# PERFORMANCE OF GOLD REFERENCE CATALYSTS IN THE WATER GAS SHIFT REACTION

**By Yatish Surendra Daya**

Submission in partial fulfilment of the requirements for the degree of
**Master of Science in Engineering**

**May 2007**




I know the meaning of plagiarism and declare that all the work in the document, save for that which is properly acknowledged, is my own.

Centre For Catalysis Research
Department of Chemical Engineering
University of Cape Town

# SYNOPSIS

The purpose of this study was to determine comparative data for 3 of the World Gold Council's reference catalysts (WGC-A - $Au/TiO_2$, WGC-B - $Au/Fe_2O_3/Al_2O_3$ and WGC-C -$Au/Fe_2O_3$) and that of a commercial low temperature water-gas shift catalyst. In this instance, Süd-Chemie's C 18-7 was chosen as the WGS catalyst.

The performance of all the catalysts was tested at conditions deemed to be found in an automotive application downstream of a methanol reformer operating at low pressure. Also, the stability of the catalysts and their response towards varying reaction conditions were investigated.

WGC-C ($Au/Fe_2O_3$) was found to have the highest activity of the reference catalysts at the standard reaction conditions. The activity of this catalyst compared favourably with that of C 18-7 at standard conditions. However, a steady deactivation was seen with this catalyst.

WGC-A ($Au/TiO_2$) was found to be the most promising catalyst. While the activity at standard conditions was low in comparison to C 18-7 and WGC-C, the catalyst was able to operate at much higher temperatures than that of the other reference catalysts, with the subsequent activity being comparable to that of C 18-7. It was also found that the catalyst was stable at elevated temperatures. Changes in reaction conditions also indicated favourable results and highlighted the stability of the catalyst. This result, together with the discovery of improved activity with increased pressure experienced with all the WGC catalysts, indicates the potential of this catalyst in future industrial applications.

# ACKNOWLEDGEMENTS

I would firstly like to thank my supervisor, Professor Jack Fletcher, for all the guidance and advice throughout the project. I would also like to acknowledge he support given to me by the rest of the academic staff in the Centre For Catalysis Research.

I would also like to thank Marc Wüst for all his support in helping me setup and operate the experimental rig. I would also like to thank Shaun Cawood and David Barkhuizen for their input in running the rig, as well as the team in the mechanical workshop for the construction of the various vessels that I required.

Special thanks goes to all the members of the Centre For Catalysis Research who made my time in the centre very fulfilling and made it a time that I will never forget.

Lastly, I would like to thank my parents and my sister for their unending support in helping me fulfill my career.

# TABLE OF CONTENTS

# LIST OF FIGURES

# LIST OF TABLES

# 1 INTRODUCTION

Gold was for a long time thought to be having no application in heterogeneous catalysis due to the metal's catalytic and chemical inertness and that no adsorption of gases, namely hydrogen and oxygen, occurred at room temperature (Bond, 1972; Schwank, 1983, 1985). However, research conducted by these authors found that gold, despite having lesser catalytic activity than Group VIII metals such as palladium, platinum and ruthenium, could influence the activity and selectivity of Group VIII metals when introduced in the form of bimetallic catalysts.

The first evidence of the possibility of catalysis by gold was found when gold particles were placed on oxidation catalysts resulting in an improvement in selectivity of the oxidation products, but at the expense of activity. Subsequently Haruta and colleagues showed that gold catalysts were active for the oxidation of carbon monoxide at ambient temperatures (Haruta *et al.*, 1987, 1989). It was further determined that, in order for gold catalysts to exhibit appreciable activity, it was necessary for the gold particles to be small (< 5 nm) and also that only certain supports were effective.

Under the guidance of these criteria, researchers discovered the potential for gold catalysis in several chemical processes, including the non-selective (Sakurai and Haruta, 1995, 1996) and selective oxidation (Haruta, 1997; Thompson, 1999) of hydrocarbons, the oxidation of hydrogen (Haruta *et al.*, 1989), the oxidation of halogenated compounds (Chen *et al.*, 1996), the hydrogenation of unsaturated hydrocarbons and combustion of hydrocarbons (Haruta, 1997), and the hydrochlorination of acetylene (Thompson, 1998; Hutchings, 2002). The water-gas shift reaction – the focus of this study – has also been extensively studied (Andreeva *et al.*, 1996a, 1996b, 1998a, 1998b, 2002a, 2002b; Fu *et al.*, 2003a, 2003b, 2005; Idakiev *et al.*, 2004).

With the recent increased interest in fuel cell technology as a possible replacement for the internal combustion engine (Fu *et al.*, 2003a), emphasis has been placed on producing the hydrogen required as fuel. One such route is the reforming of methane or methanol, followed by water-gas shift conversion and finally selective CO oxidation to produce the required hydrogen fuel (Hölzle, 2001). In each step, a catalyst, suited to the operating conditions found in fuel cells and for vehicle applications, is required. These include catalysts which:

- are not pyrophoric;
- do not require pre-reduction;
- can survive temperature excursions; and
- are tolerant of water condensation at shutdown.

(Zalc *et al.*, 2002; Fu *et al.*, 2003b; Corti *et al.*, 2005; Deng *et al.*, 2005; Gorte and Zhao, 2005; Kim and Thompson, 2005).



It is proposed that gold-based catalysts may satisfy these criteria and recent research has focused on developing gold-based catalysts that would be active both in the water-gas shift reaction and for the selective oxidation of CO.

In this study, the performance of three of the World Gold Council (WGC) reference catalysts – WGC-A ($Au/TiO_2$), WGC-B ($Au/Fe_2O_3/Al_2O_3$) and WGC-C ($Au/Fe_2O_3$) – is evaluated for the water-gas shift reaction in comparison to a typical commercial low temperature shift catalyst – $Cu/ZnO/Al_2O_3$. These comparisons are performed in the low to medium temperature shift operating range, and the effects of changing pressure, space velocity and steam/ dry gas ratio are also investigated.

# 2 BACKGROUND

## 2.1 THE WATER-GAS SHIFT REACTION

### 2.1.1 Background of the Water-Gas Shift Reaction

Pure hydrogen is required in many industrial processes, in particular the Haber ammonia synthesis process. Prior to the industrial introduction of the water-gas shift reaction in 1888, pure hydrogen was produced by the addition of metallic iron to strong acids or by the electrolysis of water. However, these processes were expensive and could not meet the demand at the time (Rhodes *et al.*, 1995).

The reaction acquired its name from the terms water-gas, which referred to an equimolar mixture of hydrogen and carbon monoxide (Twigg, 1989), and the 'shifting' of carbon monoxide (CO) and steam to carbon dioxide ($CO_2$) and hydrogen ($H_2$), according to the following:

$$CO + H_2O \Leftrightarrow CO_2 + H_2 \qquad \Delta H_{rxn} = -41.1 \text{ kJ/mol}$$

The water-gas shift reaction also provided industry with means by which to reduce carbon monoxide levels as well as to generate increased yields of pure hydrogen, since the product carbon dioxide is easier to remove than carbon monoxide (Twigg, 1989).

The water-gas shift reaction is conducted in so-called 'shift reactors' in either a single or two stage process. The reaction is thermodynamically limited if performed adiabatically in a single bed of catalyst, resulting in lower conversions as the reaction temperature increases due to the exothermic nature of the reaction (Twigg, 1989). The number of stages required is dependant on the application of the water-gas shift reaction in the overall process. A two-stage operation is utilised in ammonia synthesis, where low CO levels are required in order to avoid poisoning of the synthesis catalyst.

The first stage, or high temperature shift (HTS) stage, is conducted in the temperature range of 350 – 450°C. The second stage is referred to as the low temperature shift (LTS) stage and is conducted in the temperature range of 200 – 240°C. The industrial processes are operated at total pressures between 25 and 35 bar (Rhodes *et al.*, 1995).

### 2.1.2 High Temperature Shift

As mentioned above, high temperature shift is the first stage of the two stage water-gas shift reaction and is operated between 350 and 450°C. BASF developed the first iron and chromium oxide based catalyst for the HTS reaction (Twigg, 1989; Rhodes *et al.*, 1995). This type of catalyst is still utilised industrially in the HTS reactor. The commercial catalysts available comprise typically 90 wt% iron oxide ($Fe_2O_3$) and 10 wt% chromium oxide ($Cr_2O_3$).

The HTS stage exploits the fast kinetics of the water-gas shift reaction at high temperatures. However, as the reaction is equilibrium limited, complete conversion of the feed CO is not possible. As a result, CO levels exiting the HTS reactor are in the range 2 – 4 % (Twigg, 1989).



### 2.1.3 Low Temperature Shift

The copper based low temperature shift catalyst was first developed in the 1960s and replaced the use of a methanator to reduce carbon monoxide levels to the required levels in the range 0.1 – 0.3 % (Twigg, 1989). LTS catalysts typically comprise a mixture of copper oxide (CuO), zinc oxide (ZnO) and alumina ($Al_2O_3$) in a 1:1:1 ratio (Rhodes *et al.*, 1995).

The need for a 2-stage catalytic system derives from the fact that neither catalyst can effectively operate outside of its nominal temperature range. In the case of the iron-based HTS catalyst, this is due to it not being very active below 300°C, whereas the copper-zinc

LTS catalyst is susceptible to deactivation via sintering at temperatures above 240°C (Twigg, 1989).

### 2.1.4 Thermodynamics of the Water-Gas Shift Reaction

#### 2.1.4.1 Temperature

The water-gas shift reaction is exothermic, with $\Delta H_{rxn}$ = -41.1 kJ/mol. Therefore, the reaction temperature increases as the reaction proceeds under adiabatic conditions. However, the equilibrium constant, $K_p = (p_{H_2} . p_{CO_2})/(p_{H_2O} . p_{CO})$, decreases with increasing temperature. As mentioned previously, the reaction proceeds faster at high temperatures but, according to Le Chatelier's principle, the formation of the products is favoured at lower temperatures. Hence, the effects of temperature are contradictory and a compromise between reaction rate and conversion is needed to optimise the process.

#### 2.1.4.2 Pressure

The water-gas shift reaction is an equimolar gas phase reaction. According to Le Chatelier's principle, an increase in pressure will have no direct effect on the equilibrium. Nonetheless, it is reported that the rate of reaction increases with pressure up to 5 bar, above which the rate is insensitive to pressure (Twigg, 1989).

#### 2.1.4.3 Steam: CO ratio

A high steam to carbon monoxide ratio favours the conversion of CO. Industrially, the HTS reactor operates at $H_2O$:CO ratios in the range of 2.5-5:1 for purposes of achieving high equilibrium conversion and to limit the deposition of carbon on the catalyst. In addition, high steam content leads to thermal inefficiencies, whereas low $H_2O$:CO ratios can promote the formation of intermediate, reduced-iron species (Twigg, 1989).

### 2.1.5 Industrial Relevance and Applications

#### 2.1.5.1 Ammonia Synthesis

The process in which the water-gas shift reaction plays a vital role is in the synthesis of ammonia ($NH_3$), since water-gas shift is the only economic means of producing the quantities of hydrogen needed for the Haber process (Twigg, 1989), represented below:

$$3H_2 + N_2 \Leftrightarrow 2NH_3$$

Prior to the synthesis, both the high and low temperature shift converters are employed to maximise the yield of hydrogen and, subsequently, the amount of ammonia produced.

#### 2.1.5.2 Methanol Synthesis

The synthesis of methanol proceeds according to:

$$2H_2 + CO \Leftrightarrow CH_3OH$$

Where stoichiometry demands a 2:1 hydrogen to carbon monoxide molar ratio and consequently, only a HTS stage is employed.

#### 2.1.5.3 Possible Use of Water-Gas Shift in Automotive Fuel Cells

There has been great interest in the development of fuel cells for stationary and transportation applications. In automotive applications, the fuel cell is seen as a replacement for the internal combustion engine (Fu *et al.*, 2003a).

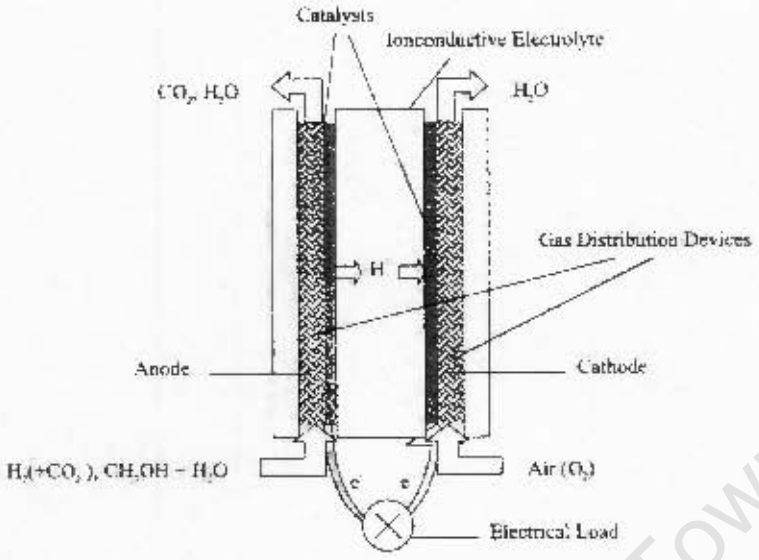


**Figure 2-1: Schematic of a Solid Polymer Fuel Cell (SPFC)** (Urban *et al.*, Applied Catalysis A: General, 2001)

A fuel cell may be considered to be an electrochemical energy converter that transforms the chemical energy of a fuel into electrical energy (Urban *et al.*, 2001). Fuel, typically hydrogen, is fed to the anode of the fuel cell where it is split into protons and electrons, and oxygen, obtained from air, is fed to the cathode. The electrons released from the oxidation of the fuel pass through an external electric circuit en route to the cathode, whereas the protons released pass through a polymer electrolyte membrane PEM which is only permeable to protons and not electric current (Hölzle, 2001). Once the protons pass through the PEM, they recombine with the electrons and oxygen to form water, the exhaust gas from a fuel cell.

Urban *et al.* (2001) have proposed that methanol can directly be added to the fuel cell. However, the presence of carbon oxide species, CO in particular, are likely to poison the platinum (Pt) based electro-catalyst making up the fuel cell anode. Hölzle (2001) proposes an alternative scheme, with a methanol or natural gas feed, and using reformers to produce a hydrogen-rich fuel that is fed to the fuel cell. This scheme has been applied

in the Daimler-Chrysler NECAR project – in particular, NECAR 3 and 5. In this scheme, natural gas and water are mixed and sent to a steam reformer to form mainly syngas – $H_2$ and CO, although side reactions, forming $CO_2$ and $H_2O$, also occur. The gas mixture then undergoes water-gas shift, both to increase the yield of $H_2$ and to reduce CO levels. As the water-gas shift reaction is equilibrium limited, unconverted CO remaining in the gas mixture still requires removal and this is achieved via a selective oxidation step where the CO is converted to $CO_2$. For a methanol feed, a similar process is followed, however water is added to the reformed gas mixture in order to induce subsequent water-gas shift.

A significant challenge remains a water-gas shift catalyst suitable to the operating conditions of the fuel cell, i.e. catalysts which exhibit similar or improved activity as compared to commercial $CuO/ZnO/Al_2O_3$, which are not pyrophoric and do not require reduction, and can tolerate temperature excursions at start-up as well as water condensation at shutdown (Zalc *et al.*, 2002; Fu *et al.*, 2003b; Corti *et al.*, 2005; Deng *et al.*, 2005; Gorte and Zhao, 2005; Kim and Thompson, 2005).

As a consequence of these demands, recent research has focused on the development of gold-based catalysts that would be active both in the water-gas shift reaction and the selective oxidation of CO. Such gold catalysts include gold-promoted ceria (Deng *et al.*, 2005; Gorte and Zhao, 2005) and gold on sulphated zirconia (Kuperman and Moir, 2005).



## 2.2 CATALYSIS BY GOLD

### 2.2.1 Applications of Gold Catalysts

Gold was for a long time thought to have no industrial application as a catalyst and, only in 1972, in one of the first studies on the catalytic properties of gold, was it reported that gold was active as an oxidative dehydrogenation catalyst when added to silver or to group VIII metals, e.g. palladium (Bond, 1972). Subsequent research by Schwank (1985)

confirmed that gold could influence the activity and selectivity of group VIII metals despite its own intrinsically low activity.

#### 2.2.1.1 Gold Supported on Iron Oxide ($Au/Fe_2O_3$)

The main application of gold supported on iron oxide is in the oxidation of CO (Guczi, 2002; Haruta *et al.*, 1989; Minocò *et al.*, 1997). Other applications include the oxidation of hydrogen (Haruta *et al.*, 1989), the hydrogenation of carbon dioxide and carbon monoxide (Sakurai and Haruta, 1995), and combustion of methanol (Haruta *et al.*, 1996).

Haruta *et al.* (1989) investigated the oxidation of CO over $Au/\alpha$-$Fe_2O_3$ and discovered that this was possible at low, even sub-ambient, temperatures. It was further reported that the supported gold catalyst displayed a longer life – 7 days – than the commercial Hopcalite catalyst used in safety masks.

It is now established that smaller gold crystallites, in the size range 4-5 nm, are necessary for appreciable activity (Guczi *et al.*, 2002) and that the size of the supported crystallites is influenced by the method of preparation used for the catalyst. Minicò *et al.* (1997) concluded that $Au/Fe_2O_3$ catalysts prepared by co-precipitation yielded smaller gold crystallites and that these were more active. It can be concluded that the oxidation of CO requires both controlled formation of small gold crystallite sizes and an appropriate support.

As mentioned previously, there is a need for removing oxidising CO in hydrogen-rich fuel streams prior to it entering a fuel cell, in view of its ability to poison the Pt-based anode. In this way, the CO in the system can be removed or reduced in concentration to acceptable levels of less than 50 ppm (Deng *et al.*, 2005; Trimm, 2005). CO oxidation is a low temperature operation and as the fuel cell would operate at approximately 80°C, problems could arise as $H_2$ oxidation occurs already at 70°C (Landon *et al.*, 2005).

Similar studies were performed by Goerke *et al.* (2004) and Luengnaruemitchai *et al.* (2005) yielding similar results.

$Au/Fe_2O_3$ has been further been shown to be active for the hydrogenation of carbon monoxide and carbon dioxide, although with higher selectivity to ethane and propane, than to methanol (Sakurai and Haruta, 1995).

#### 2.2.1.2 Gold Supported on Titanium Oxide ($Au/TiO_2$)

As with $Au/Fe_2O_3$, gold supported on titanium oxide has been extensively studied for use in CO oxidation (Iizuka *et al.*, 1997; Haruta and Daté, 2001; Daté *et al.*, 2002), methanol synthesis (Sakurai and Haruta, 1995, 1996) and combustion (Haruta *et al.*, 1996).

$Au/TiO_2$ has been shown to be a very active catalyst for CO oxidation, whereas neither gold nor $TiO_2$ alone are very active for this reaction (Haruta and Daté, 2001). The inability of the adsorbed CO to react with an oxygen molecule and for the resultant $CO_2$ to desorb from the $TiO_2$ at low temperatures, are thought to be the cause of the low activity of $TiO_2$.

In contrast, the significant activity of the $Au/TiO_2$ is thought to be due to a strong interaction between the metal and support, and which provides the site needed to activate the oxygen for $CO_2$ formation (Haruta and Daté, 2001). This catalyst was found to be active for the hydrogenation of carbon monoxide and carbon dioxide with high hydrocarbon selectivity (Sakurai and Haruta, 1995). Subsequently, the same authors found that $Au/ZnO\text{-}TiO_2$ was selective for methanol formation and attributed this observation to the gold-zinc oxide interface although the exact role of zinc was not determined (Sakurai and Haruta, 1996).

#### 2.2.1.3 Other Supported Gold Catalysts

As mentioned above, the addition of zinc oxide to gold promoted titania shifts product selectivity from hydrocarbons to methanol. Similarly, Au/ZnO alone is active for methanol synthesis and it has been claimed that the performance is similar to that of the commercial copper catalyst (Sakurai and Haruta, 1995).

The oxidation of CO was also conducted over gold supported on cobalt oxide – $Au/Co_3O_4$ – and gold supported on nickel oxide – Au/NiO (Haruta *et al.*, 1989), with activities similar to $Au/\alpha\text{-}Fe_2O_3$ despite the gold crystallites being of larger size in the case of $Co_3O_4$ and NiO supports.

Gold supported on manganese oxides – Au/MnOx – were tested as possible catalysts for the selective oxidation of CO (Torres Sanchez *et al.*, 1997). Findings included CO conversions exceeding 95% and that the catalyst was active at lower temperatures than that of Pt-based oxidation catalysts. These results were obtained at between 323 and 353 K. However, at 393 K the CO conversion decreased in favour of $H_2$ oxidation. Similar findings were reported by Luengnaruemitchai *et al.* (2005).

Various other gold-promoted metal-oxide catalysts have been tested for the oxidation of CO. Costello *et al.* (2002) and Okumura *et al.* (1998) investigated CO oxidation over $Au/Al_2O_3$. Gold-promoted ceria has recently been shown to be active for CO oxidation (Goerke *et al.*, 2004). The studies by Deng *et al.* (2005) and Panzera *et al.* (2005) yielded similar findings where $Au/CeO_2$ was active for CO oxidation but with less than total selectivity in $H_2$ containing streams.

### 2.2.2 Water-Gas Shift Reaction over Gold Catalysts

The gold catalysed water-gas shift reaction has been extensively reported in the literature, notably over $Au/\alpha\text{-}Fe_2O_3$ (Andreeva, 1996a, 1996b, 1998a, 1998b, 2002a, 2002b;

Boccuzzi, 1999; Ilieva *et al.*, 1997). Andreeva *et al.* (1998b) also investigated $Au/TiO_2$ and $Au/CoO_x$ while more recent work has focussed on $Au/CeO_2$ systems (Fu *et al.*, 2003a, 2003b, 2005; Deng *et al.*, 2005).

### 2.2.2.1 Water-Gas Shift over $Au/Fe_2O_3$

Figure 2-2 presents the findings of early studies comparing water-gas shift activity of $Au/\alpha\text{-}Fe_2O_3$, $\alpha\text{-}Fe_2O_3$ and $Au/Al_2O_3$ against a commercial copper-zinc-alumina LTS catalyst, (Andreeva *et al.*, 1996a). The gold loadings used in all cases were approximately 4%, on an atomic level.

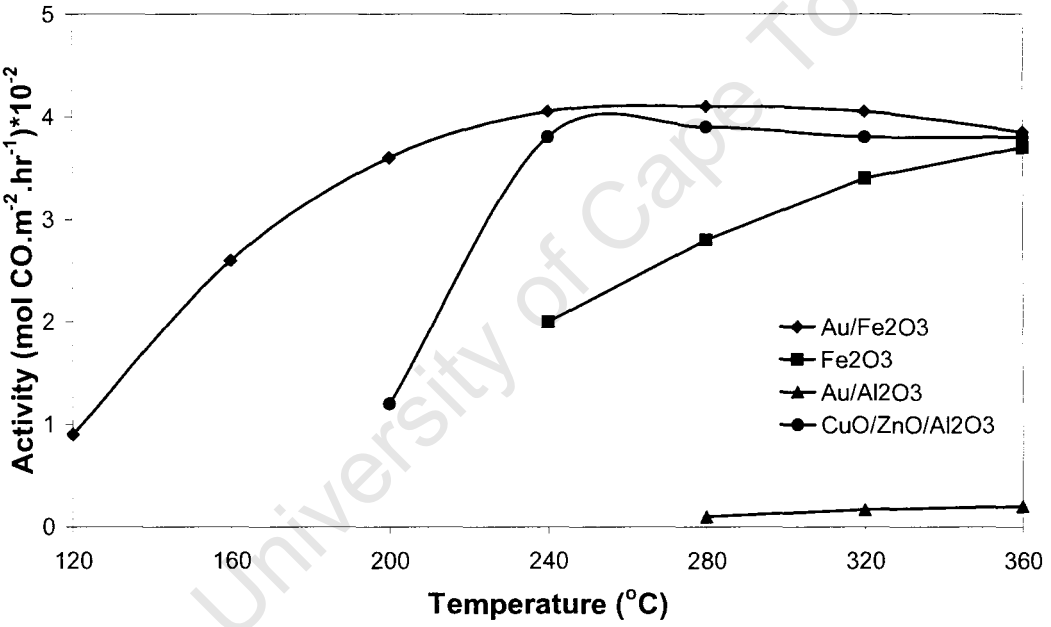




**Figure 2-2: Activity of initial Au-based catalysts compared to a commercial LTS catalyst** (Andreeva *et al.*, 1996a)

From figure 2-2, it was claimed that $Au/\alpha\text{-}Fe_2O_3$ is more active than the commercial LTS catalyst at lower temperatures. This activity was also higher than that of the gold free $Fe_2O_3$ and $Au/Al_2O_3$, which showed very little activity. It was proposed that the higher activity of $Au/\alpha\text{-}Fe_2O_3$ was due to the interaction between the gold and iron oxide support, which contained both hematite ($Fe_2O_3$) and magnetite ($Fe_3O_4$) phases. The

presence of both iron oxide phases supported the mechanism described by Andreeva *et al.* (1996b), which proposed that a spillover of activated hydroxyl groups onto the catalyst was needed and that the catalytic cycle involved a redox transfer ($Fe^{2+} \Leftrightarrow Fe^{3+}$). Ilieva *et al.* (1997) showed that this transfer occurred 140°C lower in Au/α-$Fe_2O_3$ as compared to unpromoted iron oxide, and consequently, the low temperature activity in the Au/α-$Fe_2O_3$ system. The gold-free $Fe_2O_3$ can be considered to be an HTS catalyst – conventional HTS catalysts contain approximately 90 wt% $Fe_2O_3$.

The interaction between the gold and iron oxide support was further investigated by Andreeva *et al.* (1998a) who proposed that a weaker gold-metal interaction resulted in a better catalyst, i.e. higher activity, and that this was more readily achieved via deposition-precipitation than by co-precipitation as a means of catalyst preparation.

#### 2.2.2.2 Water-Gas Shift over $Au/TiO_2$

On the basis of earlier work by Andreeva *et al.* (1996a) and the conclusion that activated hydroxyl groups and a reducible (redox active) support were necessary for activity in supported gold catalysts (notably in the case of Au/α-$Fe_2O_3$), it was not thought that $Au/TiO_2$ would be active for water-gas shift as it was not readily reducible. However, experiments conducted by this group of researchers showed that $Au/TiO_2$ prepared by deposition-precipitation was active as a water-gas shift catalyst. Three different $Au/TiO_2$ catalysts were prepared using different types of titanium based supports, namely, fresh TiOH, commercial $TiO_2$ and anatase (Andreeva *et al.*, 1998b). The gold loadings varied from 3.4 to 33 atom%, with the catalysts with lower gold loadings showing greater activity.

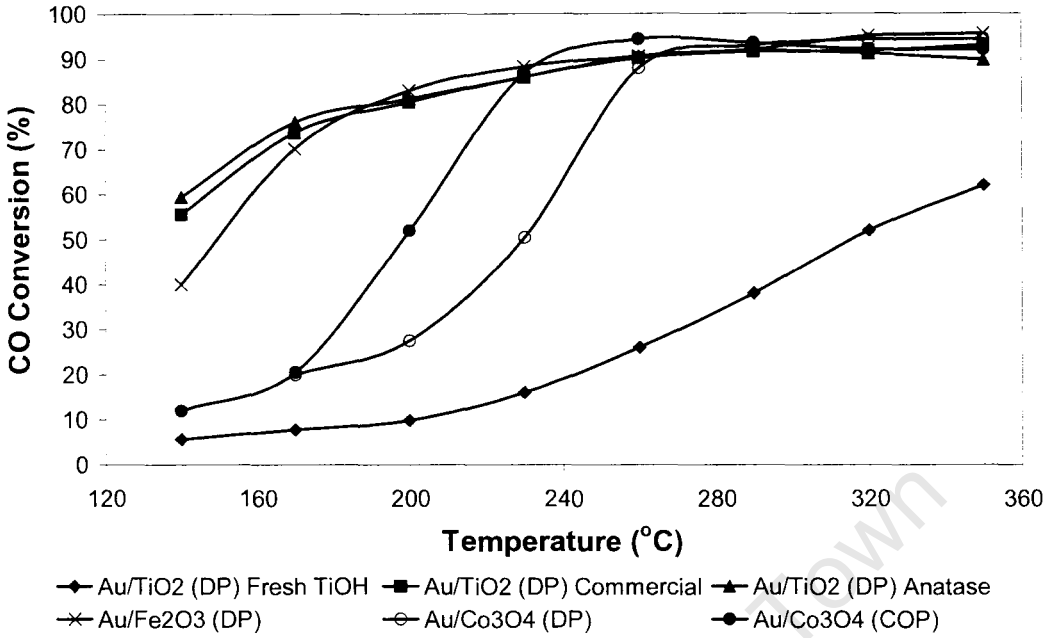


**Figure 2-3: Activity of Various Gold Based Catalysts for Water-Gas Shift** (Andreeva *et al.*, 1998b)

Whereas $Au/TiO_2$ (commercial) and $Au/TiO_2$ (anatase) were found to be very active, the catalyst prepared using fresh TiOH exhibited low activity (refer to figure 2-3).

However, catalyst characterisation revealed that the two more active catalysts contained gold particles smaller than 5 nm. A similar finding was reported by Sakurai *et al.* (1997), although no indication was given for the size of the gold crystallites on the less active catalyst – $Au/TiO_2$ (fresh TiOH). Nonetheless, the link between Au crystallite size and catalyst activity was apparent also for the $TiO_2$ based system. It was further proposed that the unexpected activity of $Au/TiO_2$ be attributed to a different mechanism to that proposed for $Au/\alpha\text{-}Fe_2O_3$, i.e. one that does not result in a redox transfer.

#### 2.2.2.3 Water-Gas Shift over Other Supported Gold Catalysts

In the same study quoted above, Andreeva *et al.* (1998b) also evaluated the water-gas shift activity of another reducible metal oxide, cobalt oxide – $Au/Co_3O_4$. Two samples were prepared, one sample by co-precipitation and the other by deposition-precipitation. It was found that both catalysts were less active than $Au/\alpha\text{-}Fe_2O_3$ and $Au/TiO_2$ and, moreover, that rapid deactivation occurred (refer to figure 2-3). Interestingly, the co-precipitated sample was the more active of the two cobalt oxide catalysts.

Analysis of the catalysts indicated the presence of CoO and inactive elemental cobalt in addition to the $Co_3O_4$. It was also found that the reduction to elemental cobalt occurred at 200°C lower for the $Au/Co_3O_4$ than for the pure support. Consequently, the rapid formation of inactive metallic Co, under the conditions of the reaction, was postulated as the reason for the rapid deactivation observed in the case of $Au/Co_3O_4$ (Andreeva *et al.*, 1998b).

More recent studies have investigated the use of ceria supported gold – $Au/CeO_2$ – as a potential LTS catalyst for use in automotive fuel cells (Andreeva *et al.*, 2002b). It has further been shown that $Au/CeO_2$ (with an atomic gold loading of 8%) exhibited higher activity across a wider temperature range (150 – 350°C) than the commercial LTS catalyst (Fu *et al.*, 2003a). Results showed that gold improved the reducibility of the cerium oxide. Interestingly, the gold loading of the catalyst – varying from 0.9 to 8.3 at% – did not influence the gold crystallite size in contrast to findings of Haruta *et al.* (1989) in the case of oxides of iron, cobalt and nickel.

A further advance In the research into water-gas shift using gold-ceria catalysts refers to a recent report by Amierio-Fonseca *et al.* (2005) as contained an a patent assigned to Johnson-Matthey where it was found that $Au/CeO_2/ZrO_2$ exhibited greater activity than commercial $CuO/ZnO/Al_2O_3$.

### 2.2.3 The Role of the Support

Iizuka *et al.* (1997, 1999) found that fine gold powder adsorbed far less CO as compared to $Au/TiO_2$ on a surface area basis and quite simply that the support – $TiO_2$ – plays a part in increasing the reactivity of the gold. Reasons for the lower activity of unsupported gold powder are claimed to be twofold. Firstly, the crystallite sizes are approximately 20 times larger than that of the supported gold catalyst and it is generally accepted that smaller crystallite size promotes higher activity and, secondly, a strong gold-metal support interaction is thought to be important. This gold-metal support interaction does not only affect gold-titania catalysts but has also been invoked for the water-gas shift reaction over $Au/Fe_2O_3$, where higher activity obtained at lower temperatures has been attributed to the interaction between the gold and iron oxide (Andreeva *et al.*, 1996a). Andreeva (2002a) further postulates that the support is able to alter the electronic properties of the small gold particles and that sufficient support surface area is essential to maintain small active metal particles.



### 2.2.4 Nature of the Active Site

The exact nature of the active site present in gold based catalysts remains a matter of speculation and is based mostly on studies of CO oxidation activity (Bond and Thompson, 2000; Costello *et al.*, 2002). To date, only one model based on water-gas shift activity has been proposed, viz. that of Ilieva *et al.* (1997) in the case of $Au/CeO_2$.

FTIR studies have shown that, in a gold based catalyst, both metallic and ionic gold are present on the support, i.e. $Au^0$ and $Au^{1+}$, with ionic gold regarded as the more active species (Minicò *et al.*, 1997). However, $Au^{3+}$ has also been reported (Bond and Thompson, 2000). Bond and Thompson (2000) suggest that both $Au^0$ or $Au^{x+}$ result in an active catalyst. They further propose that the $Au^{x+}$ acts as the 'glue' that binds the $Au^0$ to the metal-oxide support (figure 2-4), and that the structure is not fixed but depends on the extent of calcination and/or reduction. However, complete reduction of the catalyst is harmful as this glue can be lost and sintering can occur. Mechanistically, CO oxidation is

proposed to proceed via chemisorption on a metallic gold atom and via water dissociation to form a hydroxyl bonded to an ionic gold atom. When oxidised, a carboxylate group forms on the ionic gold atom and an oxygen molecule occupies a previously vacant site. Subsequent hydrogen abstraction from the carboxylate group forms carbon dioxide and a hydroperoxide ion which oxidises another carboxylate group to form more carbon dioxide and two hydroxyl groups. The mechanism is consistent with general observation that water, present either directly or resulting from $H_2$ oxidation, is necessary for stable activity.

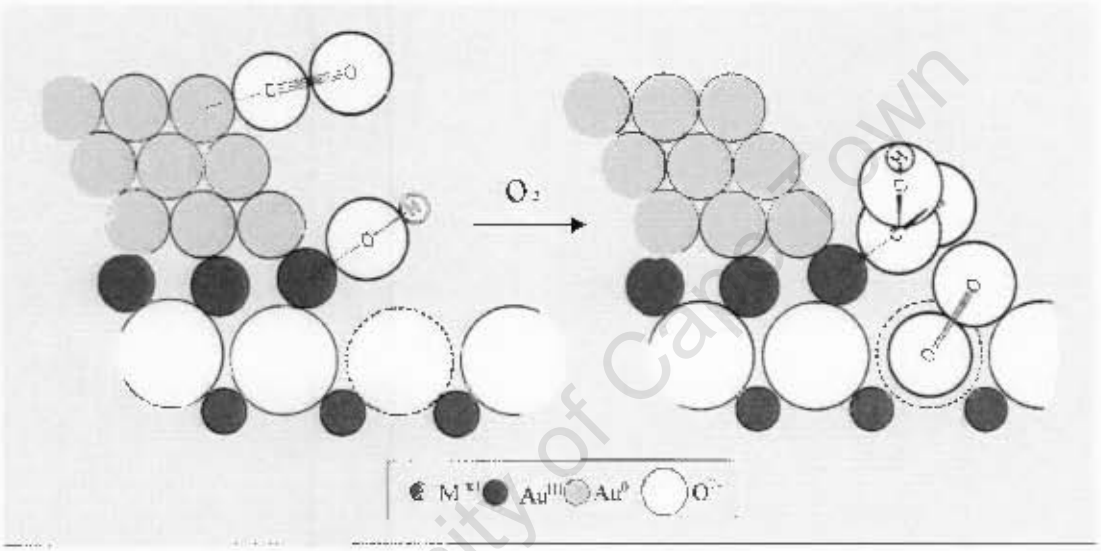


**Figure 2-4: Proposed nature of active site of gold-based catalyst for CO oxidation** (Bond and Thompson, 2000)



The need for both $Au^0$ and $Au^{x+}$ species in an active catalyst has also been proposed by Costello *et al.* (2002). They too are of the view that a hydroxyl group is bonded to the ionic gold, however, they propose that an adsorbed CO is inserted and that CO is not bound to metallic gold. Based on this model, the authors propose a reaction mechanism for both CO oxidation and the water-gas shift reaction.

Although the exact nature of the active site in gold-based water-gas shift has yet to be determined, there is significant support for the pathways that include the dissociation of water on fine gold particles followed by a spillover of activated hydroxyl groups onto the metal-oxide support which can undergo redox transfer. This has been accepted for gold supported on iron oxide (Andreeva *et al.*, 1996a; Ilieva *et al.*, 1997). Ilieva *et al.* (1997) also state that magnetite – $Fe_3O_4$ – formed after the reduction of the $Fe_2O_3$, is the "working catalytic system" for water-gas shift over Au/α-$Fe_2O_3$, as per the case in conventional HTS catalysts.

In the case of $Au/CeO_2$, the group of Flytzani-Stephanopoulos has reported that no loss in activity was observed when removing 90% of the metallic gold by NaCN leaching (Fu *et al.*, 2003b, 2005). As a consequence, it was proposed that metallic gold nanoparticles did not participate directly in the water-gas shift reaction but that the active site involved ionic gold strongly bonded into the ceria surface and subsurface layers (Fu *et al.*, 2005).



## 2.3 REACTION MECHANISMS

A definitive mechanism for the water-gas shift reaction has yet to be determined. Rather, two principle pathways have been proposed for the reaction, namely the associative and regenerative mechanisms. Both mechanisms were proposed by Armstrong and Hilditch in 1920.

### 2.3.1 Adsorptive Mechanism

The associative mechanism involves the adsorption of CO and $H_2O$ onto the surface of the catalyst. Here, an unspecified intermediate is formed which is decomposed, resulting in the formation of the products, $CO_2$ and $H_2$ (Rhodes *et al.*, 1995), as per

$$CO + H_2O \rightarrow (\text{intermediate}) \rightarrow CO_2 + H_2$$

### 2.3.2 Regenerative Mechanism

The regenerative mechanism involves a cyclic change in the oxidation state of the catalyst. The mechanism can be viewed as the lysis of water on the catalyst to produce $H_2$ and the accompanying oxidation of the catalyst surface. Subsequent surface reduction by CO to form $CO_2$ returns the catalyst to its original state (Rhodes *et al.*, 1995). This mechanism may be represented as follows:

$$H_2O + Red \rightarrow H_2 + Ox$$

$$CO + Ox \rightarrow CO_2 + Red$$

### 2.3.3 Mechanisms over Commercial Water-Gas Shift Catalysts

#### 2.3.3.1 Mechanism over LTS Catalyst

The nature of the active site and the subsequent mechanism is still unknown for the copper-zinc-alumina LTS catalyst as both the associative and regenerative mechanisms have been proposed (Rhodes *et al.*, 1995). It is also suggested that the zinc-aluminium oxide found in the catalyst plays no role in the reaction pathway but rather that copper is the active element in the catalyst. Moreover, both $Cu^0$ and $Cu^{1+}$ are present on the catalyst surface and it is generally accepted that both metallic and ionic components are needed for the catalytic activity.



#### 2.3.3.2 Mechanism over HTS Catalyst

Less debate exists with regard to the mechanism over the iron based HTS catalyst, where the regenerative mechanism has been generally accepted due to the presence of both $Fe^{2+}$ and $Fe^{3+}$ in the catalyst (Rhodes *et al.*, 1995). This suggests that the metal undergoes a redox transfer, which is required for an active catalyst.

### 2.3.4 Mechanisms over Gold-Based Water-Gas Shift Catalysts

#### 2.3.4.1 Mechanism over Au/α-$Fe_2O_3$

Au/$Fe_2O_3$ is an active water-gas shift catalyst as it can accommodate active hydroxyl groups on the surface after water is dissociated. Moreover, $Fe_2O_3$ can undergo reversible redox transfer, i.e. $Fe^{2+} \Leftrightarrow Fe^{3+}$. As a consequence, Andreeva *et al.* (1996b) proposed an associative mechanism for water-gas shift over Au/α-$Fe_2O_3$, (figure 2-4). Water adsorbs onto the catalyst and dissociates with the activated hydroxyl groups spilling over onto adjacent ferric oxide sites. Carbonate species are formed and subsequently decomposed to form carbon dioxide. This formation and decomposition occurs simultaneously with the iron oxide undergoing $Fe^{3+} \rightarrow Fe^{2+}$ redox transfer. The dissociation of water occurs with the reverse redox transfer.

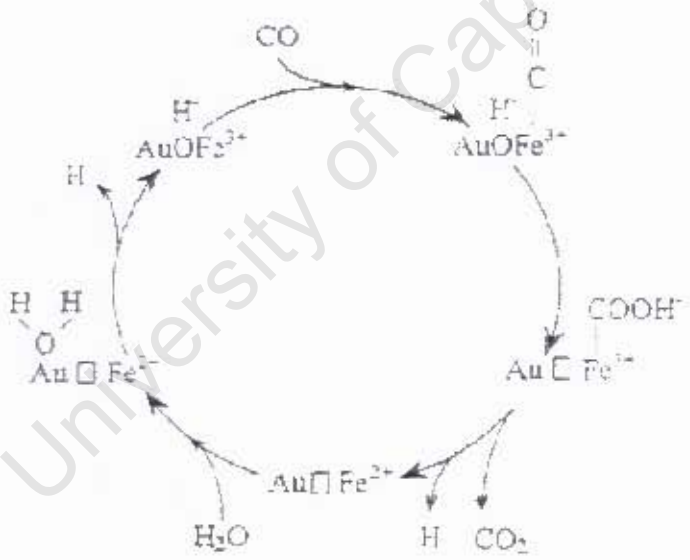


**Figure 2-5: Proposed Water-Gas Shift Reaction Mechanism over Au/α-$Fe_2O_3$** (Andreeva *et al.*, 1996b)

The same mechanism is proposed to occur over Au/$Co_3O_4$ (Andreeva *et al.*, 1998b).

### 2.3.4.2 Mechanism over $Au/TiO_2$

Infrared analysis of the active gold promoted and unpromoted $TiO_2$ catalysts revealed a higher concentration of active hydroxyl groups in the unpromoted catalyst (Andreeva *et al.*, 1998b). In the case of $Au/\alpha\text{-}Fe_2O_3$, the promoted catalyst displayed greater hydroxyl coverage. This result, combined with the non-reducible nature of $TiO_2$, has led to the proposal of an alternative mechanism to that of the mechanism over $Au/\alpha\text{-}Fe_2O_3$, as depicted in figure 2-5.

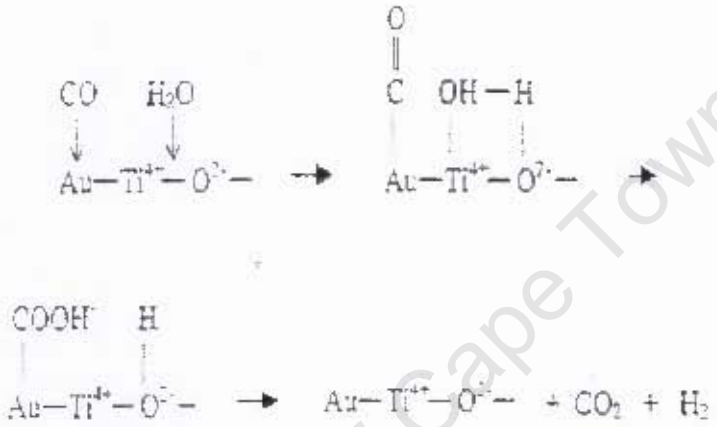


**Figure 2-6: Proposed Water-Gas Shift Reaction Mechanism over $Au/TiO_2$** (Andreeva *et al.*, 1998b)

The initial step in the mechanism is the adsorption of CO onto gold particles. Water dissociates and is adsorbed onto the titanium dioxide with a formate ($COOH^-$) species being formed on the gold. This decomposes into $CO_2$ and $H_2$ and the active catalyst is restored for further catalysis.

# 3 OBJECTIVES OF THE STUDY

The objective of this study is to determine the comparative performance of the World Gold Council's (WGC) reference catalysts – WGC-A ($Au/TiO_2$), WGC-B ($Au/Fe_2O_3/Al_2O_3$) and WGC-C ($Au/Fe_2O_3$) versus a current commercial Cu/ZnO/alumina LTS catalyst, (Süd-Chemie's C 18-7) in an automotive application downstream of a methanol reformer operating at low pressure.

In this study, the following key questions are to be investigated:

- What is the relative activity of the WGC supported gold reference catalysts in comparison to that of a commercial LTS catalyst (Süd-Chemie C 18-7)?
- What is the relative stability of the WGC reference catalysts at typical water-gas shift conditions?
- How is the performance of the WGC catalysts affected by varying reaction conditions?

# 4 EXPERIMENTAL

## 4.1 CATALYSTS

### 4.1.1 Catalysts Used

Three gold catalysts and one commercial catalyst were used in this study. The gold catalysts were supplied by the Wold Gold Council (WGC) while the commercial LTS catalyst (C 18-7) was obtained from Süd-Chemie. These catalysts and the form in which that they were applied experimentally are presented in table 4-1 below.

**Table 4-1: Catalysts used**

| Catalyst | | Supplier | Catalyst Form | Catalyst Particle Size (μm) | BET Surface Area ($m^2/g$) |
|---|---|---|---|---|---|
| C 18-7 | $CuO/ZnO/Al_2O_3$ | Süd-Chemie | Granulate | 125 – 250 | 60 |
| WGC-A | $Au/TiO_2$ | WGC | Granulate | 250 – 710 | 52 |
| WGC-B | $Au/Fe_2O_3/Al_2O_3$ | WGC | Spheres | 2200 – 4000 | 210 |
| WGC-C | $Au/Fe_2O_3$ | WGC | Granulate | 250 – 710 | 40 |

Catalyst data sheets provided by the suppliers are presented in Appendix III.

### 4.1.2 Catalyst Characterisation

#### 4.1.2.1 Catalyst Particle Size and Surface Area

The catalyst particle size range for the study is shown in table 4-1 above. For C 18-7, the commercial pellets (tablets 6 x 4.75 mm) were crushed and sieved to obtain the desired size fraction. In the case of WGC-A and WGC-C catalysts, the powder, as it was received, was pelletised at 2 tons pressure, followed by granulation and sieving to the size

fraction stated in table 4-1. The WGC-B catalyst was used in the form as supplied, viz. an egg-shell type catalyst, compromising spheres in size from 2.2 to 4.0 mm.

Furthermore, BET analysis of the gold loaded catalysts was performed to determine the surface areas of the catalysts. These results are summarised in table 4-1.

#### 4.1.2.2 Gold Loading and Particle Size

Transmission Electron Microscopy (TEM) was conducted on the gold catalysts to determine the sizes of the gold particles (figure 4-1). Analysis of the TEM images for WGC-A and WGC-C showed gold particles in the range 2 – 5.5 nm and 2.5 – 4.5 nm respectively. However, the TEM images obtained in the case of WGC-B were difficult to interpret as the gold particles could not be clearly seen.



**Table 4-2: Gold loaded catalyst data**

| Catalyst | Gold content wt % | Gold Particle Size Range (nm) |
|---|---|---|
| WGC-A | 1.5 | 2 – 5.5 |
| WGC-B | 0.3 | |
| WGC-C | 5.0 | 2.5 – 4.5 |

Gold content of the catalysts was not determined independently and the reported values are those provided by the WGC (refer to table 4-2).

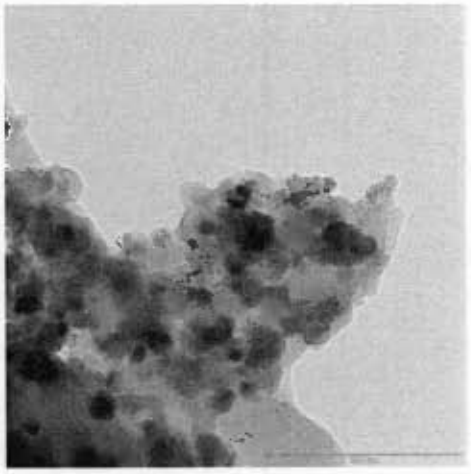

WGC-A ($Au/TiO_2$)

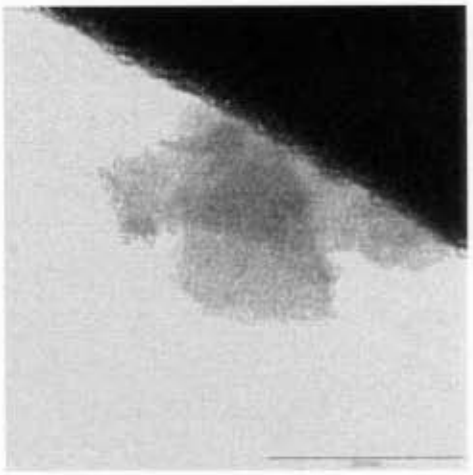

WGC-B ($Au/Fe_2O_3/Al_2O_3$)

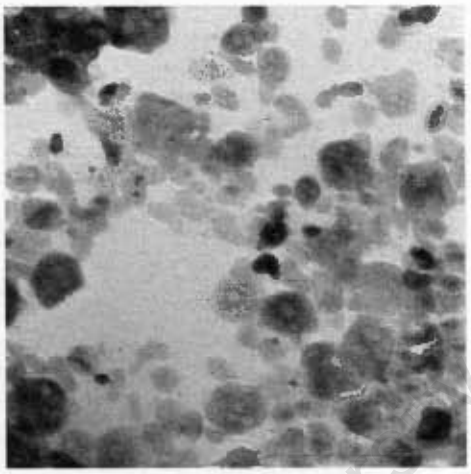

WGC-C ($Au/Fe_2O_3$)

Scale: 200 nm

**Figure 4-1: TEM micrographs of gold catalysts**



#### 4.1.2.3 Temperature Programmed Reduction (TPR)

TPR experiments were conducted on all the catalysts tested. Approximately 0.1 g of catalyst was used in each run. Well defined reduction of the catalyst was observed for both C 18-7 and WGC-C. No reduction of WGC-A was observed. This was expected as both Au and $TiO_2$ are non-reducible, resulting in WGC-A being non-reducible. Also, no reduction in WGC-B was observed, possibly due to the low Au loading. The TPR traces of all the catalysts can be seen in chapter 5.

## 4.2 WATER-GAS SHIFT TEST APPARATUS

The flowsheet of the experimental apparatus used in this study is shown in figure 4-2. The apparatus consists of a down-flow packed bed reactor preceded by a gaseous and liquid feed system and followed by a condenser to remove unconverted water prior to depressurisation via a back-pressure regulator.

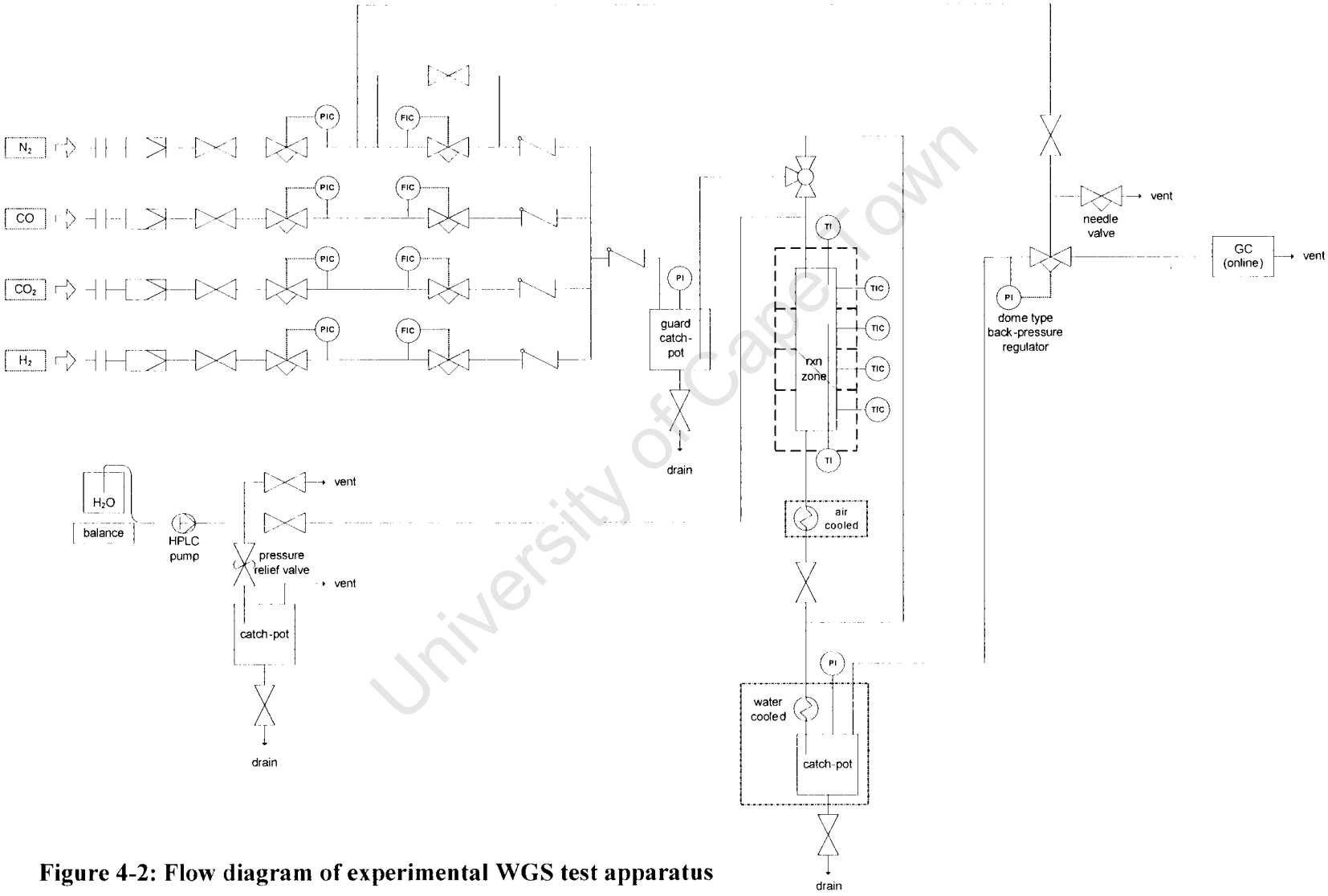


**Figure 4-2: Flow diagram of experimental WGS test apparatus**

### 4.2.1 Feed

The reactor feed consists of a gaseous feed and a liquid feed. Gaseous feed, comprising of hydrogen, nitrogen, carbon monoxide and carbon dioxide, is supplied from a central manifold as individual components via mass flow controllers (Brooks Instruments 5850S series, $H_2$ and $N_2$ 0 - 200 sccm; CO and $CO_2$ 0 - 50 sccm) to the reactor. Deionised liquid water is fed by an isocratic HPLC pump (Laballiance Series 1+, 0.01 - 10 ml/min).

### 4.2.2 Guard Catch Pot

A 1 litre catch pot (internal diameter 85 mm, internal length 180 mm) is placed before the reactor to collect any liquid water that might proceed back towards the mass flow controllers under circumstances of system blockage and acts merely to protect the mass flow controllers from such an event. Non-return valves located after the mass flow controllers and before the catch pot act as an additional safety feature to protect the mass flow controllers.



### 4.2.3 Reactor

The reactor body comprises a stainless steel tube with an approximate length of 360 mm and internal diameter of 16 mm. An axial thermowell, to accommodate a $\frac{1}{16}$" thermocouple (Unitemp J type), runs from the bottom of the reactor to approximately 30 mm from the top of the reactor. The top reactor assembly, which incorporates the gas and water feed connections, joins to the reactor body by means of a ¾" VCR fitting. This assembly also comprises a fixed thermocouple which projects some 5 mm into the top of the packed bed, once assembled. Reactor feed and effluent lines are connected to the reactor body via ¼" VCR fittings.

The reactor is placed inside a concentric heating jacket comprising 4 independent heating zones (Unitemp coil heaters), viz. two pre-heat zones, followed by the catalyst bed zone and a subsequent post bed trim zone. The pre-heat and trim zones are individually controlled by means of temperature controllers (Gefran 600) while the

catalyst bed zone is controlled by means of a programmable temperature controller (Gefran 800P). The entire assembly is insulated using glasswool insulation to maintain stable temperature control.

### 4.2.4 Condensers

Condensation of the unconverted water in the reactor effluent occurs in two stages: in an air-cooled coil followed by a water-cooled coil. The air-cooled coil comprises a 2000 mm length of ¼" stainless steel tubing coiled with a diameter of 100 mm. The water-cooled condensation stage consists of a similar smaller coil placed in a water bath (Endocal RTE-8) cooled to approximately 2°C.

The condensed water is collected in a knock-out vessel (length 80 mm, internal diameter 40 mm) directly following the water-cooled coil and maintained at 2°C. The vessel is specifically designed to eliminate back-mixing of the product gas, ensuring virtually plug-flow behaviour in the lines from the reactor to the online gas chromatographic analysis. Condensed water is collected periodically from the knock-out vessel via a valve under action of the system pressure.



### 4.2.5 Back-Pressure Regulator

A back-pressure regulator supplied by Grove Valve & Regulator Co. maintains the system operating pressure and is situated downstream of the condensers and knock-out vessel. The operating pressure on the diaphragm is provided by nitrogen.

### 4.2.6 Adaptations for Sampling

To allow for the unconverted feed gas to be analysed, 3-way valves are placed before and after the reactor. Switching of these valves so that the reactor is bypassed allows for the composition of the dry feed gas to be analysed via a gas chromatograph equipped with both a thermal conductivity detector (TCD) and, subsequently, by a flame ionisation detector (FID), after methanation.

## 4.3 OPERATING CONDITIONS

### 4.3.1 Standard Operating Conditions

Preliminary experiments conducted on the commercial LTS catalyst indicated a decrease in catalyst activity until a steady-state condition, where a negligible activity loss is observed with time, was reached after approximately 72 hours. Consequently, all catalysts were tested at a set of standard conditions until steady-state conditions were reached. The standard conditions applied are provided in table 4-3. In order to evaluate the extent of catalyst deactivation during an experimental run, the standard conditions were periodically reset to determine the 'standard catalytic activity' with time-on-stream.

**Table 4-3: Standard conditions**

| | |
|---|---|
| Temperature | 200°C |
| Pressure | 2 bar (absolute) |
| Steam: Dry Gas Ratio | 1:1 (mol/mol) |
| $WHSV_{dry}$ | 4.0 $hr^{-1}$ |
| $SGHSV_{dry}$ (C 18-7) | 10000 $hr^{-1}$ |



It should be noted that the $SGHSV_{dry}$ stated above is for commercial LTS catalyst only, since bulk densities differ for the various catalysts.

### 4.3.2 Reaction Conditions for Performance Evaluations

For the purposes of testing the performance of the catalysts in the water-gas shift reaction, the reaction conditions are changed and their effect on the conversion is noted. The parameters considered are reactor temperature, pressure, space velocity and steam to dry gas ratio.

#### 4.3.2.1 Temperature

Temperature is the most important parameter considered in this study. In order to study the effect of reaction temperature on the conversion, the entire temperature range available to water gas shift (200 – 350°C) is considered. Also, in order to determine the "light-off" point of the catalyst, the temperature is reduced to 130°C and the temperatures are increased in 10°C increments.

In order to maintain a gas phase reaction, the water in the catalyst zone has to remain above its dew point. At the standard reaction conditions of 2 bar (absolute) and a steam to dry gas ratio is 1:1, the dew point of water is 121°C. Therefore, to prevent condensation of water in the system, and subsequent catalyst deactivation of the commercial LTS catalyst, the lowest reaction temperature considered is 130°C.

#### 4.3.2.2 Pressure

The standard reactor pressure is set at 2 bar. Increased pressures of 4 and 8 bar have also been considered for the purposes of testing the effect of pressure on the catalyst activity, with the necessary minimum operating temperature adjusted due to the changing dew point.

#### 4.3.2.3 Space Velocity

A standard gas hourly space velocity on a dry basis ($SGHSV_{dry}$) of 10000 $hr^{-1}$ is used for the commercial LTS catalyst to ensure that the reaction is not equilibrium limited. This corresponds to a weight hourly space velocity on a dry basis ($WHSV_{dry}$) of 4 $hr^{-1}$. As the $SGHSV_{dry}$ used is only relevant for the commercial LTS catalyst, the experiments are conducted at a constant $WHSV_{dry}$ of 4.0 $hr^{-1}$.

For all the catalysts tested, experiments are conducted at half and double the standard $WHSV_{dry}$, i.e. 2 $hr^{-1}$ and 8 $hr^{-1}$.

#### 4.3.2.4 Steam: Dry Gas Ratio

The standard steam/dry gas ratio on a molar basis chosen for the experiments is 1:1. Steam/dry gas ratios of 0.5 and 2.0 (mol/mol) have been used to determine its effect on catalyst activity.

## 4.4 EXPERIMENTAL OPERATING PROCEDURE

### 4.4.1 Catalyst Loading Procedure

In order to load the reactor, the reactor body is placed in a bench vice so that the reactor is loaded from the bottom upwards for a final packing as depicted in figure 4-3.

Silane treated glasswool is inserted at the reactor exit to ensure that no catalyst or inert packing is lost from the reactor bed. The temperature trim zone at the bottom of the reactor and the lower half of the reaction zone (the bottom 15 cm of the reactor) is packed first with granulate SiC (500-750 μm). The catalyst bed, consisting of 1 g of catalyst diluted in 5 $cm^3$ of the inert silicon carbide, is loaded next. The remaining portion of the reactor is then filled with SiC until the tip of the thermowell running along the length of the reactor is covered. After each zone is packed, the reactor is tapped to ensure that the contents are fully settled and compact. Finally, another plug of glasswool is placed on top of the completed packing prior to the connection of the reactor body to the reactor top assembly via the VCR fitting.

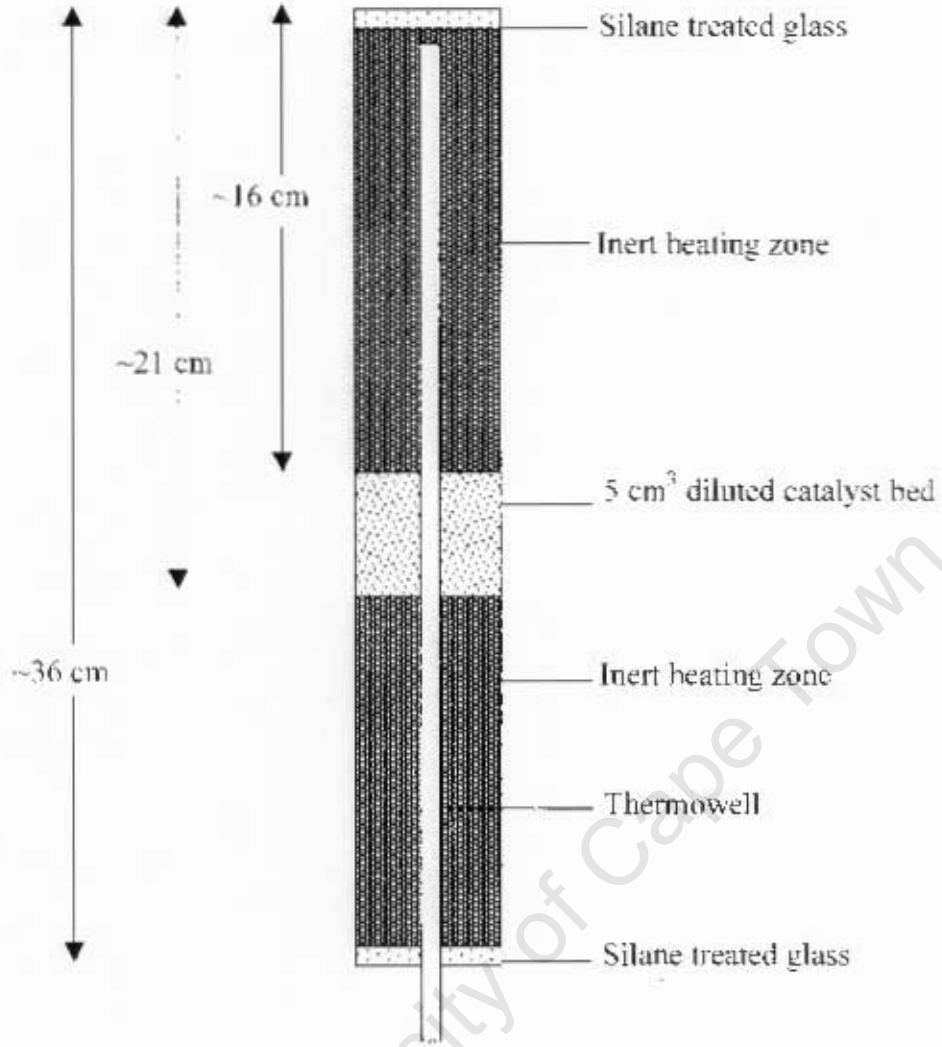


**Figure 4-3: Diagrammatic representation of the reactor packing**



### 4.4.2 Reactor Leak Test

The packed reactor is placed in the heating jacket and the water feed, gas feed and reactor exit lines are connected. On completion, nitrogen, bypassing the mass flow controller, is passed through the system at 21 bar. This procedure not only pressurises but also purges the system of air. Soapy water is applied to the connections to determine if any leaks are evident. Upon satisfactory completion of the leak test, the system is depressurised to atmospheric pressure.

### 4.4.3 Catalyst Activation/ Reduction

The commercial LTS catalyst required pre-treatment considered typical for such catalysts and involves ramping the catalyst bed zone to 200°C at 1°C/min under a 200 sccm stream comprising 2 vol% $H_2$ in $N_2$. Whereas the catalyst zone temperature is ramped automatically by the zone programmer, the preheat and trim zone temperatures are incrementally increased by 10°C every 10 minutes. To complete the reduction process, pure $H_2$ at 80 sccm is passed over the catalyst for 1 hour at 200°C.

The three gold catalysts were calcined at 250°C prior to packaging and shipping from the WGC. These catalysts underwent the same pre-reduction as described above after being loaded into the reactor and the performing of the subsequent comparative performance tests.



### 4.4.4 Reactor Operation

#### 4.4.4.1 Dry Gas Composition

The four reaction gases are obtained individually from the gas manifold and their flowrates are controlled by individual mass flow controllers (refer to section 4.2.1). The feed gas composition is the approximate gas composition of the product of methanol reforming as reported by Edwards *et al.* (1998). Table 4-4 lists the compositions of the feed gas and the flowrates of each gas at the standard $WHSV_{dry}$ of 4.0 $hr^{-1}$, resulting in a total dry gas flowrate of 74.7 sccm.

**Table 4-4: Feed gas composition and flowrates**

| | Composition (vol %) | Flowrate (sccm) for $WHSV_{dry}$ = 4 $hr^{-1}$ |
|---|---|---|
| Hydrogen | 40 | 29.9 |
| Nitrogen | 40 | 29.9 |
| Carbon Monoxide | 5 | 3.7 |
| Carbon Dioxide | 15 | 11.2 |

#### 4.4.4.2 Start Up Procedure

Upon completion of the reactor leak test (refer to section 4.4.2) and catalyst activation/ reduction (refer to section 4.4.3), and whilst the system is still at 200°C and under pure $H_2$, the operating pressure is set to 2 bar (absolute) via the back-pressure regulator. Three-way valves located before and after the reactor are switched so as to isolate the reactor at pressure under $H_2$ and to bypass the feed directly to the air- and water-cooled effluent condensers and knock-out vessel. Due to the large dead volume associated with the guard vessel located prior to the reactor, the total flowrate of the feed gas is increased to 250 sccm; with the individual flowrates such as to provide the standard gas composition (refer to table 4-4). After approximately 15 minutes (approximately twice the guard vessel volume), the total flowrate and composition is set as per table 4-4.

The water pump is started and primed to remove any air bubbles in the lines but the reactor is bypassed by switching a 3-way valve located prior to the reactor. Once the pump is primed, the desired flowrate is set and the pump continues to pump with the reactor still bypassed.

Bypass gas samples are sequentially analysed by gas chromatography until the gas composition is found to be constant, after which the 3-way valves prior to and after the reactor are switched to direct both the dry gas and water flows through the reactor, the product recovery system and to effluent analyses. This point is determined to be the start of the water-gas shift (WGS) experiment.

#### 4.4.4.3 On-line Procedures

The following procedures are applied to alter specific reaction conditions during the WGS performance test. In all cases, after alteration of conditions, the system is allowed to stabilise for 3 hours prior to the resumption of effluent stream analysis.

**Temperature**

When changing the reaction temperature, the set-points of the 4 temperature controllers are adjusted according to pre-determined values in order to obtain the desired temperature profile in the reactor.

**Pressure**

Reactor pressure is adjusted by increasing or decreasing the $N_2$ loading pressure on the back pressure regulator by means of the supply $N_2$ pressure regulator and bleed valves, respectively.

**Space Velocity**

Altering of the space velocity involves simultaneous adjustment of both the feed gas and water flowrates such that the steam: dry gas ratio is maintained. The individual feed gas flowrates are adjusted by changing each of the mass flow controller set points and the water flowrate is adjusted by changing the pump setting.

**Steam: Dry Gas Ratio**

In all cases, a change in the steam/dry gas ratio is effected by means of a change in water flowrate only whilst maintaining a constant dry gas flowrate.



#### 4.4.4.4 Shut-down Procedure

Upon completing an experimental run, the water pump is switched off, after which the 3-way valves before and after the reactor are switched so as to bypass dry feed gas for analysis with a view to ascertaining the stability of feed composition and dry gas analysis over the duration of the experiment.

On completion of the post-experiment dry gas analyses, gate valves on the delivery manifold are shut so that no more gas enters the system. The BPR is vented to

atmosphere via the bleed valve and the system depressurised. The heating is turned off and the reactor is allowed to cool to ambient temperature after which the reactor is removed, unloaded and made ready for subsequent experiments.

## 4.5 FEED AND PRODUCT GAS ANALYSIS

### 4.5.1 Gas Chromatography

#### 4.5.1.1 Sampling Procedure

On-line sampling of the bypass feed and de-watered product gas stream is achieved via an automated 6-way sampling valve, fitted with a 100µl sample loop. During normal test operation, the valve is set so that the gaseous stream flows through the sample loop to vent and analysis is initiated by switching the sample loop in-line with the chromatographic carrier gas, after which the valve switches back to its original position.

A single compositional data point comprises the average of 3 consecutive sample 'injections' and analyses.

#### 4.5.1.2 Chromatographic Analysis

The $CO_2$ is separated from the product gas in the first, Hayesep, column while the remaining components eluting from the first column passes through the second, molsieve, column via the programmed action of a second 6-way valve. $H_2$, $N_2$ and, to a lesser degree, CO and $CO_2$, are detected by the TCD after which they pass through a methaniser where the CO and $CO_2$ are converted to methane which is quantified accurately in the ensuing FID. Analysis of a sample takes approximately 4 minutes. Full chromatographic conditions are listed in table 4.5, and sample chromatographs are provided in figures 4-4 and 4-5 for TCD and FID analyses respectively. Typical component elution times are tabulated in table 4-6.

**Table 4-5: Chromatographic conditions**

| | Hayesep | Molsieve |
|---|---|---|
| Column packing | Hayesep N | Molsieve 13X |
| Column length | 2 m | 1.3 m |
| Column diameter (OD) | ⅛ " | ⅛ " |
| Column material | Stainless steel | Stainless steel |
| Column temperature | 50°C | |
| Methaniser temperature | 380°C | |
| Detector temperature (TCD filament) | 150°C | |
| Detector temperature (FID) | 250°C | |
| Carrier (Argon) Flowrate | 30 ml/min | |



The analytical system comprises a gas chromatograph (GC) fitted with an automated gas sampling valve, two columns (Hayesep and molsieve columns in series) with a thermal conductivity detector (TCD), methaniser and flame ionisation detector (FID) in series.

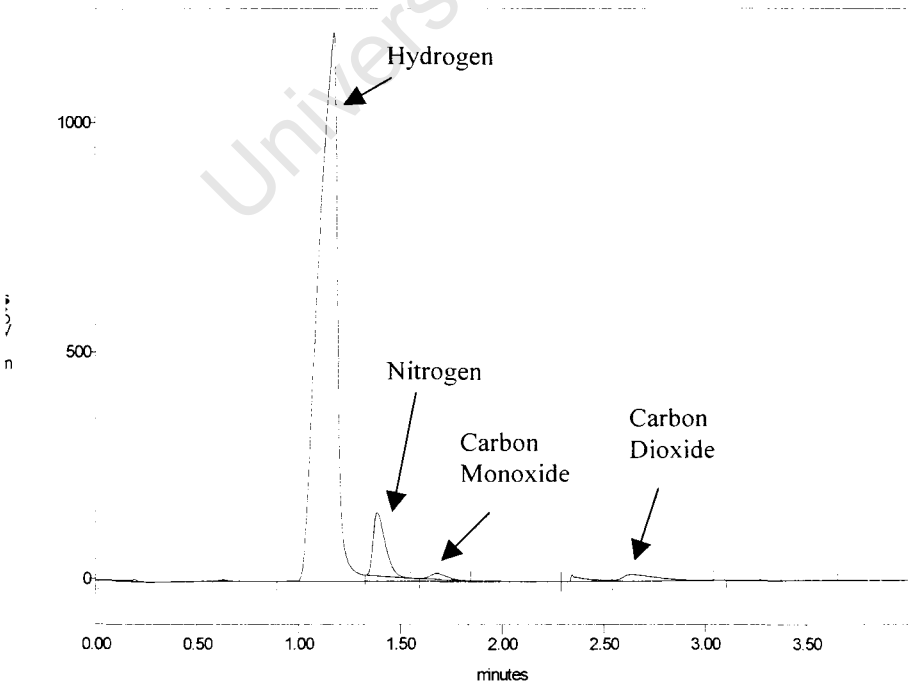


**Figure 4-4: Typical chromatogram from TCD**

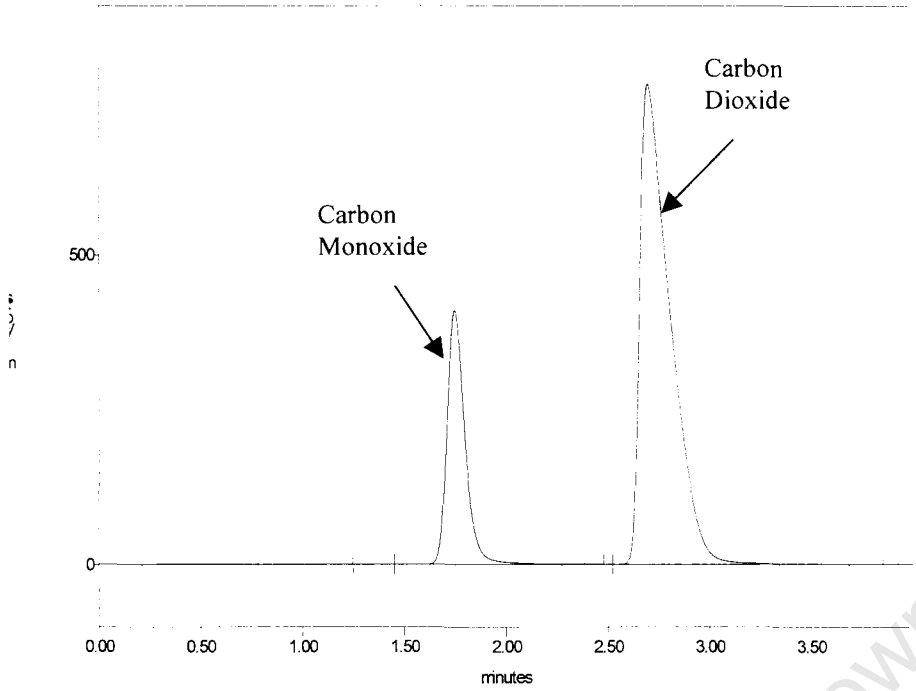


**Figure 4-5: Typical chromatogram from FID after methanation**

**Table 4-6: Chromatographic elution times for all components**

| Component | TCD Elution Time (minutes) | FID Elution Time (minutes) |
|---|---|---|
| Nitrogen | 1.2 | - |
| Hydrogen | 1.4 | - |
| Carbon Monoxide | 1.7 | 1.7 |
| Carbon Dioxide | 2.7 | 2.7 |

### 4.5.2 Data Work Up

Using the data obtained from the FID trace (i.e. the analyte responses for CO and $CO_2$ obtained as methane), the conversion of CO ($X_{CO}$) is as follows:

$$X_{co} = \frac{F_{CO,feed} - F_{CO,product}}{F_{CO,feed}} \qquad \textbf{Equation 4-1}$$

$$X_{CO} = \frac{F_{feed}.x_{CO,feed} - F_{product}.x_{CO,product}}{F_{feed}.x_{CO,feed}} \qquad \textbf{Equation 4-2}$$

$$F_{product} = F_{feed} + F_{feed}.x_{CO,feed}.X_{CO} \qquad \textbf{Equation 4-3}$$

$$X_{CO} = \frac{\left(1 - \frac{x_{CO,product}}{x_{CO,feed}}\right)}{1 + x_{CO,product}} \qquad \textbf{Equation 4-4}$$

where $x_{CO,product}$ is obtained from a single-point calibration using a standard calibration mixture containing 5 mol% CO, corresponding to the amount of CO in the feed dry gas mixture at standard conditions (and previously shown to be within the FID linear range); $F_{feed}$ is the total molar dry gas flowrate into the system, and $x_{CO.feed}$ is the molar composition of CO in the feed dry gas mixture (i.e. 0.052).

# 5 RESULTS

A summary of all experiments conducted is presented in table 5-1.

**Table 5-1: Summary of experimental runs**

| Experiment | Catalyst | Temperature (°C) | Pressure (bar a) | $WHSV_{dry}$ ($hr^{-1}$) | S:DG* (mol/mol) |
|---|---|---|---|---|---|
| 1 | LTS | 135 – 200 | 2 | 4 | 1:1 |
| 2 | LTS | 130 – 205 | 2, 4, 8 | 2, 4, 8 | 0.5:1, 1:1, 2:1 |
| 3 | WGC-B | 125 – 275 | 2 | 4.0 | 1:1 |
| 4 | WGC-B | 125, 185, 205 – 275 | 2, 4, 8 | 2, 4, 8 | 0.5:1, 1:1, 2:1 |
| 5 | WGC-C | 190 | 2 | 4 | 1:1 |
| 6 | WGC-C | 130 – 235 | 2 | 4 | 1:1 |
| 7 | WGC-C | 165, 190 | 2, 4, 8 | 2, 4, 8 | 0.5:1, 1:1, 2:1 |
| 8 | WGC-A | 155 – 315 | 2, 4, 8 | 2, 4, 8 | 0.5:1, 1:1, 2:1 |

* S:DG – Steam/Dry gas ratio

## 5.1 PRELIMINARY FINDINGS

### 5.1.1 Initial Deactivation of Catalysts

Initial experiments on the commercial LTS catalyst revealed a slight deactivation over the first 2-3 days on stream, after which catalyst performance becomes stable. A similar pattern is also evident for the gold reference catalysts. Consequently, in all experiments, the catalyst activity is allowed to stabilise under standard conditions (refer to table 4-3) for 72 hours prior to the adjustment of experimental conditions and evaluation of performance.

Figure 5-1 shows this initial deactivation in the case of both LTS ($Cu/ZnO/Al_2O_3$) catalyst and WGC-A ($Au/TiO_2$) catalysts at standard conditions. For the C 18-7 catalyst, the CO conversion decreased from approximately 90% to 85% in a period of approximately 72 hours after which the conversion was deemed to be constant with time-on-stream. In the case of the WGC-A catalyst, the CO conversion decreased from approximately 25% to 12% over a similar period of time before stabilising.

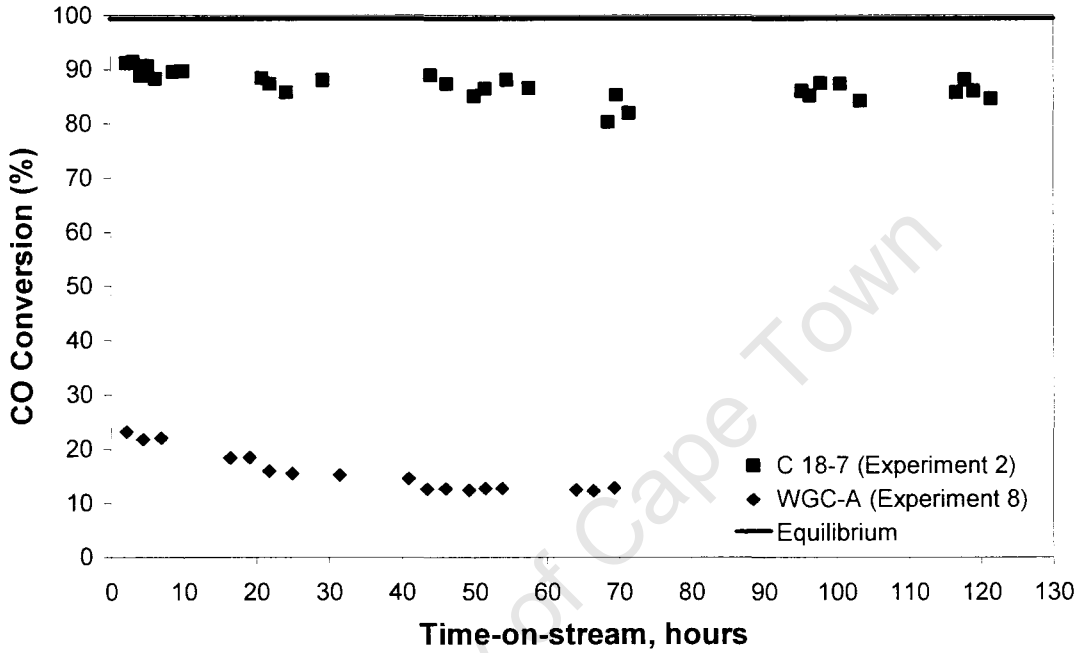


**Figure 5-1: Initial deactivation of commercial LTS ($Cu/ZnO/Al_2O_3$) catalyst (experiment 2) and WGC-A ($Au/TiO_2$) (experiment 8) at standard conditions**

### 5.1.2 Experimental Reproducibility

Figure 5-2 shows the initial deactivation of 2 separate experiments using $Au/Fe_2O_3$, (i.e. experiments 5 and 6) over a period of some 90 hours. Good reproducibility is observed as both experiments are initially at 97% CO conversion - close to equilibrium - and the activity decreases to 75% over the 90 hour period.

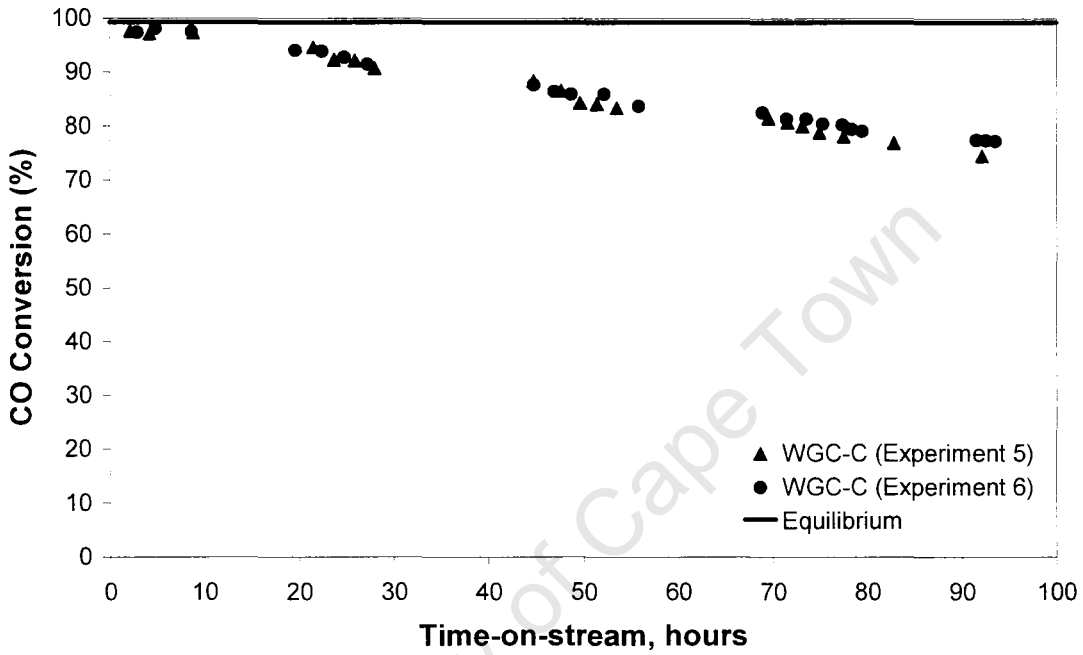


**Figure 5-2: Experimental reproducibility for the WGC-C ($Au/Fe_2O_3$) catalyst at standard conditions**

## 5.2 COMMERCIAL LOW-SHIFT CATALYST, C 18-7 ($Cu/ZnO/Al_2O_3$)

### 5.2.1 Effect of Temperature

The effect of temperature was evaluated at otherwise standard conditions by varying temperature stepwise from 135 – 205°C in approximately 10°C increments, followed by decreasing the temperature from 190 to 130°C, again in 10°C increments over a period of approximately 320 hours. The results of this experiment are presented in figure 5-3. From the good co-incidence of conversion values for the increasing and decreasing temperature series, it can clearly be seen that catalyst activity is stable throughout the experimental period (of some 12 days). CO conversion increased steadily with increasing temperature as expected and approaches equilibrium conversion above 200°C (as is expected from industrial practice).



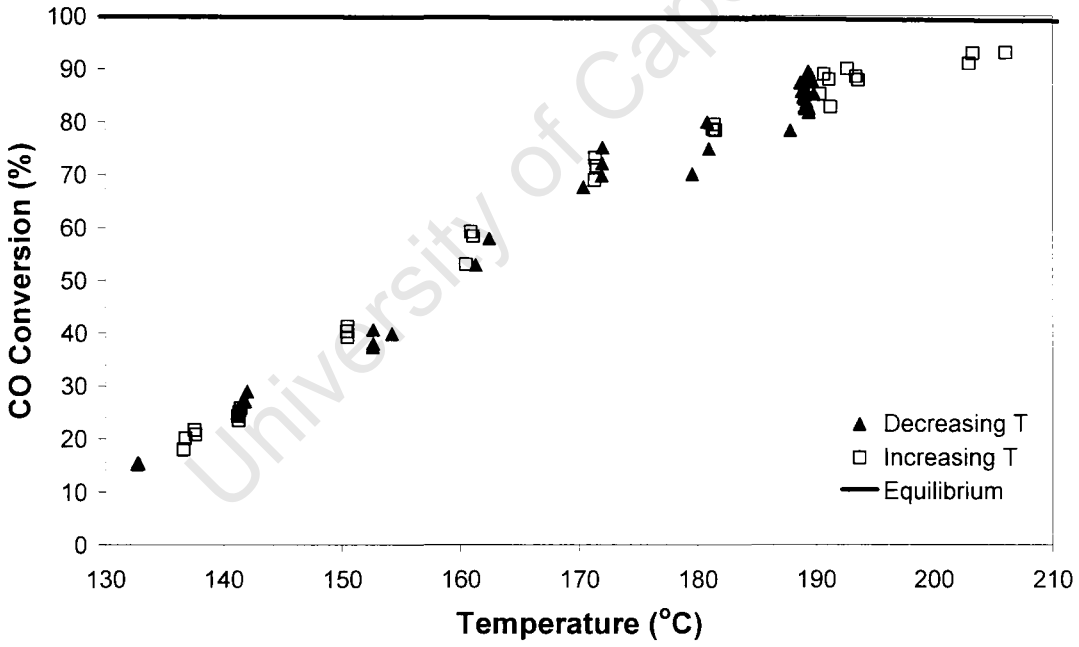


**Figure 5-3: Performance of LTS ($Cu/ZnO/Al_2O_3$) catalyst at varying temperatures (experiment 2)**

### 5.2.2 Effect of Space Velocity

The standard space velocity condition of this study ($SGHSV_{dry}$ = 10000 $hr^{-1}$) was chosen to be sufficiently high as to keep the catalyst away from equilibrium in its typical temperature range of 195 – 210°C. This value corresponds to a weight hourly space velocity ($WHSV_{dry}$) of 4.0 $hr^{-1}$. Tests at $WHSV_{dry}$ of 2.0 and 8.0 $hr^{-1}$ were conducted to evaluate the response of the catalyst to lower and higher duties respectively.

In order to remain kinetically limited, the tests were conducted at 160°C, where the CO conversion at standard conditions was approximately 60%. As expected, the conversion of CO decreased with increasing space velocity (figure 5-4).

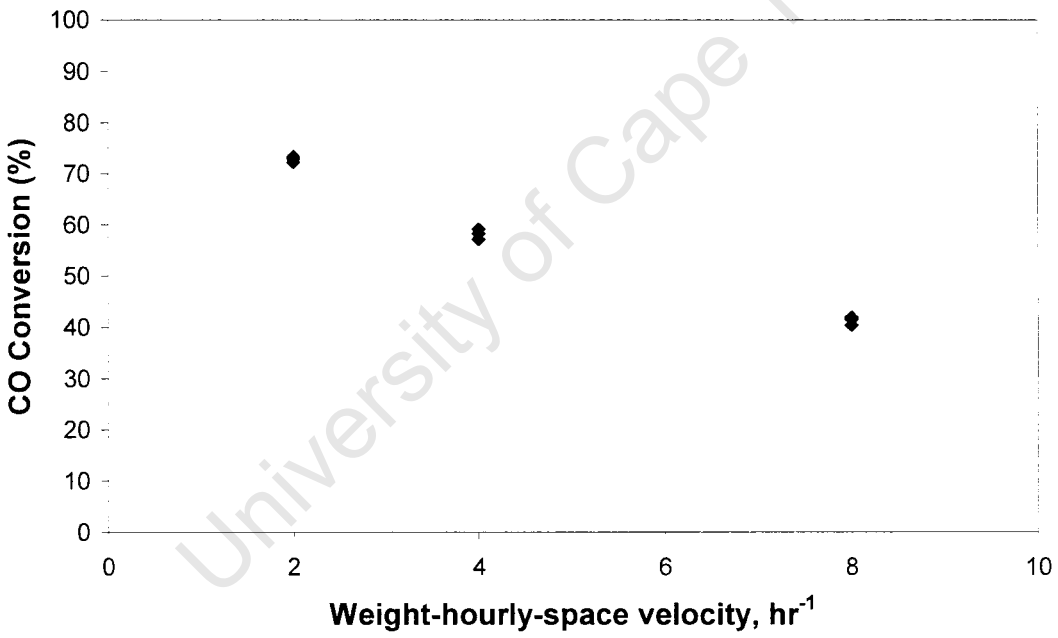


**Figure 5-4: Effect of space velocity on LTS ($Cu/ZnO/Al_2O_3$) performance at 160°C and otherwise standard conditions (experiment 2)**

### 5.2.3 Effect of Steam: Dry Gas Ratio

In testing the influence of this parameter, the flowrate of water was altered at constant dry gas flowrate and, consequently, increasing steam:dry gas ratio is concomitant with increasing overall flowrate (and decreasing contact time). After initial stabilization of catalyst activity over 72 hours, the experimental sequence comprised tests at molar steam/dry gas ratios of 1 (standard), 0.5 and 2. The results of these experiments are presented in figure 5-5, where the data point annotations (values in square brackets) refer to the test sequence. It can be seen that upon returning to the standard steam/ dry gas ratio (1:1) after the tests at the two extreme values, lower CO conversion was recorded than the original value. Consequently, these findings suggest that the catalyst had been altered in some way by the changing reaction conditions.

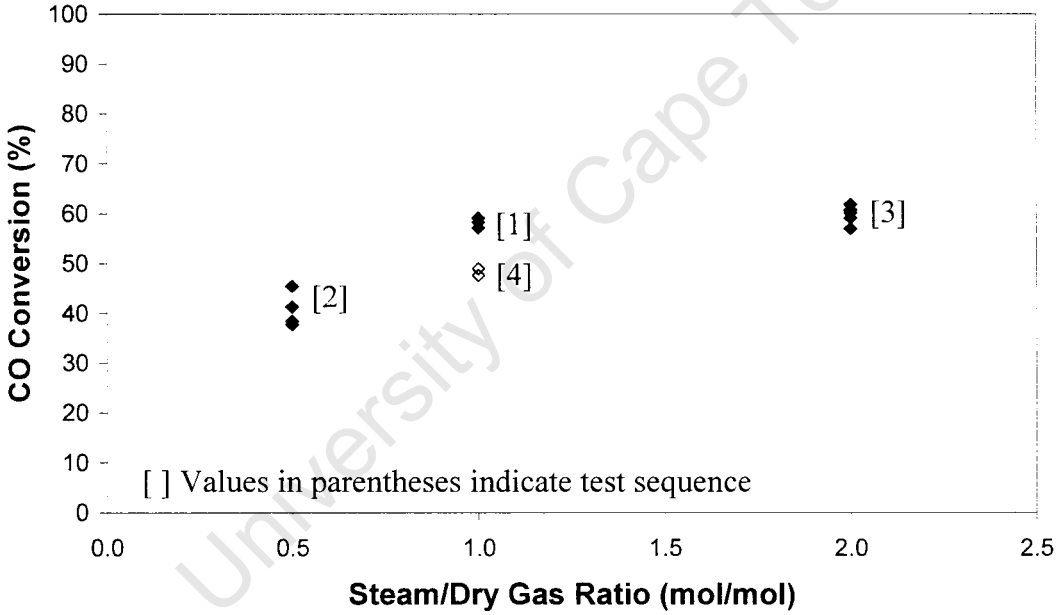




**Figure 5-5: Effect of steam: dry gas ratio on LTS ($Cu/ZnO/Al_2O_3$) performance at 160$^0$C and otherwise standard conditions (experiment 2)**

### 5.2.4 Effect of Pressure

The influence of reaction pressure on catalyst activity is presented in figure 5-6. It should be noted, however, that this series of experiments was conducted on the catalyst after the steam:dry gas experiments of section 5.2.3 and, consequently, that the starting point for this test series is the possibly slightly deactivated catalyst resulting from the steam:dry gas test series. Again in figure 5-6, data annotations in square brackets indicate the sequence of the test series from which it can be seen that the catalyst performance remains stable across the experimental pressure series.

By determining the equivalent reaction rates at 2, 4 and 8 bar respectively, it can be seen that the rate for CO conversion is roughly proportional to $1/\sqrt{P}$, as previously reported for $Cu/ZnO/Al_2O_3$ catalysts (Twigg, 1989).

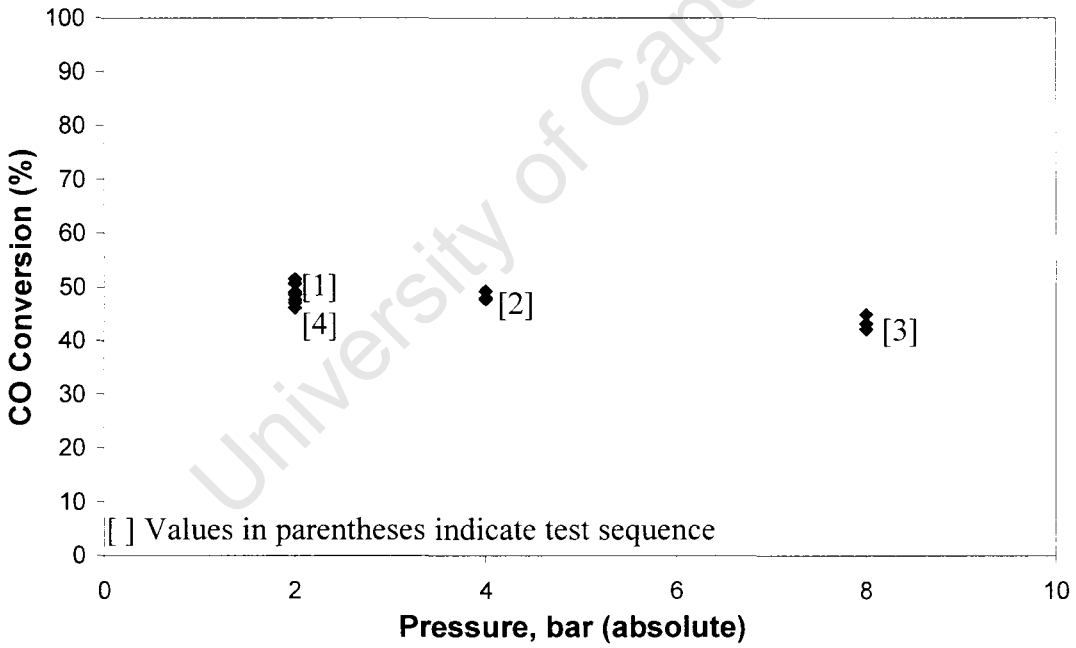


**Figure 5-6: Effect of pressure on LTS ($Cu/ZnO/Al_2O_3$) catalyst at 160°C and otherwise standard conditions (experiment 2)**

### 5.2.5 TPR Analysis

From figure 5-7, it can be seen that at approximately 150°C, some activity takes place on the LTS catalyst, with a overlapping of two peaks occurring at 220°C. These peaks are attributed to the reduction of Cu. The catalyst returns to the base line at 260°C

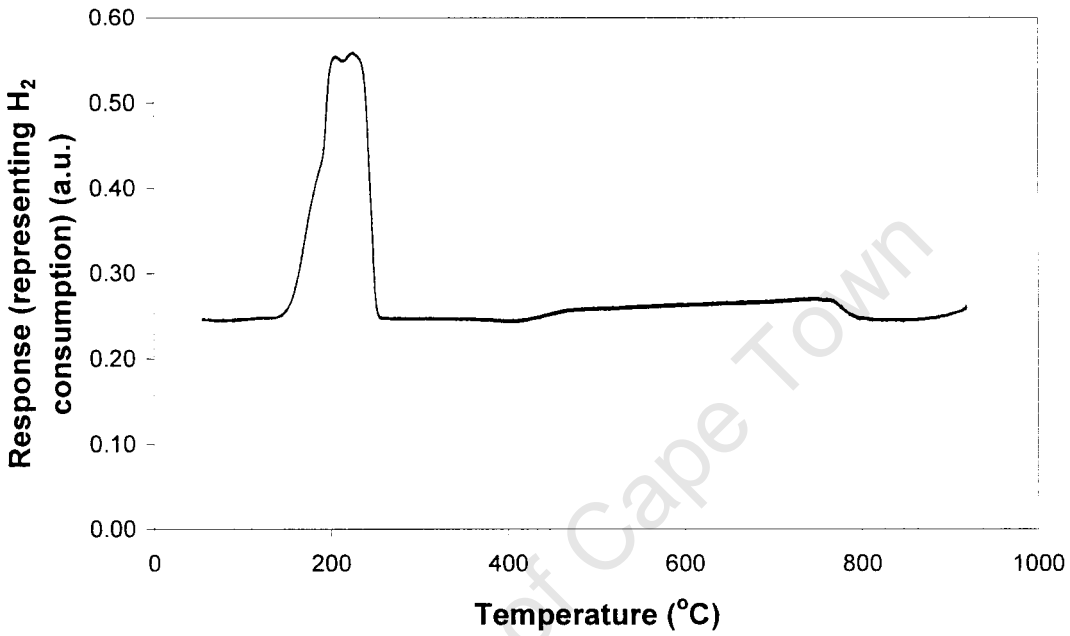


**Figure 5-7: TPR Analysis of LTS ($Cu/ZnO/Al_2O_3$) catalyst**

## 5.3 WGC TYPE A CATALYST – $Au/TiO_2$

As the $Au/TiO_2$ catalyst performance proved to be remarkably stable, only a single experimental run was conducted. Moreover, the catalyst was observed to attain its steady-state activity more rapidly than any of the catalysts of this study.

### 5.3.1 Initial Deactivation

CO conversion versus time-on-stream is presented in figure 5-8 from which it can be seen that the catalyst activity stabilizes within two days-on-stream. For consistency with the testing protocols of the other catalysts of this study, performance experiments were conducted only after 70 hours.

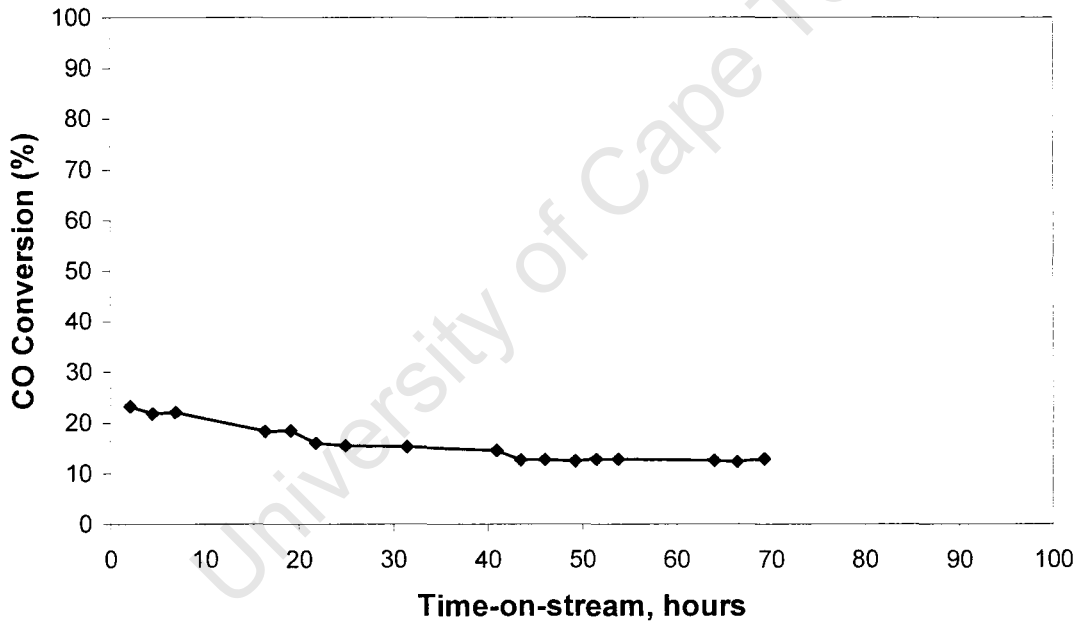




**Figure 5-8: Initial deactivation of WGC-A ($Au/TiO_2$) at standard conditions (experiment 8)**

### 5.3.2 Effect of Temperature

The conversion of CO increased with temperature, but due to the lower activity relative to $Cu/ZnO/Al_2O_3$, equilibrium conversion was approached only at high temperatures, above 315°C (figure 5-9).

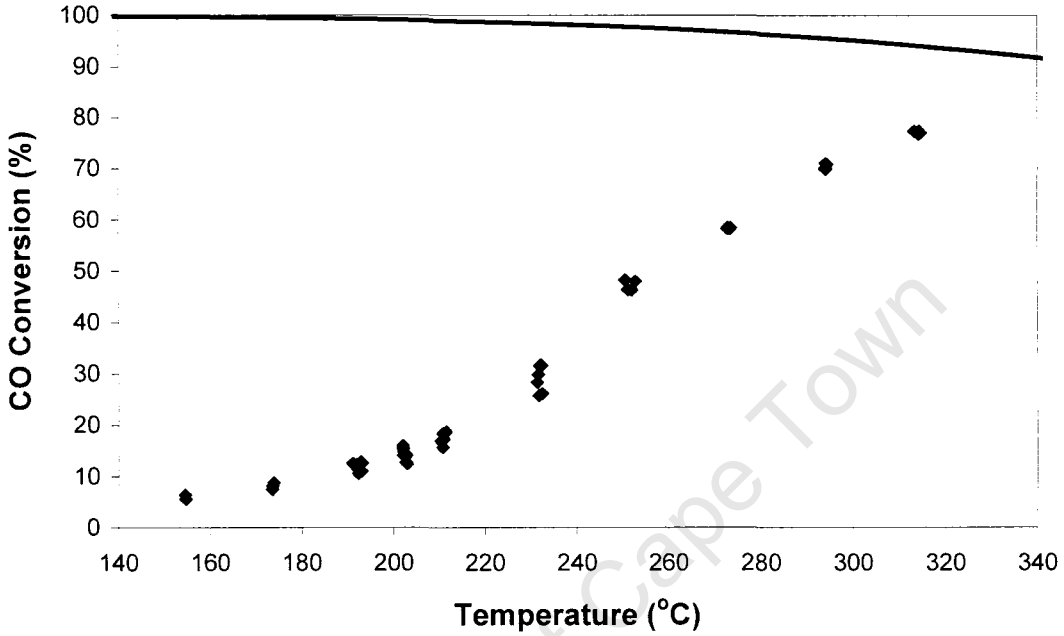


**Figure 5-9: Effect of temperature on WGC-A ($Au/TiO_2$) at otherwise standard conditions (experiment 8)**

### 5.3.3 Effect of Space Velocity

As per the case with C 18-7, $WHSV_{dry}$ of 2.0, 4.0 and 8.0 $hr^{-1}$ were tested. However, in this case, standard conditions were re-established after each change in space velocity so as to determine to what extent and under which conditions catalyst stability might be degraded. For reasons of the low catalyst activity observed at standard conditions, the space velocity, steam/dry gas ratio and pressure series were all conducted at 250°C.

As expected, increasing space velocity resulted in decreasing CO conversion (refer to figure 5-10). It was further observed that, upon returning to the standard space velocity approximately 40 hours after the start of the test, the CO conversion did not differ significantly to that prior to the test, again confirming good catalyst stability under the applied conditions, notably the relatively high temperature of 250°C.



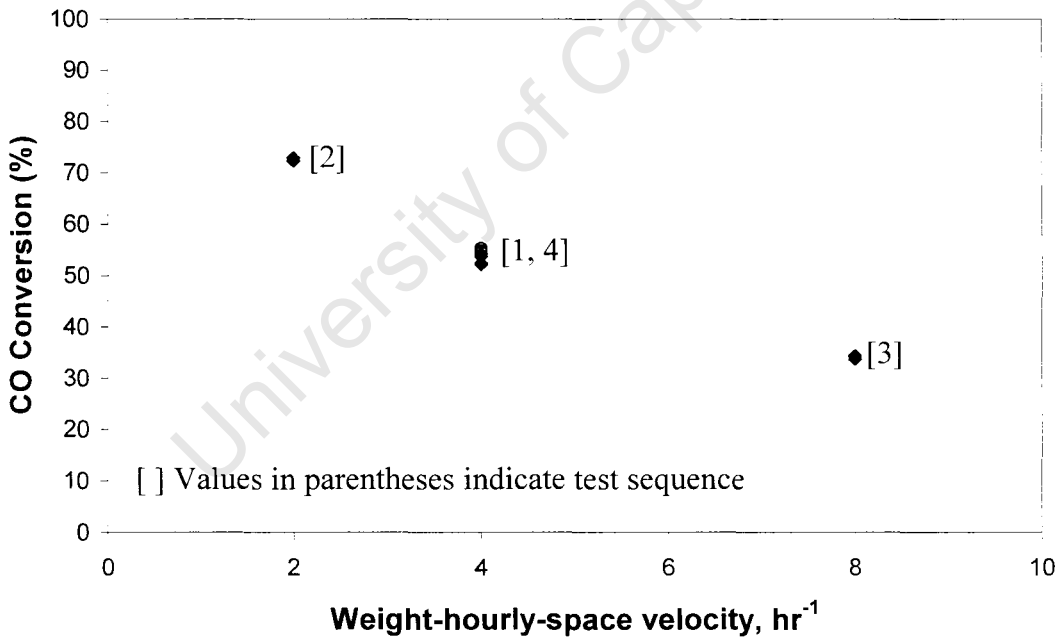


**Figure 5-10: Effect of space velocity on WGC-A ($Au/TiO_2$) at 250°C and otherwise standard conditions (experiment 8)**

### 5.3.4 Effect of Steam: Dry Gas Ratio

The effect of steam/dry gas ratio on CO conversion is shown on figure 5-11 for a constant temperature of 250°C and otherwise standard conditions from which it is apparent that increased steam/dry gas ratio suppresses CO conversion. Numbers in square brackets in figure 5-11 indicate the sequence of the rest conditions applied.

It is important to note, however, that due to the changing total steam flowrate (at fixed dry gas flow rate) in these experiments, overall contact time is decreasing with increasing steam/dry gas ratio in figure 5-15. It is noteworthy that some catalyst deactivation may have occurred as a result of the low steam/dry gas ratio of 0.5:1 (mol/mol).



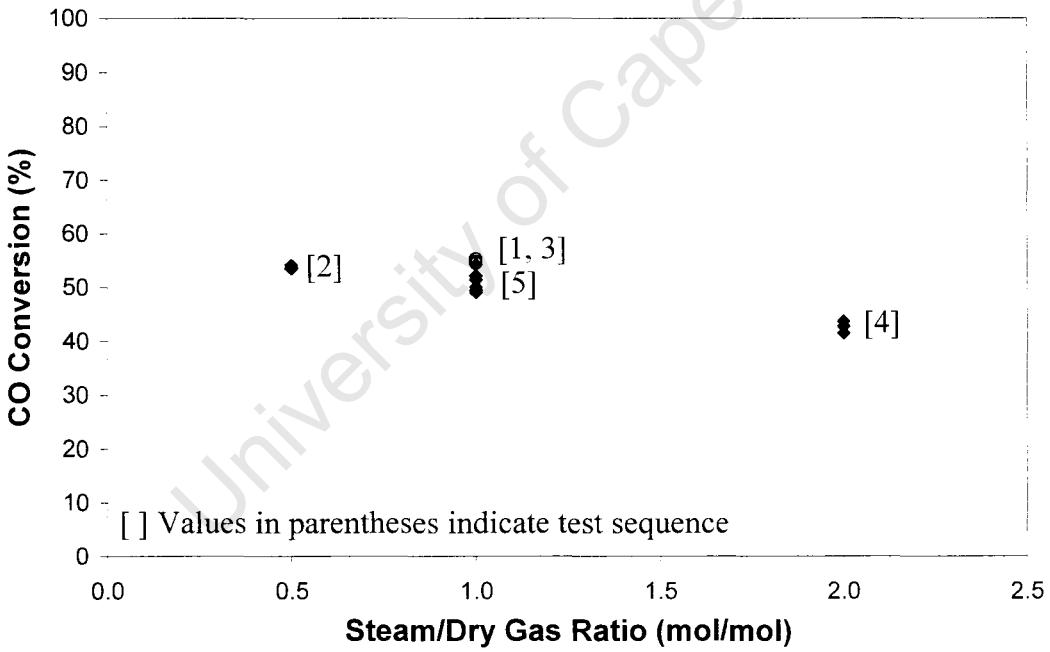


**Figure 5-11: Effect of steam: dry gas ratio of WGC-A ($Au/TiO_2$) at 250°C and otherwise standard conditions (experiment 8)**

### 5.3.5 Effect of Pressure

Increasing the pressure results in increased CO conversion (figure 5-12), contrary to the case for C 18-7 (figure 5-6). No noteworthy evidence could be seen for catalyst deactivation during the pressure series.

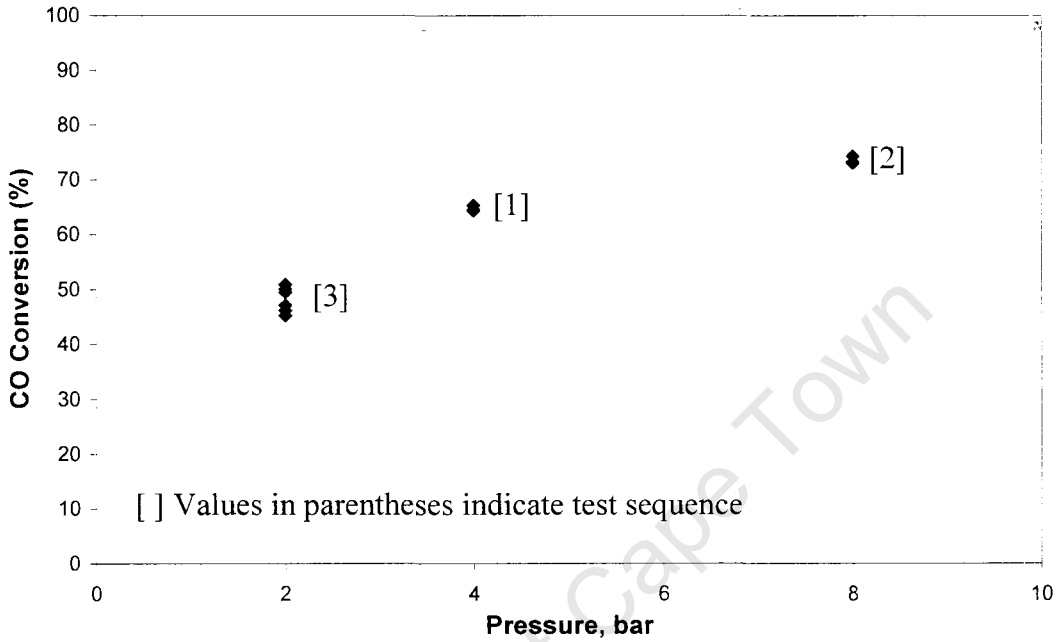


**Figure 5-12: Effect of pressure on WGC-A ($Au/TiO_2$) at 250°C and otherwise standard conditions (experiment 8)**

### 5.3.6 TPR Analysis

As can be seen from figure 5-13, no reduction of the catalyst occurs. This is, however, expected, as Au and $TiO_2$ are both non-reducible species.

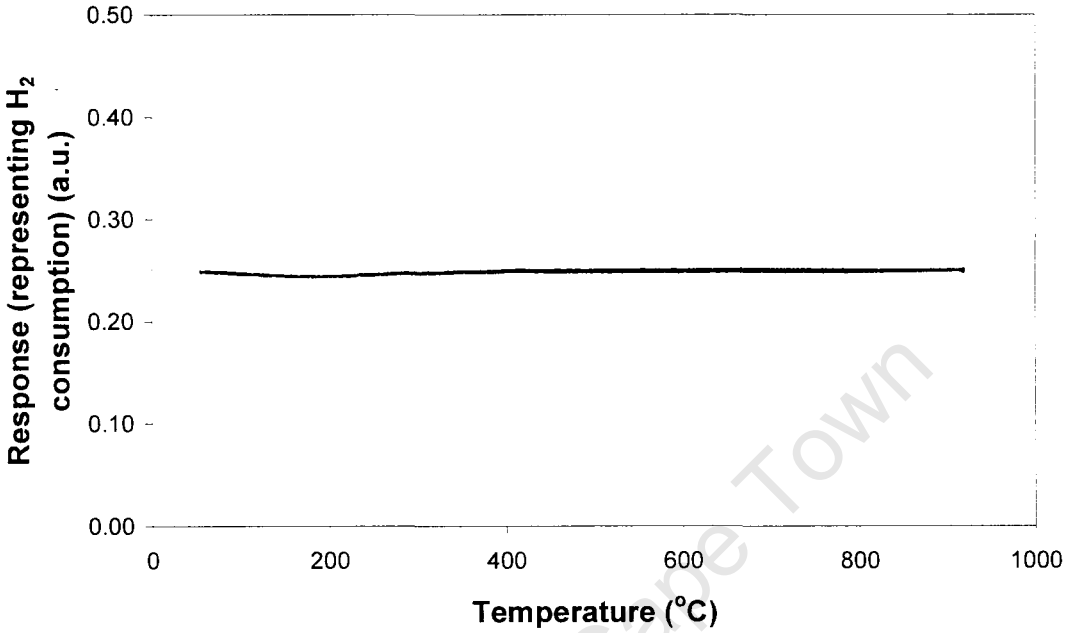


**Figure 5-13: TPR Analysis of WGC-A ($Au/TiO_2$) catalyst**

## 5.4 WGC TYPE B CATALYST – $Au/Fe_2O_3/Al_2O_3$

Two tests were performed on the WGC-B catalyst – the first to determine the effect of temperature until the catalyst was deemed to be deactivated, and the second to evaluate the influence of the remaining parameters (i.e. space velocity, steam/ dry gas ratio and pressure).

### 5.4.1 Initial Deactivation

A similar period of deactivation is seen in the type B gold catalyst (refer to figure 5-14) as in the case of the commercial LTS catalyst, with the initial conversion declining from some 25% to a largely steady value of approximately 16% after two days on stream.

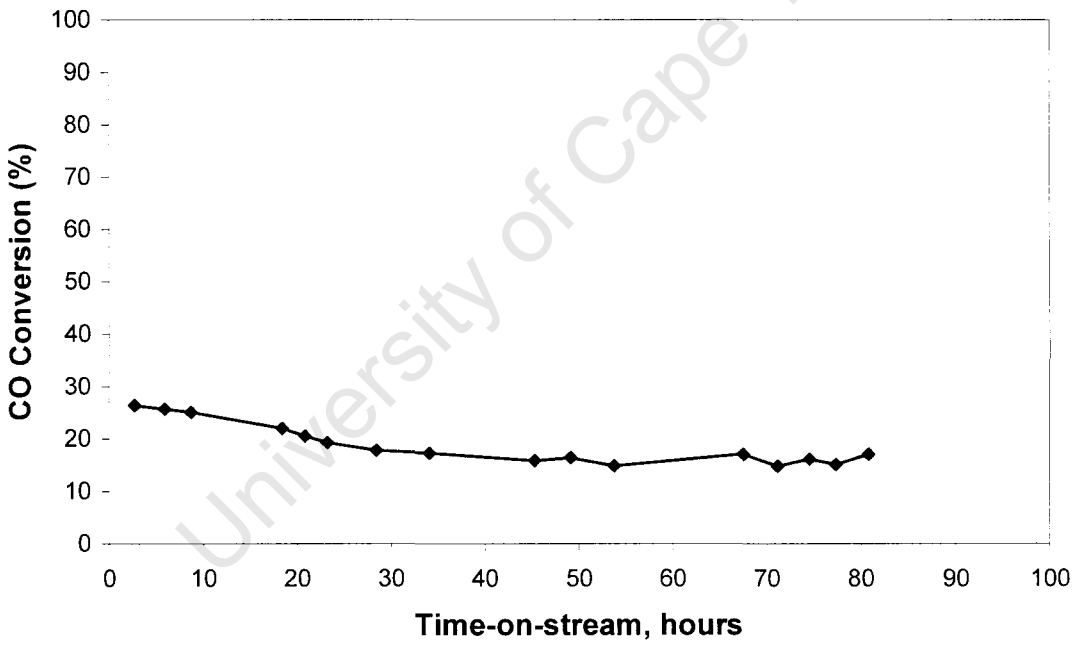


**Figure 5-14: Initial deactivation of WGC-B ($Au/Fe_2O_3/Al_2O_3$) at standard conditions (experiment 3)**

### 5.4.2 Effect of Temperature

CO conversion increases with increasing temperature up to approximately 220°C, however the maximum conversion (20% at 220°C) remains far below the equilibrium level (figure 5-15). Above 220°C, CO conversion decreases gradually with increasing temperature up to 250°C. Already at 250°C, catalyst stability was observed to be declining as shown by the several data points at this temperature in figure 5-15, and collected over a 40 hour period. Subsequent tests at higher temperatures showed little further influence on CO conversion.

Subsequent tests in experiment 4 at 225, 215 and 205°C revealed substantially reduced catalytic activity when compared to the initial CO conversion levels found in experiment 3 in this temperature range (figure 5-15) and suggesting that some irreversible catalyst deactivation is effected at temperatures above 250°C, and possibly even above 220°C.

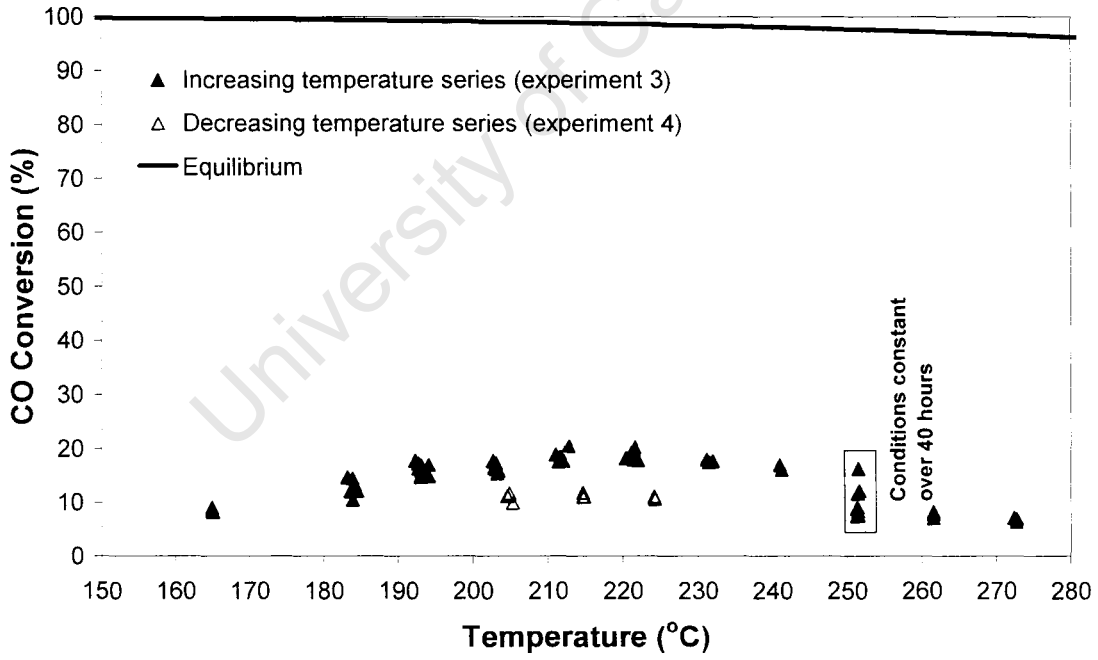


**Figure 5-15: Effect of temperature on WGC-B ($Au/Fe_2O_3/Al_2O_3$) (experiment 3 and 4)**

### 5.4.3 Effect of Space Velocity

As per the case with all catalysts tested, $WHSV_{dry}$ of 2.0, 4.0 and 8.0 $hr^{-1}$ were tested. The findings of these experiments are presented in figure 5-16 where data annotations in square brackets indicate the experimental sequence.

From figure 5-16, a monotomically declining trend in CO conversion with increasing space velocity is apparent, as expected. Moreover, CO conversion remains essentially constant in the range of 15 – 17% at standard conditions throughout the experimental series.

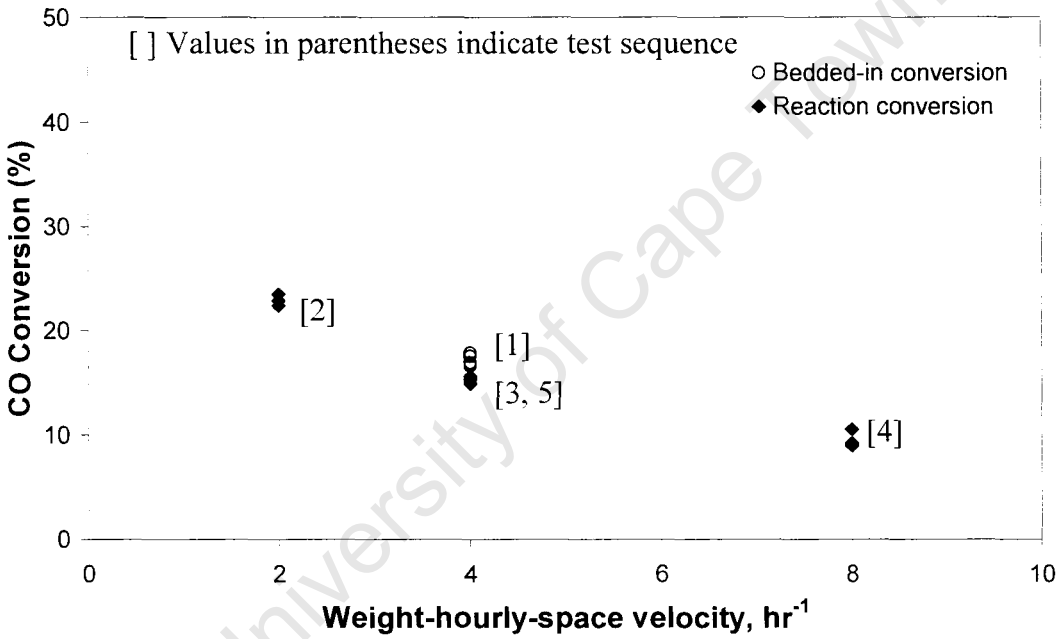


**Figure 5-16: Effect of space velocity on WGC-B ($Au/Fe_2O_3/Al_2O_3$) at 190°C and otherwise standard conditions (experiment 4)**

### 5.4.4 Effect of Steam: Dry Gas Ratio

The results of a series of experiments at varying steam/dry gas ratio are presented in figure 5-17 where data annotations in square brackets indicate the experimental sequence. By and large, in going from a molar steam/dry gas ratio of 1 to 2 and back to 1 again, shows little effect on conversion. However, at the lower steam/dry gas ratio of 0.5 mol/mol, CO conversion is reduced and, moreover, on subsequently re-establishing standard conditions (i.e. steam/dry gas = 1), catalyst activity appears slightly depressed as compared to previous levels.

It is important to note, however, that due to the changing total steam flowrate (at fixed dry gas flow rate) in these experiments, overall contact time is decreasing with increasing steam/dry gas ratio in figure 5-17.

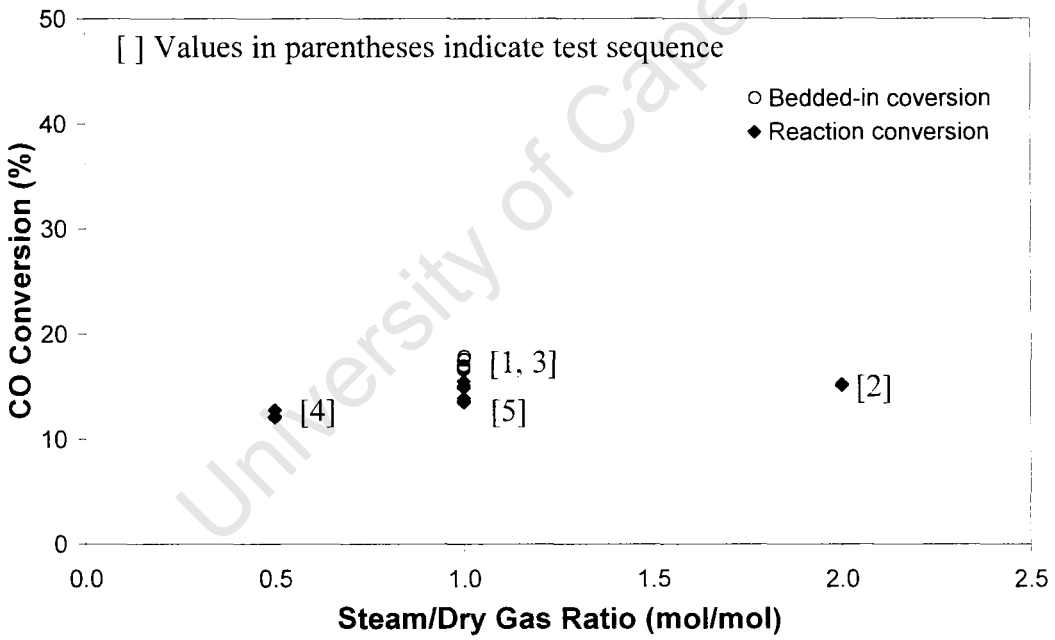


**Figure 5-17: Effect of steam: dry gas ratio on WGC-B ($Au/Fe_2O_3/Al_2O_3$) at 190°C and otherwise standard conditions (experiment 4)**

### 5.4.5 Effect of Pressure

From figure 5-18, it can be seen that in the case of the WGC-B gold catalyst, an increase in pressure results in an increase in CO conversion. At standard conditions (2 bar pressure), CO conversion levels before and after the experimental series are 14% and 11% respectively.

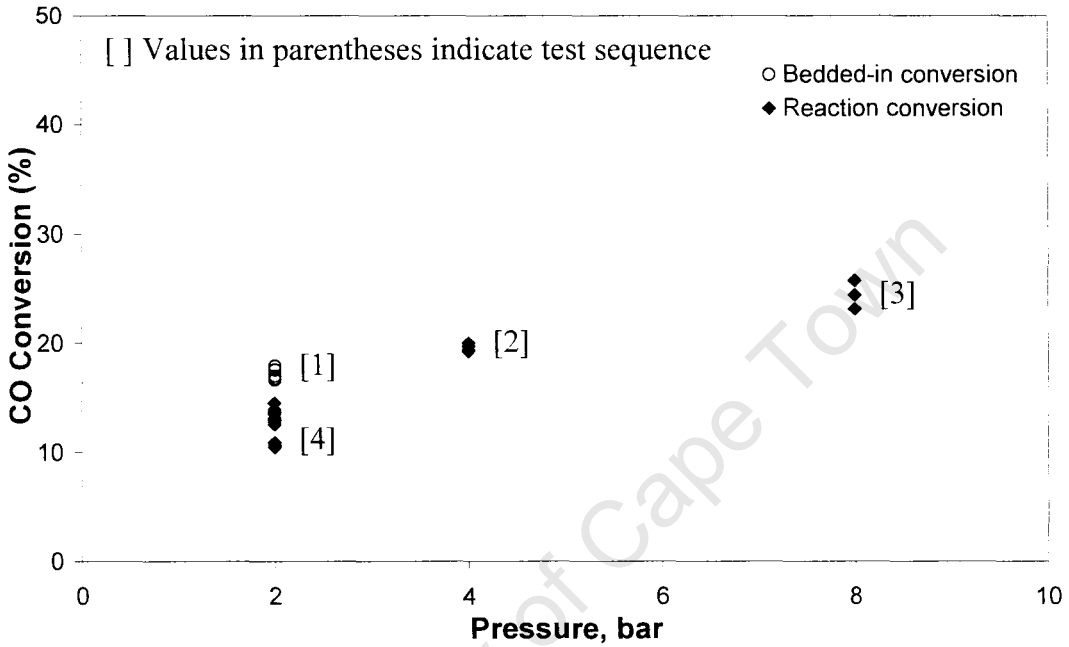


**Figure 5-18: Effect of pressure on WGC-B ($Au/Fe_2O_3/Al_2O_3$) at 190°C and otherwise standard conditions (experiment 4)**

### 5.4.6 TPR Analysis

The TPR analysis of WGC-B ($Au/Fe_2O_3/Al_2O_3$) yielded no positive results due to the low loading of Au (0.3 wt%) and relative low loading of $Fe_2O_3$ (11.6 wt%). It is however unclear whether to attribute the apparent peak at 600°C to the reduction of the iron species or to drift. It should also be noted that the drop in response at the end of the temperature range is due to the end of the ramping of the temperature in the experiment.

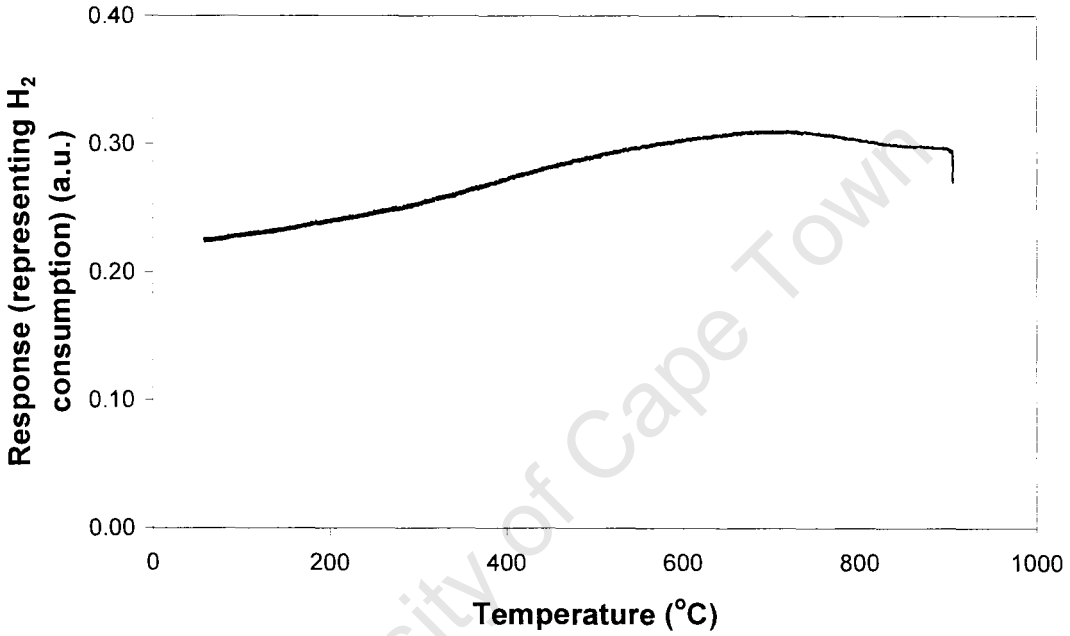


**Figure 5-19: TPR Analysis of WGC-B ($Au/Fe_2O_3/Al_2O_3$) catalyst**

## 5.5 WGC TYPE C CATALYST – $Au/Fe_2O_3$

Due to the very pronounced deactivation with time-on-stream, it was necessary to conduct three separate experimental series on the $Au/Fe_2O_3$ (WGC-C) catalyst.

### 5.5.1 Deactivation of Catalyst

Figure 5-20 presents the time-on-stream performance of the WGC-C catalyst at standard conditions, from which it is clearly seen that the catalyst deactivates rapidly and continuously. The experiment was terminated when 50% CO conversion was reached after approximately 200 hours on stream.

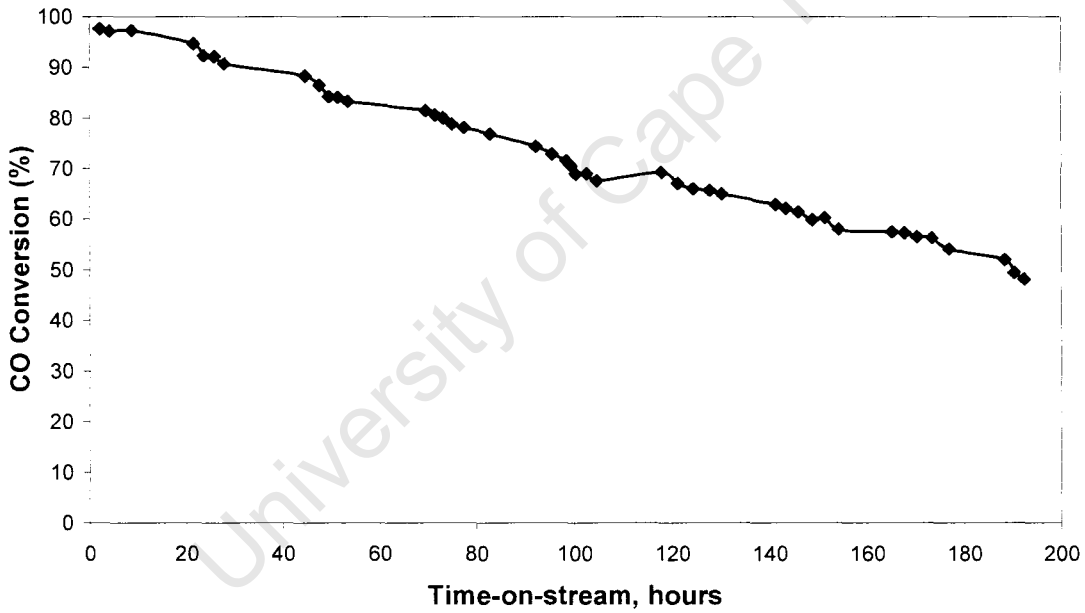




**Figure 5-20: Deactivation of WGC-C ($Au/Fe_2O_3$) at standard conditions (experiment 5)**

### 5.5.2 Effect of Temperature

Given the observed rapid deactivation of the $Au/Fe_2O_3$ catalyst (figure 5-20), the effect of temperature was evaluated on a fresh catalyst charge starting after 92 hours on stream at standard conditions and shown in figure 5-21 by the open symbol. This initial CO conversion of approximately 80% is consistent with the same value after 92 hours in experiment 5 (figure 5-20). The temperature was subsequently reduced to 130°C and the increasing temperature series collected over approximately a further 100 hours on stream (until 235°C), reaching the initial temperature condition of 195°C some 70 hours after initiating the series. The deactivation was further proved as, when the temperature was returned to 175 and 195°C respectively, the CO conversion was approximately 15% lower (not shown in figure 5-21)

As expected, CO conversion increases with increasing temperature, however, reaching a maximum at approximately 215°C, above which the conversion declines. It is significant that the series CO conversion level at 195°C (solid symbol in figure 5-21), although lower than the starting level at this temperature (open symbol in figure 5-21), is much less depressed than may have been expected based on a 70 hour time-on-stream interval between data collection. Indeed, based on figure 5-20, a CO conversion level closer to 65% is evident at 160 hours time-on-stream (i.e. 70 hours after the 92 hour starting point). This lower deactivation apparent from the above in figure 5-21 may, however, be ascribed to the ensuing 70 hour interim period accruing at average temperatures significantly lower than the standard condition of experiment 5 (figure 5-21). Similarly, above 215°C, deactivation becomes rapid (figure 5-21). Importantly, the conversion-temperature performance up to 200°C may be considered a true measure of the performance for the WGC-C ($Au/Fe_2O_3$) catalyst after approximately 100 hours on stream at otherwise standard conditions.

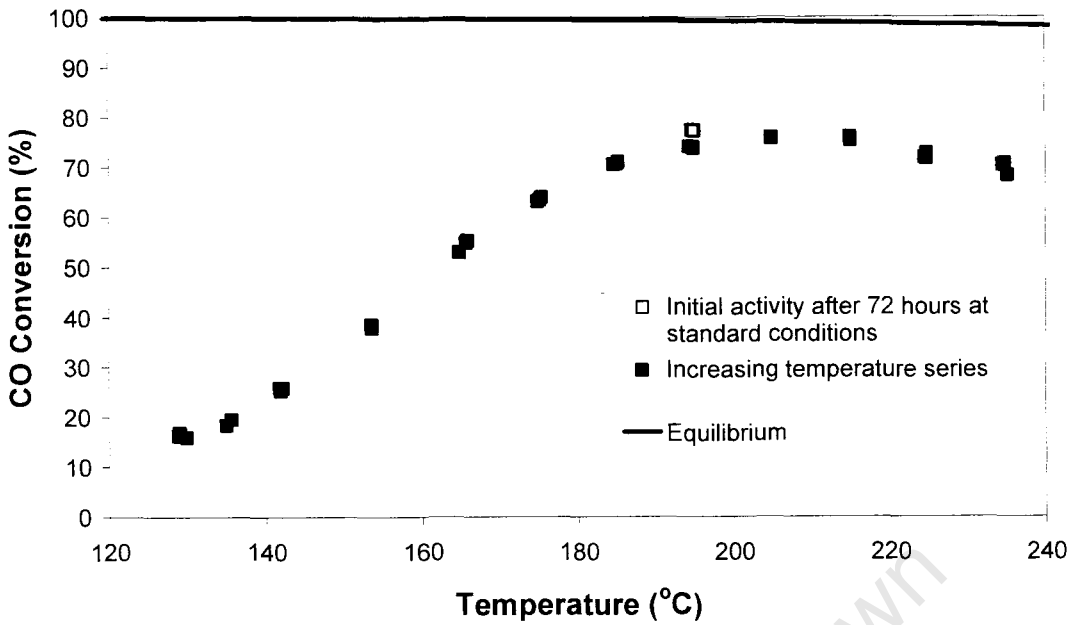


**Figure 5-21: Effect of temperature on WGC-C ($Au/Fe_2O_3$) at otherwise standard conditions (experiment 6)**

### 5.5.3 Effect of Pressure

In a fresh test series (experiment 7), the influence of pressure, space velocity, and steam/dry gas ratio were evaluated sequentially after the same bedding-in period of 92 hours at standard conditions as per experiment 6. However, in order to avoid equilibrium control, the pressure, space velocity and steam/dry gas tests were conducted at 165°C. The initial CO conversion at this condition at the start of the pressure test series was 40% (open symbol in figure 5-19).

As with the type B gold catalyst, CO conversion increased with increasing pressure. It can further be seen that some deactivation occurs during the experimental series.

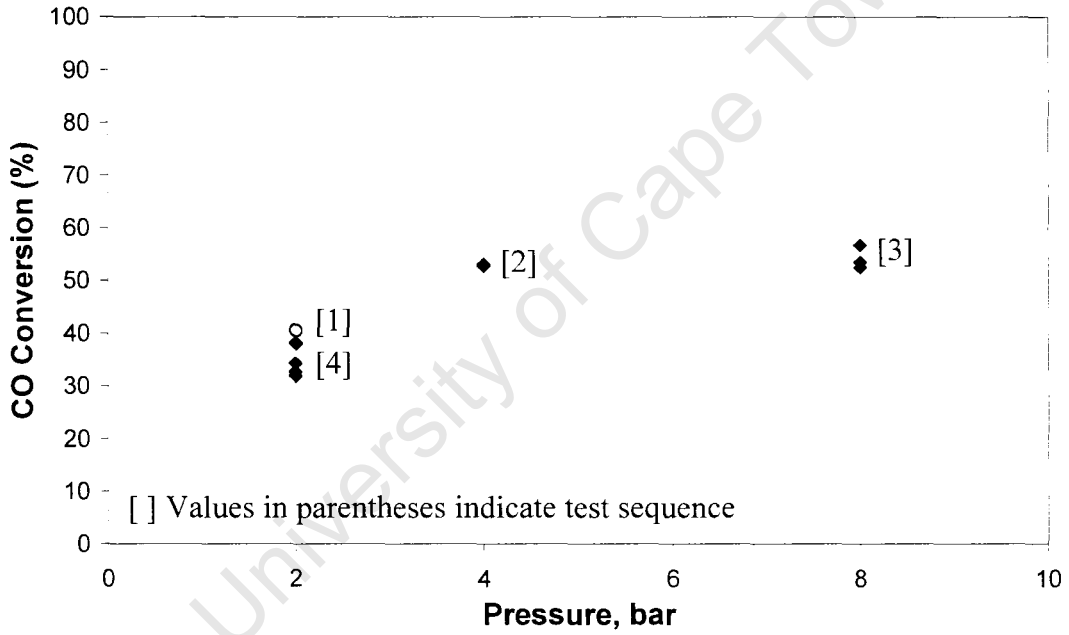


**Figure 5-22: Effect of pressure on WGC-C ($Au/Fe_2O_3$) at 165°C and otherwise standard conditions (experiment 7)**

### 5.5.4 Effect of Space Velocity

The influence of space velocity is shown in figure 5-23 for the WGC-C ($Au/Fe_2O_3$) catalyst. Although the standard catalyst activity at 165°C is significantly lower than that for the earlier pressure series, the catalyst does not deactivate to any significant extent during the space velocity tests. CO conversion declines monotonically with increasing space velocity as expected.

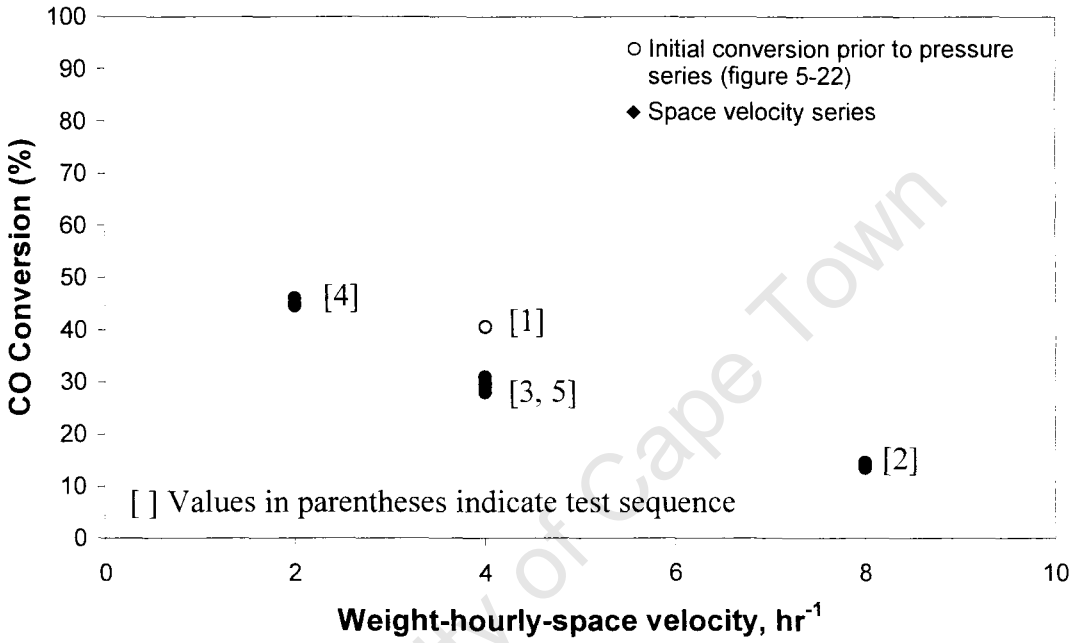


**Figure 5-23: Effect of space velocity on WGC-C ($Au/Fe_2O_3$) at 165°C and otherwise standard conditions (experiment 7)**

### 5.5.5 Effect of Steam: Dry Gas Ratio

The effect of increasing steam/dry gas ratio is to increase CO conversion as expected (see figure 5-24).

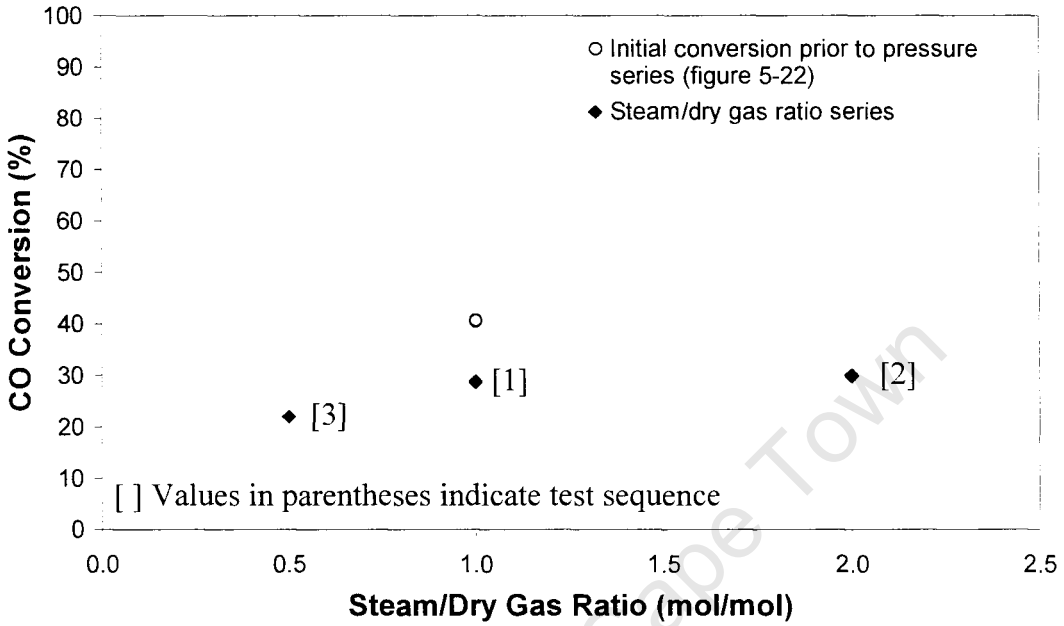


**Figure 5-24: Effect of steam: dry gas ratio on WGC-C ($Au/Fe_2O_3$) at 165$^0$C and otherwise standard conditions (experiment 7)**

### 5.5.6 TPR Analysis

From figure 5-25, the TPR analysis of WGC-C shows that the first peak is seen at approximately 260°C, with subsequent peaks at 620 and 720°C. The first peak can be attributed to the reduction of $Fe_2O_3$ to $Fe_3O_4$, while the high temperature peaks denote the reduction of $Fe_3O_4$ to metallic Fe. Further analysis of the TPR results can be seen in section 6.2.

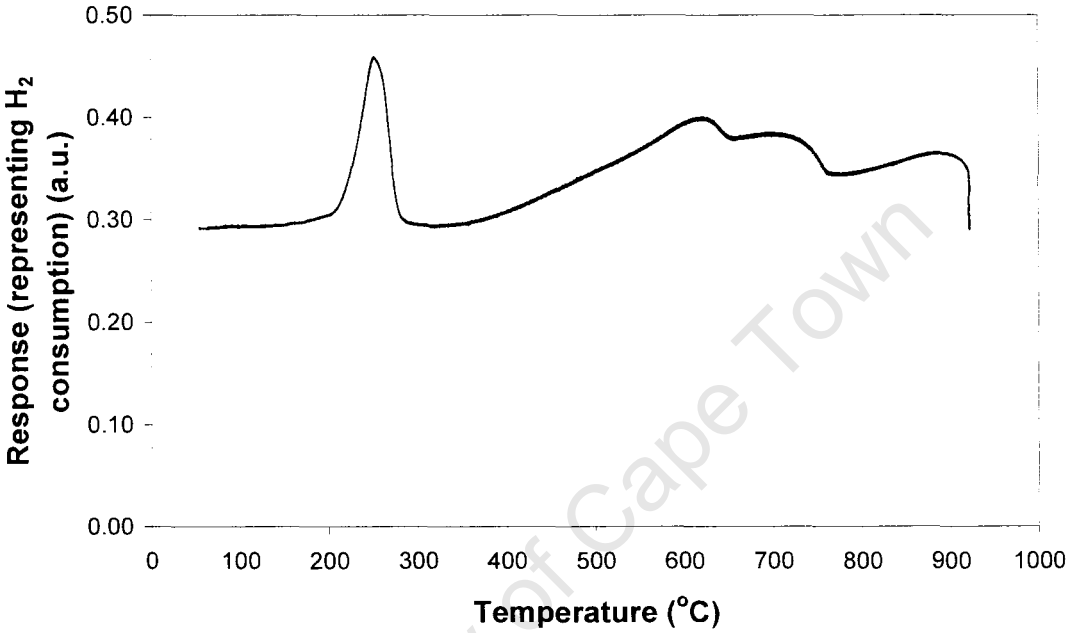


**Figure 5-25: TPR Analysis of WGC-C ($Au/Fe_2O_3$) catalyst**

# 6 DISCUSSION

## 6.1 INFLUENCE OF REACTION VARIABLES

### 6.1.1 Temperature

All of the catalysts tested exhibited similar trends under the same reaction conditions, but the changes in activity varied with each catalyst. For example, the conversion of CO increased with temperature for all catalysts tested but the commercial LTS catalyst and WGC-A exhibited greater changes with temperature as opposed to the gold promoted iron catalysts.

It should also be noted that although the conversion of CO over the commercial LTS catalyst approached the equilibrium conversion, it did not reach equilibrium. WGC-A also approached equilibrium but whether equilibrium would be reached was not investigated. This was due to the temperature of the reaction at the highest CO conversion (77 % at 315°C) over this catalyst being higher than that of the highest temperature tested over the other catalysts, in this case, 285°C over WGC-B (experiment 3). These results can be seen in figure 6-1 which shows the temperature dependency of all the catalysts tested using the averages of the data obtained.



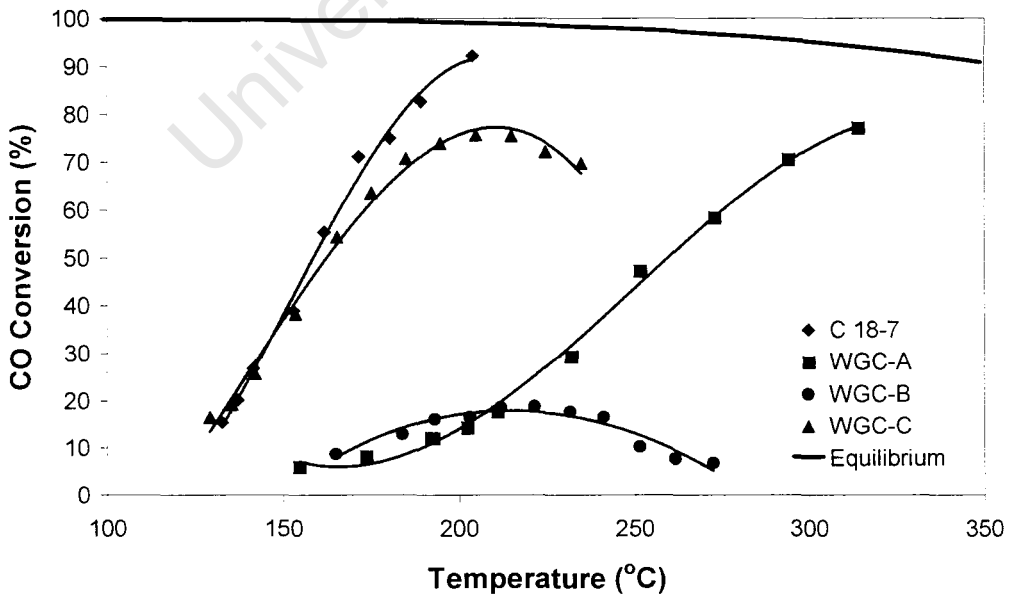


**Figure 6-1: Influence of Temperature on all catalysts tested**

### 6.1.2 Pressure

The changes in CO conversion with changing pressure differed in the commercial LTS catalyst as opposed to the gold-promoted reference catalysts. Increased pressure resulted in an increase in the CO conversion over the WGC reference catalysts, but the conversion of CO decreased with increasing pressure over the commercial LTS catalyst (refer to figure 6-2). This was due to the rate of reaction being inversely proportional to the pressure (Twigg, 1989). However, these decreases in activity were fairly small, as can be seen from the decrease from 48% to 43% when the pressure is increased from 2 bar to 8 bar. The increased activity over the gold-promoted suggests that the rate of reaction was proportional to the operating pressure. It also suggests that an improved activity can be achieved when operating under elevated pressures.

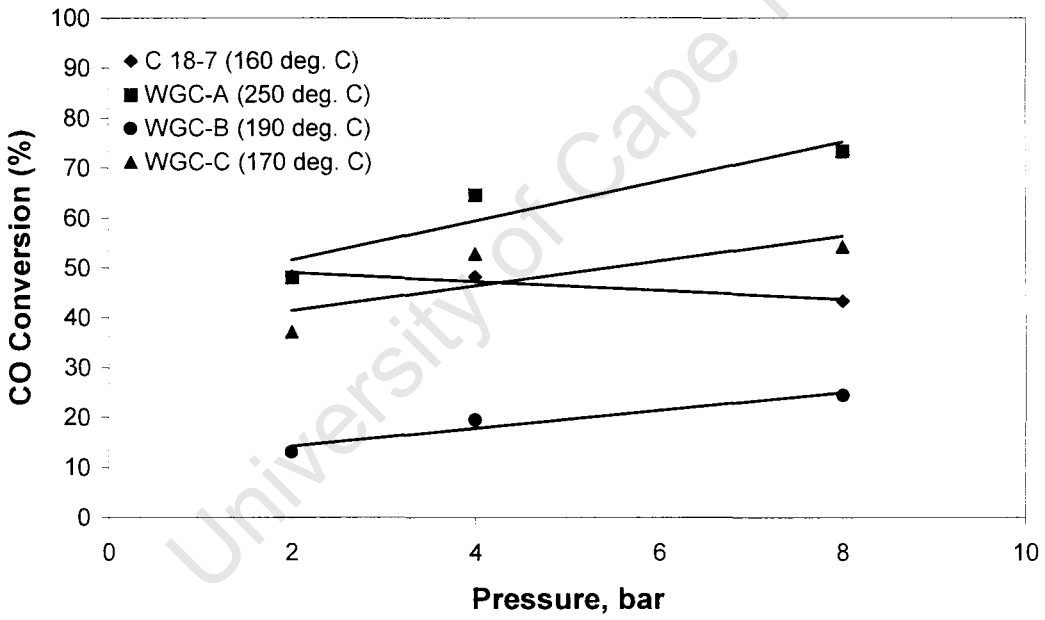




**Figure 6-2: Influence of pressure on catalysts tested (temperature at which catalyst tested in brackets)**

### 6.1.3 Steam/ Dry Gas Ratio

Increasing the steam/ dry gas ratio resulted in increased CO conversion, and conversely, a decreased ratio resulted in decreased CO conversion. This was the case

with C 18-7, WGC-C and WGC-B, but the opposite trend was seen on WGC-A. This can be seen in figure 6-3, using the averages of the data obtained.

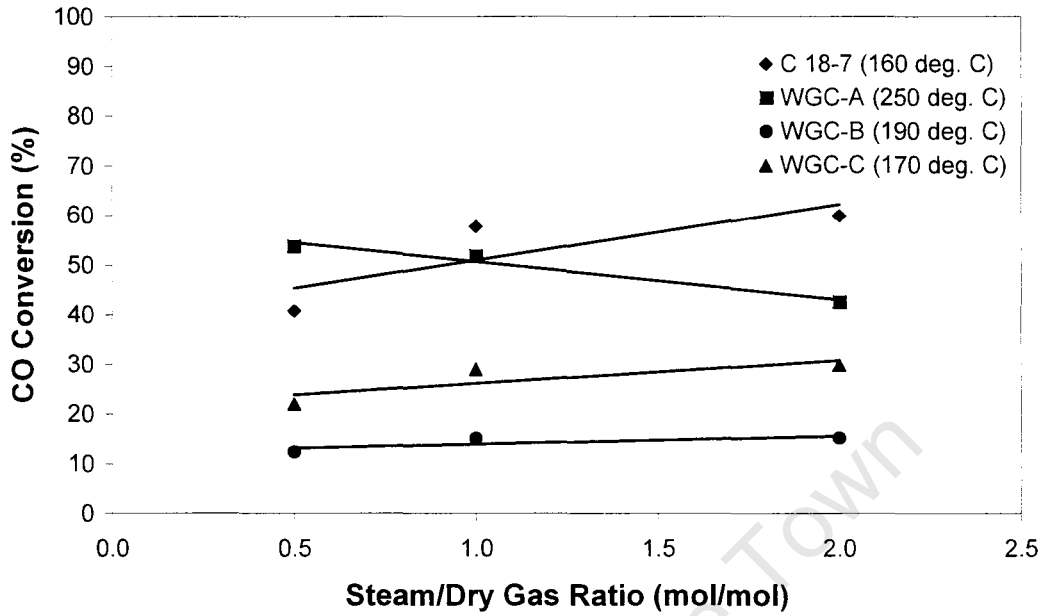


**Figure 6-3: Influence of Steam: Dry gas ratios on catalysts tested (temperature at which catalyst tested in brackets)**



However, changing the steam/ dry gas ratio caused some problems with respect to the state of the catalyst, in particular after the catalyst is exposed to decreased water levels. Upon returning to standard conditions, the resultant CO conversion was lower than that found earlier in the time-on-stream period at the same conditions. This relative decrease in activity was more evident after tests on the lower steam/ dry gas ratio were performed.

### 6.1.4 Space Velocity

The catalysts tested all reacted as expected when exposed to changing space velocities, i.e., higher conversion was observed with lower space velocity and vice versa. Also, no marked catalyst deactivation was observed with the experiments.

## 6.2 CATALYST STABILITY

WGC-C, iron oxide with a 5 wt % Au loading, produced the highest CO conversion (~77%) of all the WGC catalysts tested at standard conditions i.e. T=195°C, P = 2 bar, WHSV = 4.0 $hr^{-1}$ and steam: dry gas = 1:1. This result compared favourably with the activity determined by Andreeva and colleagues (Andreeva *et al*, 1996b, 1998a), where CO conversions of above 80% were obtained using 3 wt% $Au/Fe_2O_3$ prepared by deposition-precipitation, at 200°C, space velocity of 4000 $hr^{-1}$ and steam/ dry gas ratio of 0.7 in a stream containing 4.88 vol% CO.

When testing the WGC-C catalyst up to 215°C, it was thought that a steady state conversion had been reached. However, the catalyst then experienced a constant deactivation with time, and as a result, a steady state condition was never again reached. It was discovered in subsequent tests performed on this catalyst that this deactivation was evident in all experiments. As a result, the subsequent CO conversions obtained were slightly lower than they should have been if no deactivation occurred. No such time-on-stream deactivation was observed with C 18-7 and WGC-A while WGC-B experienced deactivation with the temperature elevated to above 215°C.

These differences in stability can also be attributed to the reduction of the catalysts. As mentioned in chapter 4, all the catalysts were pre-reduced at 200°C. As WGC-A is non-reducible, it is found to be very stable at elevated temperatures. From figure 5-7, it is seen that a double peak is observed at approximately 200°C. This indicates the reduction of copper in C 18-7. No further reduction is seen at higher temperatures and it can be assumed that this catalyst would also be stable at higher temperatures. However, the maximum temperature tested on C 18-7 was 200°C. No significant reduction was seen on WGC-B as it is predominantly composed of $Al_2O_3$ and due to the low gold loading.

However, WGC-C was found to be reducible, with the reduction being attributed to the reduction of the Fe species. The results also compared favourably to that of Venugopal and Scurrell (2004) on 3 wt% Au on $Fe_2O_3$ (refer to figure 5-25). Peaks associated with the reduction of iron were found at approximately 250°C, 620°C and 720°C. The final 2 peaks were attributed to the reduction of magnetite ($Fe_3O_4$) to metallic iron, while the lower temperature peak, when reducing bulk $Fe_2O_3$, was attributed to the reduction of hematite to magnetite. On the gold-promoted catalyst tested by Venugopal and Scurrell, 2 low temperature peaks were found, 1 attributed to the reduction stated above ($Fe_2O_3$ ➔ $Fe_3O_4$) and the other to the reduction of an $Au_xO_y$ species. In the case of the WGC catalyst, only 1 low temperature peak at 250°C was found. Whether the reduction of a gold species occurs in this case has yet to be determined.

## 6.3 COMPARATIVE PERFORMANCE OF CATALYSTS

The rate data obtained from the catalyst tests at standard conditions can be seen in table 6-1. It can be seen that WGC-B has the highest reaction rate of the WGC catalysts when the data is calculated with respect to the gold loading. The reaction rate per mol metal (Au vs Cu) is also determined to be greater than that of C 18-7. However, as the Au loading (0.3 wt %) is approximately 100 times smaller than that of the Cu loading (33.6 wt %) in C 18-7, this comparison is of limited meaning.

When considering the rates with respect to the total catalyst loading (i.e. 1 g), C 18-7 has the highest reaction rate. Sakurai *et al* (1997) quoted the reaction rate of a LTS catalyst to be 5 times greater than that of co-precipitated $Au/Fe_2O_3$ with a 5 % gold loading. However, these were at 100°C and conversions of below 20%. It is interesting to note that the reaction rate of WGC-C is comparable to that of C 18-7 in this instance.

**Table 6-1: Rate Data at Standard Conditions and Activation Energies**

| Catalyst | Rate ($g_{CO}/g_{Au}.s$) | Rate ($g_{CO}/g_{catalyst}.s$) *1000 | $E_A$ (kJ/mol) |
|---|---|---|---|
| C 18-7 | 0.234 | **78.68** | 72.7 |
| WGC-A | 0.719 | 10.79 | 32.9 |
| WGC-B | **4.718** | 14.15 | 23.7 |
| WGC-C | 1.385 | **69.23** | 47.5 |

Using the rate data, activation energies were calculated for each case and can also be seen in table 6-1. The activation energies of the WGC catalysts compare favourably with that of Sakurai *et al* (1997). However, the activation energies determined for the LTS catalyst in the same study as well as by Choi *et al* (2003) was much lower than that calculated in this study.

The final comparison of the data used in this study is to look at the temperatures for CO conversions of 20, 50 and 75%, respectively, at standard conditions. From table 6-2, it can be seen that WGC-C is on par with C 18-7 at low conversion (i.e. 20%). At the higher conversions, C 18-7 exhibits the greatest activity. WGC-A once again shows comparative results which would imply that WGC-A would make a very good water-gas shift catalyst in the low- to medium-shift temperature range. Catalyst deactivation would need to be considered before using a particular catalyst, and as WGC-C showed a trend of constant deactivation (refer to section 6.2), it would not make an effective catalyst at this stage.

**Table 6-2: Temperature and Conversion Data at standard conditions**

| Catalyst | $T_{X=20\%}$ (°C) | $T_{X=50\%}$ (°C) | $T_{X=75\%}$ (°C) |
|---|---|---|---|
| C 18-7 | 137 | **156** | **176** |
| WGC-A | 215 | 257 | 308 |
| WGC-B | 220* | - | - |
| WGC-C | **136** | 162 | 191 |

* The maximum conversion attained with WGC-B was 19%

# 7 CONCLUSION

This work has successfully completed comparing the performance of the three reference World Gold Council catalysts in the water-gas shift reaction to that of the commercially used low temperature shift catalyst, i.e. C 18-7 ($Cu/ZnO/Al_2O_3$). This comparison entailed the testing of the activity of all catalysts with changes in temperature, space velocity, steam/ dry gas ratio and operating pressure.

Of the gold reference catalysts tested at the standard operating conditions, it was found that WGC-C ($Au/Fe_2O_3$) was the most active. However, it was discovered that this catalyst deactivated with time. It should also be noted that, at the standard operating conditions, C 18-7 produced the highest activity of all the catalyst tested.

WGC-B ($Au/Fe_2O_3/Al_2O_3$) had the lowest overall activity – the maximum conversion obtained was 20% – and deactivation was experienced at above 220°C.

WGC-A ($Au/TiO_2$) produced the most favourable results. Although the activity at standard conditions was low, the catalyst exhibited large changes in activity with increased temperature. This indicates that catalyst could yield favourable results if utilised in a single stage water-gas shift operation in the medium temperature range of 250 to 350°C. This catalyst was also found to be the most stable when subjected to varying reaction conditions.

Another important conclusion obtained from this study was that, unlike C 18-7, increased pressure favours the conversion of CO in all Au-based catalysts evaluated.

It is recommended that future work undertaken on the WGC-A gold reference catalyst include testing in the medium and high temperature shift range and at elevated pressures.

# 8 REFERENCES


Andreeva, D., Idakiev, V., Tabakova, T. & Andreev, A., Low-Temperature Water-Gas Shift Reaction over Au/α-$Fe_2O_3$, *Journal of Catalysis* **158** (1996a) 354 – 355

Andreeva, D., Idakiev, V., Tabakova, T. & Andreev, A. & Giovanoli, R., Low-Temperature Water-Gas Shift Reaction on Au/α-$Fe_2O_3$, *Applied Catalysis A: General* **134** (1996b) 275 – 283

Andreeva, D., Tabakova, T., Idakiev, V., Christov, P. & Giovanoli, R., Au/α-$Fe_2O_3$ catalyst for water-gas shift reaction prepared by deposition-precipitation, *Applied Catalysis A: General* **169** (1998a) 9 – 14

Andreeva, D., Tabakova, T., Idakiev, V. & Giovanoli, R., Low-Temperature Water-Gas Shift Reaction on Au/$TiO_2$, Au/α-$Fe_2O_3$, and Au/$Co_3O_4$, *Bulgarian Chemical Communications*, Vol. 30 Numbers 1-4 (1998b) 59 – 67

Andreeva, D., Low Temperature Water Gas Shift over Gold Catalysts, *Gold Bulletin* **35** 3 (2002a) 82 – 88

Andreeva, D., Idakiev, V., Tabakova, T., Ilieva, L., Falaras, P., Bourlinos, A. & Travlos, A., Low-temperature water-gas shift reaction over Au/$CeO_2$ catalysts, *Catalysis Today* **72** (2002b) 51 – 57

Boccuzzi, F., Chiorino, A., Manzoli, M., Andreeva, D. & Tabakova, T., FTIR Study of the Low-Temperature Water-Gas Shift Reaction on Au/$Fe_2O_3$ and Au/$TiO_2$ Catalysts, *Journal of Catalysis* **188** (1999) 176 – 185

Bocuzzi, F., Chiorino, A., Manzoli, M., Andreeva, D., Tabakova, T., Ilieva, L. & Iadakiev, V., Gold, silver and copper catalysts supported on $TiO_2$ for pure hydrogen production, *Catalysis Today* **75** (2002) 169–175

Boccuzzi, F., Chiorino, A. & Manzoli, M., FTIR Study of Methanol Decomposition, *Journal of Power Sources*, **118** (2003) 304 - 310

Bond, G., The Catalytic Properties of Gold (Potential applications in the chemical industry), *Gold Bulletin* **5** (1972) 11 – 13

Bond, G. & Thompson, D., Catalysis by Gold, *Catalysis Reviews – Science & Engineering* **41** 3&4 (1999) 319 – 388

Bond, G. & Thompson, D., Gold-Catalysed Oxidation of Carbon Monoxide, *Gold Bulletin* **33** 2 (2000) 41 – 51

Cameron, D., Holliday, R. & Thompson, D., Gold's Future Role in Fuel Cell Systems, *Journal of Power Sources*, **118** (2003) 298 – 303

Chen, B., Bai, C., Cook, R., Wright, J. & Wang, C., Gold/cobalt oxide catalysts for oxidative destruction of dichloromethane, *Catalysis Today* **30** (1996) 15 - 20

Corto, C.W., Holliday, R.J. & Thompson, D.T., Commercial aspects of gold catalysis, *Applied Catalysis A: General* **291** (2005) 253 - 261

Costello, C, Kung, M., Oh, H., Wang, Y. & Kung, H., Nature of the active site for CO oxidation on highly active Au/$\gamma$-$Al_2O_3$, *Applied Catalysis A: General* **232** (2002) 159 – 168

Daté, M., Ichihashi, T., Yamashita, T., Chiorino, A., Boccuzzi, F. & Haruta, M., Performance of Au/$TiO_2$ catalyst under ambient conditions, *Catalysis Today* **72** (2002) 89 – 94

Debeila, M., Coville, N., Scurrell, M. & Hearne, G., DRIFTS studies of the interaction of nitric oxide and carbon monoxide on Au-$TiO_2$, *Catalysis Today* **72** (2002) 79 – 87

Deng, W., De Jesus, J., Saltsburg, H. & Flytzani-Stephanopoulos, M., Low-content gold-ceria catalysts for the water-gas shift and preferential CO oxidation reactions, *Applied Catalysis A: General* **291** (2005) 126 – 135

Edwards, N., Ellis, S.R., Frost, J.C., Golunski, S.E., van Keulen, A.N.J., Lindewald, N.G. & Reinkingh, J.G., On-board hydrogen generation for transport applications: the HotSpot methanol processor, *Journal of Power Sources* **71** (1998) 123 - 128

Fu, Q., Kudriavtseva, S., Salstburg, H. & Flytzani-Stephanopoulos, M., Gold-ceria catalysts for low-temperature water-gas shift reaction, *Chemical Engineering Journal* **93** (2003a) 41 – 53

Fu, Q., Saltsburg, H. & Flytzani-Stephanopoulos, M., Active Nonmetallic Au and Pt Species on Ceria-Based Water-Gas Shift Catalysts, *Science* **301** (2003b) 935 – 938

Fu, Q., Deng, W., Saltsburg, H. & Flytzani-Stephanopoulos, M., Activity and stability of low-content gold-cerium oxide catalysts for the water-gas shift reaction, *Applied Catalysis B; Environmental* **56** (2005) 57 – 68

Goerke, O., Pfeifer., P. & Schubert, K., Water gas shift reaction and selective oxidation of CO in microreactors, *Applied Catalysis A: General* **263** (2004) 11 – 18

Gorte, R.J. & Zhao, S., Studies of the water-gas-shift reaction with ceria-supported precious metals, *Catalysis Today* **104** (2005) 18 – 24

Guczi, L., Horváth, D., Pászti, Z. & Petõ, G., Effect of treatments on gold nanoparticles: Relation between morphology, electron structure and catalytic activity in CO oxidation, *Catalysis Today* **72** (2002) 101 – 105

Haruta, M., Kobayashi, T., Sano, H. & Yamada, H., Novel gold catalysts for the oxidation o carbon monoxide at a temperature far below 0°C, *Chemistry Letters* **829** (1987) 405 – 408

Haruta, M., Yamada, N., Kobayashi, T. & Iijima, S., Gold Catalysts Prepared by Coprecipitation for Low-Temperature Oxidation of Hydrogen and of Carbon Monoxide, *Journal of Catalysis* **115** (1989) 301 – 309

Haruta, M., Ueda, A., Tsubota, S. & Torres Sanchez, R., Low-temperature catalytic combustion of methanol and its decomposed derivatives over supported gold catalysts, *Catalysis Today* **29** (1996) 443 – 447

Haruta, M., Size- and support-dependency in the catalysis of gold, *Catalysis Today* **36** (1997) 153 – 166

Haruta, M. & Daté, M., Advances in the catalysis of Au nanoparticles, *Applied Catalysis A: General* **222** (2001) 427 – 437

Hölzle, M., Intelligent chemistry without combustion – the fuel cell en route to being the energy converter of the future, 2001, Electronic http://www.basf.de/basf/html/d/kampagne/imagekampagne/pdf/necar5engl.pdf Accessed: 14 May 2003

Hua, J., Wei, K., Zheng. Q. & Lin., X., Influence of Calcination Temperature on the Structure and Catalytic Performance of Au/iron Oxide Catalysts **259** (2004) 121 - 130

Hutchings, G., Gold catalysis in chemical processing, *Catalysis Today* **72** (2002) 11 – 17

Idakiev, V., Tabakova, T., Yuan, Z.-Y. & Su, B.-L., Gold Catalysts Supported on Mesoporous Titania for Low-Temperature Water-Gas Shift Reaction, *Applied Catalysis A: General* **270** (2004) 135 - 141

Iizuka, Y., Fujiki, H., Yamauchi, N., Chijiiwa, T., Arai, S., Tsubota, S. & Haruta, M., Adsorption of CO on gold supported on $TiO_2$, *Catalysis Today* **36** (1997) 115 – 123

Iizuka, Y., Tode, T., Takao, T., Yatsu, K., Takeuchi, T., Tsubota, S. & Haruta, M., A Kinetic and Adsorption Study of CO Oxidation over Unsupported Fine Gold Powder and over Gold Supported on Titanium Dioxide, *Journal of Catalysis* **187** (1999) 50 - 58

Ilieva, L., Andreeva, D. & Andreev, A., TPR and TPD investigation of Au/α-$Fe_2O_3$, *Thermochimica Acta* **292** (1997) 169 – 174

Jacobs, G., Chenu, E., Patterson, P.M., Williams, L., Sparks, D., Thomas, G. & Davis, B.H., Water-gas Shift: Comparative Screening of Metal Promoters for Metal/Ceria Systems and Role of the Metal, *Applied Catalysis A: General* **258** (2004) 203 - 214

Kim, C.H. & Thompson, L., Deactivation of Au/$CeO_x$ Water Gas Shift Catalysts, *Journal of Catalysis* **229** (2005) 600 – 608

Landon, P., Ferguson, J., Solsana, B.E., Garcia, T., Carley, A.F., Herzing, A.A., Kiely, C.J., Golunski, S.E. & Hutchings, G.J., Selective oxidation of CO in the presence of H2, H2O and CO2 via gold for use in fuel cells, *Chemical Communication* (2005) 3385 – 3387

Luengnaruemitchai, A., Osuwan, S. & Gulari, E., Comparative Studies of Low-Temperature Water-Gas Shift Reaction over Pt/$CeO_2$, Au/$CeO_2$, and Au/$Fe_2O_3$, *Catalysis Communications* **4** (2003) 215 – 221

Luengnaruemitchai, A., Thoa, D.T.K., Osuwan, S. & Gulari, E., A comparative study of Au/$MnO_x$ and Au/$FeO_x$ catalysts for the catalytic oxidation of CO in hydrogen rich stream, *International Journal of Hydrogen Energy* **30** (2005) 981– 987

Minicò, S., Scirè, S., Crisafulli, C., Visco, A. & Galvagno, S., FT-IR study of $Au/Fe_2O_3$ catalysts for CO oxidation at low temperature, *Catalysis Letters* **47** (1997) 273 – 276

Okumura, M., Nakamura, S., Tsubota, S., Nakamura, T., Azuma, M. & Haruta, M., Chemical vapour deposition of gold on $Al_2O_3$, $SiO_2$, and $TiO_2$ for the oxidation of CO and of $H_2O$, *Catalysis Letters* **51** (1998) 53 – 58

Panzera, G., Modaferri, V., Candamano, S., Donato, A., Frusteri, F. & Antonucci, P.L., CO selective oxidation on ceria-supported Au catalysts for fuel cell applications, *Journal of Power Sources* **135** (2005) 177 – 183

Rhodes, C., Hutchings, G. & Ward, A., Water-gas shift reaction: finding the mechanistic boundary, *Catalysis Today* **23** (1995) 43 – 58

Roberts, S., Performance of Gold Catalysts for Low Temperature Water Gas Shift, 2001

Sakurai, H., & Haruta, M., Carbon dioxide and carbon monoxide hydrogenation over gold supported on titanium, iron, and zinc oxides, *Applied Catalysis A: General* **127** (1995) 93 – 105

Sakurai, H., & Haruta, M., Synergism in methanol synthesis from carbon dioxide over gold catalysts supported on metal oxides, *Catalysis Today* **29** (1996) 361 – 365

Sakurai, H., Ueda, A., Kobayashi, T. & Haruta, M., Low-temperature water-gas shift reaction over gold deposited on $TiO_2$, *Chemical Communications* (1997) 271 – 272

Schwank, J., Catalytic Gold: Applications of Elemental Gold in Heterogeneous Catalysis, *Gold Bulletin* **16** (1983) 103 – 110

Schwank, J., Gold in bi-metallic catalysts, *Gold Bulletin* **18** (1985) 2 – 10

Tabakova, T., Bocuzzi, F., Manzoli, M., Sobczak, J.W., Idakiev, V. & Andreeva, D., Effect of Synthesis Procedure on the Low-Temperature WGS Activity of Au/ceria Catalysts, *Applied Catalysis B: Environmental* **49** (2004) 73 - 81

Thompson, D., New Advances in Gold Catalysis Part I*, *Gold Bulletin* **31** 4 (1998) 111 - 118

Thompson, D., New Advances in Gold Catalysis Part II*, *Gold Bulletin* **32** 1 (1999) 12 – 19

Twigg, M., The Water-gas Shift Reaction, *Catalyst Handbook* (2nd Edition), Wolfe Publishing Ltd., 1989, 283 – 339

Torres Sanchez, R., Ueda, A., Tanaka, K. & Haruta, M., Selective Oxidation of CO in Hydrogen over Gold Supported o Manganese Oxides, *Journal of Catalysis* **168** (1997) 125 – 127

Trimm, D.L., Minimisation of carbon monoxide in a hydrogen stream for fuel ell application, *Applied Catalysis A: General* **296** (2005) 1 – 11

Urban, P., Funke, A., Müller, J., Himmen, M. & Docter, A., Catalytic processes in solid polymer electrolyte fuel cell systems, *Applied Catalysis A: General* **221** (2001) 459 – 470

Venugopal, A. & Scurrell, M.S., Low Temperature Reductive Pretreatment of $Au/Fe_2O_3$ Catalysts, TPR/TPO Studies and Behaviour in the Water-gas Shift Reaction, *Applied Catalysis A: General* **258** (2004) 241 – 249

Zalc, J.M., Sokolovskii, V., & Löffler, D. G., Are Noble Metal-Based Water-Gas Shift Catalysts Practical for Automotive Fuel Processing? *Journal of Catalysis* **206** (2002) 169 – 171

# APPENDIX I

# LIST OF CATALYSTS TESTED AND EXPERIMENTAL CONDITIONS TESTED

| Experiment | Catalyst | Temperature (°C) | Pressure (bar a) | $WHSV_{dry}$ ($hr^{-1}$) | S:DG* (mol/mol) |
|---|---|---|---|---|---|
| 1 | LTS | 135 – 200 | 2 | 4 | 1:1 |
| 2 | LTS | 130 – 205 | 2, 4, 8 | 2, 4, 8 | 0.5:1, 1:1, 2:1 |
| 3 | WGC-B | 125 – 275 | 2 | 4.0 | 1:1 |
| 4 | WGC-B | 125, 185, 205 – 275 | 2, 4, 8 | 2, 4, 8 | 0.5:1, 1:1, 2:1 |
| 5 | WGC-C | 190 | 2 | 4 | 1:1 |
| 6 | WGC-C | 130 – 235 | 2 | 4 | 1:1 |
| 7 | WGC-C | 165, 190 | 2, 4, 8 | 2, 4, 8 | 0.5:1, 1:1, 2:1 |
| 8 | WGC-A | 155 – 315 | 2, 4, 8 | 2, 4, 8 | 0.5:1, 1:1, 2:1 |

* S:DG – Steam/Dry gas ratio* S:DG – Steam/Dry gas ratio

# APPENDIX II

# EXPERIMENTAL DATA

**EXPERIMENT 1 - Commercial LTS Catalyst (Sud-Chemie C 18-7)**

| | | |
|---|---|---|
| **Pressure** | 2.0 | bar (absolute) |
| **WHSV** | 4.0 | $hr^{-1}$ |
| **S/DG** | 1.0 | mol/mol |

| Time-on-stream (hours) | Temperature (°C) | $X_{CO}$ (%) | C balance (%) | $x_{CO}$ (%) | $x_{CO_2}$ (%) | $F_{CO}$ (ml/min) | $F_{CO_2}$ (ml/min) | $F_{CO+CO_2}$ (ml/min) |
|---|---|---|---|---|---|---|---|---|
| 21.9 | **199.8** | **98.0** | 109.2 | 0.0012 | 0.2070 | 0.09 | 16.21 | 16.30 |
| 28.3 | **198.8** | **97.3** | 110.0 | 0.0017 | 0.2083 | 0.13 | 16.30 | 16.43 |
| 39.3 | **198.4** | **98.1** | 111.1 | 0.0012 | 0.2108 | 0.09 | 16.51 | 16.60 |
| 42.5 | **198.8** | **95.3** | 112.1 | 0.0029 | 0.2114 | 0.22 | 16.53 | 16.75 |
| 45.6 | **198.7** | **84.3** | 111.5 | 0.0098 | 0.2050 | 0.73 | 15.92 | 16.65 |
| 48.1 | **198.8** | **98.2** | 110.9 | 0.0011 | 0.2105 | 0.08 | 16.48 | 16.57 |
| 64.4 | **190.9** | **90.6** | 111.4 | 0.0059 | 0.2077 | 0.44 | 16.19 | 16.64 |
| 66.4 | **188.8** | **93.0** | 111.7 | 0.0044 | 0.2094 | 0.33 | 16.35 | 16.68 |
| 67.8 | **189.2** | **95.2** | 111.2 | 0.0030 | 0.2096 | 0.23 | 16.38 | 16.61 |
| 78.8 | **175.7** | **80.7** | 111.8 | 0.0121 | 0.2039 | 0.90 | 15.80 | 16.70 |
| 79.8 | **176.0** | **83.4** | 111.9 | 0.0104 | 0.2053 | 0.78 | 15.94 | 16.72 |
| 87.7 | **158.1** | **61.6** | 110.8 | 0.0240 | 0.1928 | 1.77 | 14.77 | 16.54 |
| 89.9 | **158.7** | **61.0** | 110.5 | 0.0244 | 0.1919 | 1.80 | 14.70 | 16.50 |
| 91.7 | **158.6** | **59.4** | 111.0 | 0.0254 | 0.1922 | 1.87 | 14.71 | 16.58 |
| 99.8 | **147.2** | **46.4** | 111.0 | 0.0335 | 0.1860 | 2.45 | 14.12 | 16.57 |
| 101.4 | **147.5** | **50.7** | 110.7 | 0.0308 | 0.1874 | 2.26 | 14.27 | 16.53 |
| 112.0 | **135.5** | **13.8** | 111.0 | 0.0539 | 0.1706 | 3.86 | 12.72 | 16.58 |
| 113.6 | **136.4** | **19.8** | 110.2 | 0.0502 | 0.1718 | 3.61 | 12.85 | 16.46 |
| 115.5 | **136.3** | **13.4** | 112.3 | 0.0542 | 0.1730 | 3.89 | 12.89 | 16.77 |
| 120.1 | **147.5** | **28.6** | 111.0 | 0.0447 | 0.1774 | 3.23 | 13.34 | 16.57 |
| 121.4 | **147.4** | **21.8** | 111.8 | 0.0489 | 0.1758 | 3.52 | 13.17 | 16.69 |
| 135.5 | **157.5** | **46.9** | 111.4 | 0.0332 | 0.1870 | 2.43 | 14.21 | 16.64 |
| 136.9 | **158.2** | **45.8** | 112.0 | 0.0339 | 0.1877 | 2.48 | 14.25 | 16.73 |
| 141.4 | **167.0** | **61.4** | 113.3 | 0.0241 | 0.1976 | 1.78 | 15.14 | 16.92 |
| 143.1 | **168.0** | **63.3** | 111.8 | 0.0230 | 0.1956 | 1.70 | 15.01 | 16.70 |
| 144.2 | **167.8** | **58.7** | 112.6 | 0.0258 | 0.1949 | 1.90 | 14.91 | 16.81 |
| 160.4 | **177.9** | **87.1** | 112.3 | 0.0081 | 0.2079 | 0.61 | 16.17 | 16.78 |
| 162.0 | **176.5** | **89.6** | 111.7 | 0.0065 | 0.2078 | 0.49 | 16.19 | 16.68 |
| 163.9 | **178.0** | **93.2** | 112.0 | 0.0043 | 0.2102 | 0.32 | 16.41 | 16.73 |
| 167.0 | **177.8** | **96.1** | 111.6 | 0.0024 | 0.2108 | 0.18 | 16.49 | 16.67 |
| 170.0 | **177.2** | **94.7** | 110.8 | 0.0033 | 0.2085 | 0.25 | 16.30 | 16.55 |
| 184.0 | **176.7** | **93.7** | 110.2 | 0.0039 | 0.2069 | 0.30 | 16.16 | 16.46 |
| 186.1 | **177.6** | **91.2** | 110.6 | 0.0055 | 0.2065 | 0.41 | 16.11 | 16.52 |
| 188.9 | **177.8** | **87.4** | 113.4 | 0.0079 | 0.2101 | 0.59 | 16.35 | 16.94 |
| 191.0 | **178.1** | **90.1** | 109.4 | 0.0062 | 0.2037 | 0.46 | 15.88 | 16.34 |
| 194.5 | **177.2** | **89.5** | 109.5 | 0.0066 | 0.2037 | 0.49 | 15.87 | 16.36 |
| 207.8 | **177.4** | **88.6** | 109.4 | 0.0072 | 0.2028 | 0.54 | 15.79 | 16.33 |
| 209.9 | **177.7** | **88.8** | 109.4 | 0.0070 | 0.2031 | 0.52 | 15.82 | 16.34 |

**EXPERIMENT 2 - Commercial LTS Catalyst (Sud-Chemie C 18-7)**

| | | |
|---|---|---|
| **Pressure** | 2.0 | bar (absolute) |
| **WHSV** | 4.0 | $hr^{-1}$ |
| **S/DG** | 1.0 | mol/mol |

| Time-on-stream (hours) | Temperature (°C) | $X_{CO}$ (%) | C balance (%) | $x_{CO}$ (%) | $x_{CO_2}$ (%) | $F_{CO}$ (ml/min) | $F_{CO_2}$ (ml/min) | $F_{CO+CO_2}$ (ml/min) |
|---|---|---|---|---|---|---|---|---|
| 1.0 | **189.8** | **76.96** | 100.27 | 0.0115 | 0.1820 | 0.86 | 14.11 | 14.97 |
| 2.2 | **189.5** | **91.21** | 99.31 | 0.0044 | 0.1858 | 0.33 | 14.50 | 14.83 |
| 3.1 | **189.6** | **91.44** | 99.44 | 0.0042 | 0.1861 | 0.32 | 14.53 | 14.85 |
| 4.1 | **189.8** | **88.86** | 98.76 | 0.0055 | 0.1838 | 0.42 | 14.33 | 14.75 |
| 5.1 | **189.2** | **90.67** | 99.12 | 0.0046 | 0.1852 | 0.35 | 14.45 | 14.80 |
| 6.2 | **189.3** | **88.26** | 98.09 | 0.0058 | 0.1823 | 0.44 | 14.21 | 14.65 |
| 8.6 | **189.2** | **89.59** | 98.38 | 0.0052 | 0.1834 | 0.39 | 14.30 | 14.69 |
| 9.9 | **189.0** | **89.72** | 99.02 | 0.0051 | 0.1846 | 0.38 | 14.40 | 14.79 |
| 20.8 | **187.2** | **88.42** | 94.13 | 0.0058 | 0.1748 | 0.43 | 13.63 | 14.06 |
| 21.9 | **187.4** | **87.34** | 95.20 | 0.0063 | 0.1764 | 0.47 | 13.75 | 14.22 |
| 24.2 | **190.0** | **85.81** | 94.63 | 0.0071 | 0.1747 | 0.53 | 13.60 | 14.13 |
| 29.2 | **189.0** | **88.04** | 94.82 | 0.0059 | 0.1759 | 0.45 | 13.71 | 14.16 |
| 44.0 | **189.5** | **88.94** | 94.75 | 0.0055 | 0.1761 | 0.41 | 13.74 | 14.15 |
| 46.2 | **189.9** | **87.32** | 96.85 | 0.0063 | 0.1795 | 0.47 | 13.99 | 14.46 |
| 50.0 | **190.0** | **85.10** | 96.91 | 0.0074 | 0.1788 | 0.56 | 13.92 | 14.47 |
| 51.5 | **189.2** | **86.45** | 96.14 | 0.0067 | 0.1778 | 0.51 | 13.85 | 14.36 |
| 54.5 | **189.4** | **88.11** | 94.83 | 0.0059 | 0.1760 | 0.44 | 13.72 | 14.16 |
| 57.6 | **190.0** | **86.59** | 95.52 | 0.0067 | 0.1767 | 0.50 | 13.76 | 14.27 |
| 68.6 | **189.8** | **80.34** | 96.17 | 0.0098 | 0.1755 | 0.73 | 13.63 | 14.36 |
| 69.6 | **189.5** | **85.28** | 96.18 | 0.0073 | 0.1774 | 0.55 | 13.81 | 14.36 |
| 71.4 | **190.0** | **81.98** | 96.79 | 0.0090 | 0.1773 | 0.67 | 13.78 | 14.46 |
| 95.3 | **189.1** | **86.04** | 89.84 | 0.0069 | 0.1656 | 0.52 | 12.90 | 13.42 |
| 96.4 | **189.9** | **85.16** | 89.80 | 0.0074 | 0.1652 | 0.55 | 12.86 | 13.41 |
| 97.8 | **189.8** | **87.49** | 89.85 | 0.0062 | 0.1662 | 0.47 | 12.95 | 13.42 |
| 100.6 | **188.7** | **87.32** | 90.18 | 0.0063 | 0.1667 | 0.47 | 12.99 | 13.47 |
| 103.3 | **189.1** | **84.26** | 89.98 | 0.0078 | 0.1651 | 0.59 | 12.85 | 13.44 |
| 116.6 | **188.8** | **85.73** | 89.26 | 0.0071 | 0.1644 | 0.53 | 12.80 | 13.33 |
| 117.8 | **189.2** | **88.11** | 89.66 | 0.0059 | 0.1661 | 0.44 | 12.95 | 13.39 |
| 118.9 | **189.2** | **86.03** | 90.16 | 0.0070 | 0.1662 | 0.52 | 12.94 | 13.47 |
| 121.4 | **189.0** | **84.60** | 90.16 | 0.0077 | 0.1656 | 0.58 | 12.89 | 13.47 |
| 123.6 | **189.4** | **89.45** | 90.19 | 0.0052 | 0.1676 | 0.39 | 13.08 | 13.47 |
| 128.6 | **188.9** | **11.89** | 89.35 | 0.0455 | 0.1339 | 3.29 | 10.05 | 13.34 |
| 129.9 | **187.9** | **78.34** | 89.49 | 0.0108 | 0.1618 | 0.81 | 12.56 | 13.37 |
| 130.9 | **187.7** | **63.74** | 89.42 | 0.0182 | 0.1558 | 1.35 | 12.00 | 13.36 |
| 140.1 | **189.1** | **82.74** | 93.13 | 0.0086 | 0.1706 | 0.64 | 13.26 | 13.91 |
| 141.4 | **189.1** | **82.47** | 67.36 | 0.0087 | 0.1210 | 0.65 | 9.41 | 10.06 |
| 142.5 | **189.4** | **82.57** | 94.28 | 0.0087 | 0.1727 | 0.65 | 13.43 | 14.08 |
| 144.7 | **189.4** | **81.75** | 94.90 | 0.0091 | 0.1736 | 0.68 | 13.49 | 14.17 |
| 148.2 | **189.3** | **83.71** | 93.71 | 0.0081 | 0.1721 | 0.61 | 13.39 | 14.00 |
| 166.2 | **179.6** | **70.09** | 93.72 | 0.0150 | 0.1667 | 1.12 | 12.88 | 14.00 |
| 168.2 | **181.0** | **74.86** | 93.55 | 0.0126 | 0.1682 | 0.94 | 13.03 | 13.97 |
| 172.8 | **180.9** | **79.94** | 92.97 | 0.0100 | 0.1692 | 0.75 | 13.14 | 13.89 |
| 175.5 | **170.4** | **67.61** | 93.08 | 0.0163 | 0.1644 | 1.21 | 12.69 | 13.90 |
| 176.4 | **172.0** | **75.05** | 92.93 | 0.0125 | 0.1671 | 0.93 | 12.95 | 13.88 |
| 177.4 | **172.0** | **72.13** | 93.08 | 0.0140 | 0.1662 | 1.04 | 12.86 | 13.90 |
| 178.4 | **171.9** | **69.76** | 93.44 | 0.0152 | 0.1660 | 1.13 | 12.83 | 13.95 |

**EXPERIMENT 2 - Commercial LTS Catalyst (Sud-Chemie C 18-7)**

| | | |
|---|---|---|
| **Pressure** | 2.0 | bar (absolute) |
| **WHSV** | 4.0 | $hr^{-1}$ |
| **S/DG** | 1.0 | mol/mol |

| Time-on-stream (hours) | Temperature (°C) | $X_{CO}$ (%) | C balance (%) | $x_{CO}$ (%) | $x_{CO_2}$ (%) | $F_{CO}$ (ml/min) | $F_{CO_2}$ (ml/min) | $F_{CO+CO_2}$ (ml/min) |
|---|---|---|---|---|---|---|---|---|
| 191.1 | **162.4** | **57.87** | 93.53 | 0.0213 | 0.1613 | 1.57 | 12.40 | 13.97 |
| 191.9 | **161.3** | **52.88** | 93.34 | 0.02385 | 0.15893 | 1.76 | 12.18 | 13.94 |
| 195.4 | **152.6** | **37.41** | 93.17 | 0.03193 | 0.15220 | 2.34 | 11.58 | 13.91 |
| 196.0 | **152.6** | **40.66** | 92.52 | 0.03022 | 0.15229 | 2.22 | 11.60 | 13.82 |
| 197.5 | **152.6** | **38.05** | 93.00 | 0.03159 | 0.15214 | 2.31 | 11.58 | 13.89 |
| 198.5 | **154.2** | **39.80** | 92.74 | 0.03067 | 0.15236 | 2.25 | 11.60 | 13.85 |
| 213.3 | **141.4** | **26.34** | 92.19 | 0.03779 | 0.14564 | 2.75 | 11.02 | 13.77 |
| 214.5 | **141.3** | **24.68** | 91.98 | 0.03867 | 0.14452 | 2.81 | 10.92 | 13.74 |
| 215.5 | **142.0** | **28.93** | 92.08 | 0.03641 | 0.14650 | 2.65 | 11.10 | 13.75 |
| 216.5 | **141.8** | **27.10** | 92.62 | 0.03738 | 0.14681 | 2.72 | 11.11 | 13.83 |
| 220.0 | **132.8** | **15.36** | 92.75 | 0.04366 | 0.14209 | 3.16 | 10.69 | 13.85 |
| 221.3 | **132.7** | **15.37** | 93.82 | 0.04366 | 0.14421 | 3.16 | 10.85 | 14.01 |
| 222.4 | **132.7** | **15.24** | 92.70 | 0.04373 | 0.14195 | 3.16 | 10.68 | 13.85 |
| 235.8 | **137.5** | **21.64** | 92.63 | 0.04029 | 0.14452 | 2.93 | 10.91 | 13.83 |
| 236.8 | **137.6** | **20.82** | 92.83 | 0.04073 | 0.14458 | 2.96 | 10.91 | 13.86 |
| 237.8 | **136.8** | **20.07** | 93.73 | 0.04114 | 0.14604 | 2.98 | 11.01 | 14.00 |
| 239.1 | **136.6** | **17.97** | 93.88 | 0.04226 | 0.14544 | 3.06 | 10.96 | 14.02 |
| 242.4 | **141.3** | **23.46** | 95.11 | 0.03932 | 0.15021 | 2.86 | 11.35 | 14.21 |
| 243.4 | **141.3** | **25.15** | 94.84 | 0.03842 | 0.15037 | 2.79 | 11.37 | 14.16 |
| 244.4 | **141.5** | **25.78** | 93.44 | 0.03808 | 0.14787 | 2.77 | 11.18 | 13.96 |
| 245.3 | **141.2** | **24.33** | 93.78 | 0.03886 | 0.14793 | 2.83 | 11.18 | 14.01 |
| 259.5 | **150.4** | **40.34** | 92.93 | 0.03039 | 0.15296 | 2.23 | 11.65 | 13.88 |
| 260.6 | **150.4** | **41.25** | 93.40 | 0.02991 | 0.15424 | 2.19 | 11.76 | 13.95 |
| 261.5 | **150.4** | **39.17** | 94.05 | 0.03100 | 0.15466 | 2.27 | 11.77 | 14.05 |
| 264.3 | **160.5** | **52.98** | 93.12 | 0.02379 | 0.15855 | 1.76 | 12.15 | 13.91 |
| 265.5 | **160.9** | **59.15** | 93.91 | 0.02061 | 0.16259 | 1.53 | 12.50 | 14.02 |
| 266.6 | **161.1** | **58.32** | 93.29 | 0.02104 | 0.16105 | 1.56 | 12.38 | 13.93 |
| 269.5 | **171.4** | **73.16** | 93.37 | 0.01345 | 0.16722 | 1.00 | 12.94 | 13.95 |
| 270.5 | **171.3** | **68.93** | 93.22 | 0.01560 | 0.16523 | 1.16 | 12.76 | 13.92 |
| 271.4 | **171.5** | **71.54** | 93.46 | 0.01427 | 0.16674 | 1.06 | 12.90 | 13.96 |
| 283.5 | **181.3** | **78.56** | 94.66 | 0.01071 | 0.17186 | 0.80 | 13.34 | 14.14 |
| 284.7 | **181.5** | **78.34** | 93.90 | 0.01082 | 0.17030 | 0.81 | 13.21 | 14.02 |
| 285.7 | **181.5** | **79.44** | 94.22 | 0.01027 | 0.17136 | 0.77 | 13.30 | 14.07 |
| 289.2 | **190.7** | **88.92** | 94.42 | 0.00551 | 0.17551 | 0.41 | 13.69 | 14.10 |
| 290.2 | **191.1** | **87.98** | 95.12 | 0.00598 | 0.17647 | 0.45 | 13.76 | 14.21 |
| 291.2 | **191.2** | **82.74** | 93.85 | 0.00861 | 0.17196 | 0.64 | 13.37 | 14.02 |
| 292.4 | **190.4** | **85.19** | 93.18 | 0.00737 | 0.17166 | 0.55 | 13.36 | 13.92 |
| 308.3 | **193.6** | **87.80** | 90.06 | 0.00607 | 0.16671 | 0.46 | 13.00 | 13.45 |
| 309.4 | **192.7** | **89.93** | 90.13 | 0.00500 | 0.16770 | 0.38 | 13.09 | 13.46 |
| 310.4 | **193.4** | **88.49** | 91.56 | 0.00572 | 0.16986 | 0.43 | 13.24 | 13.67 |
| 314.8 | **206.1** | **93.00** | 91.95 | 0.00347 | 0.17239 | 0.26 | 13.47 | 13.73 |
| 315.8 | **203.3** | **92.84** | 90.77 | 0.00355 | 0.17008 | 0.27 | 13.29 | 13.56 |
| 317.1 | **203.0** | **90.93** | 90.13 | 0.00451 | 0.16810 | 0.34 | 13.12 | 13.46 |
| 319.6 | **161.3** | **58.30** | 90.44 | 0.02105 | 0.15551 | 1.56 | 11.95 | 13.51 |
| 333.9 | **161.4** | **57.17** | 91.21 | 0.02163 | 0.15653 | 1.60 | 12.02 | 13.62 |

**EXPERIMENT 2 - Commercial LTS Catalyst (Sud-Chemie C 18-7)**

| | | |
|---|---|---|
| **Pressure** | 2 | bar (absolute) |
| **WHSV** | **8** | **$hr^{-1}$** |
| **S/DG** | 1 | mol/mol |

| Time-on-stream (hours) | Temperature ($^{o}C$) | $X_{CO}$ (%) | C balance (%) | $x_{CO}$ (%) | $x_{CO_2}$ (%) | $F_{CO}$ (ml/min) | $F_{CO_2}$ (ml/min) | $F_{CO+CO_2}$ (ml/min) |
|---|---|---|---|---|---|---|---|---|
| 336.6 | **160.1** | **41.54** | 96.42 | 0.02975 | 0.16030 | 2.18 | 12.22 | 14.40 |
| 337.7 | **161.2** | **40.40** | 96.58 | 0.03035 | 0.16013 | 2.23 | 12.20 | 14.42 |
| 338.8 | **161.2** | **41.92** | 94.64 | 0.02956 | 0.15695 | 2.17 | 11.97 | 14.13 |

**EXPERIMENT 2 - Commercial LTS Catalyst (Sud-Chemie C 18-7)**

| | | |
|---|---|---|
| **Pressure** | 2.0 | bar (absolute) |
| **WHSV** | **2.0** | **$hr^{-1}$** |
| **S/DG** | 1.0 | mol/mol |

| Time-on-stream (hours) | Temperature ($^{o}C$) | $X_{CO}$ (%) | C balance (%) | $x_{CO}$ (%) | $x_{CO_2}$ (%) | $F_{CO}$ (ml/min) | $F_{CO_2}$ (ml/min) | $F_{CO+CO_2}$ (ml/min) |
|---|---|---|---|---|---|---|---|---|
| 356.8 | **161.3** | **72.88** | 86.39 | 0.01359 | 0.15362 | 1.01 | 11.89 | 12.90 |
| 359.7 | **161.6** | **72.23** | 89.27 | 0.01392 | 0.15893 | 1.04 | 12.30 | 13.33 |
| 365.4 | **161.7** | **73.33** | 88.61 | 0.01336 | 0.15809 | 1.00 | 12.24 | 13.23 |

**EXPERIMENT 2 - Commercial LTS Catalyst (Sud-Chemie C 18-7)**

| | | |
|---|---|---|
| **Pressure** | 2.0 | bar (absolute) |
| **WHSV** | 4.0 | $hr^{-1}$ |
| **S/DG** | **0.5** | **mol/mol** |

| Time-on-stream (hours) | Temperature ($^{o}C$) | $X_{CO}$ (%) | C balance (%) | $x_{CO}$ (%) | $x_{CO_2}$ (%) | $F_{CO}$ (ml/min) | $F_{CO_2}$ (ml/min) | $F_{CO+CO_2}$ (ml/min) |
|---|---|---|---|---|---|---|---|---|
| 380.4 | **161.3** | **41.31** | 89.86 | 0.02988 | 0.14733 | 2.19 | 11.23 | 13.42 |
| 381.4 | **161.6** | **45.47** | 90.64 | 0.02770 | 0.15060 | 2.04 | 11.50 | 13.54 |
| 382.5 | **161.2** | **37.73** | 91.32 | 0.03176 | 0.14870 | 2.33 | 11.31 | 13.64 |
| 383.4 | **159.8** | **38.45** | 89.93 | 0.03138 | 0.14628 | 2.30 | 11.13 | 13.43 |

**EXPERIMENT 2 - Commercial LTS Catalyst (Sud-Chemie C 18-7)**

| | | |
|---|---|---|
| **Pressure** | 2.0 | bar (absolute) |
| **WHSV** | 4.0 | $hr^{-1}$ |
| **S/DG** | **2.0** | **mol/mol** |

| Time-on-stream (hours) | Temperature (°C) | $X_{CO}$ (%) | C balance (%) | $x_{CO}$ (%) | $x_{CO_2}$ (%) | $F_{CO}$ (ml/min) | $F_{CO_2}$ (ml/min) | $F_{CO+CO_2}$ (ml/min) |
|---|---|---|---|---|---|---|---|---|
| 386.4 | **161.3** | **60.94** | 89.10 | 0.01969 | 0.15399 | 1.46 | 11.85 | 13.31 |
| 387.5 | **161.2** | **60.47** | 89.46 | 0.01993 | 0.15449 | 1.48 | 11.88 | 13.36 |
| 388.7 | **161.0** | **60.09** | 89.31 | 0.02012 | 0.15404 | 1.49 | 11.85 | 13.34 |
| 390.5 | **161.8** | **60.66** | 89.46 | 0.01983 | 0.15458 | 1.47 | 11.89 | 13.36 |
| 391.4 | **162.4** | **61.87** | 88.92 | 0.01921 | 0.15401 | 1.42 | 11.86 | 13.28 |
| 393.5 | **162.0** | **60.75** | 88.80 | 0.01978 | 0.15333 | 1.47 | 11.80 | 13.26 |
| 394.5 | **161.6** | **60.13** | 89.05 | 0.02010 | 0.15355 | 1.49 | 11.81 | 13.30 |
| 404.1 | **161.2** | **59.11** | 88.79 | 0.02063 | 0.15263 | 1.53 | 11.73 | 13.26 |
| 405.1 | **161.2** | **57.01** | 89.22 | 0.02171 | 0.15261 | 1.61 | 11.72 | 13.33 |

**EXPERIMENT 2 - Commercial LTS Catalyst (Sud-Chemie C 18-7)**

| | | |
|---|---|---|
| **Pressure** | 2.0 | bar (absolute) |
| **WHSV** | 4.0 | $hr^{-1}$ |
| **S/DG** | **1.0** | **mol/mol** |

| Time-on-stream (hours) | Temperature (°C) | $X_{CO}$ (%) | C balance (%) | $x_{CO}$ (%) | $x_{CO_2}$ (%) | $F_{CO}$ (ml/min) | $F_{CO_2}$ (ml/min) | $F_{CO+CO_2}$ (ml/min) |
|---|---|---|---|---|---|---|---|---|
| 408.0 | **160.9** | **49.01** | 89.60 | 0.02586 | 0.15004 | 1.90 | 11.48 | 13.38 |
| 409.0 | **160.9** | **47.65** | 90.48 | 0.02657 | 0.15120 | 1.95 | 11.56 | 13.51 |

**EXPERIMENT 2 - Commercial LTS Catalyst (Sud-Chemie C 18-7)**

| | | |
|---|---|---|
| **Pressure** | **4.0** | **bar (absolute)** |
| **WHSV** | 4.0 | $hr^{-1}$ |
| **S/DG** | 1.0 | mol/mol |

| Time-on-stream (hours) | Temperature (°C) | $X_{CO}$ (%) | C balance (%) | $x_{CO}$ (%) | $x_{CO_2}$ (%) | $F_{CO}$ (ml/min) | $F_{CO_2}$ (ml/min) | $F_{CO+CO_2}$ (ml/min) |
|---|---|---|---|---|---|---|---|---|
| 411.9 | **161.6** | **47.92** | 88.77 | 0.02642 | 0.14797 | 1.94 | 11.31 | 13.26 |
| 412.9 | **161.6** | **49.22** | 88.50 | 0.02575 | 0.14797 | 1.90 | 11.32 | 13.22 |
| 414.5 | **161.7** | **47.69** | 88.43 | 0.02654 | 0.14720 | 1.95 | 11.25 | 13.21 |

**EXPERIMENT 2 - Commercial LTS Catalyst (Sud-Chemie C 18-7)**

| | | |
|---|---|---|
| **Pressure** | **8.0** | **bar (absolute)** |
| **WHSV** | 4.0 | $hr^{-1}$ |
| **S/DG** | 1.0 | mol/mol |

| Time-on-stream (hours) | Temperature (°C) | $X_{CO}$ (%) | C balance (%) | $x_{CO}$ (%) | $x_{CO_2}$ (%) | $F_{CO}$ (ml/min) | $F_{CO_2}$ (ml/min) | $F_{CO+CO_2}$ (ml/min) |
|---|---|---|---|---|---|---|---|---|
| 427.9 | **161.3** | **42.12** | 88.22 | 0.02945 | 0.14447 | 2.16 | 11.01 | 13.18 |
| 428.9 | **162.1** | **43.11** | 88.07 | 0.02893 | 0.14459 | 2.12 | 11.03 | 13.15 |
| 430.8 | **162.4** | **44.85** | 88.73 | 0.02803 | 0.14659 | 2.06 | 11.19 | 13.25 |

**EXPERIMENT 2 - Commercial LTS Catalyst (Sud-Chemie C 18-7)**

| | | |
|---|---|---|
| **Pressure** | 2.0 | bar (absolute) |
| **WHSV** | 4.0 | $hr^{-1}$ |
| **S/DG** | 1.0 | mol/mol |

| Time-on-stream (hours) | Temperature ($^{o}C$) | $X_{CO}$ (%) | C balance (%) | $x_{CO}$ (%) | $x_{CO2}$ (%) | $F_{CO}$ (ml/min) | $F_{CO2}$ (ml/min) | $F_{CO+CO2}$ (ml/min) |
|---|---|---|---|---|---|---|---|---|
| 433.1 | **160.6** | **50.65** | 86.25 | 0.02500 | 0.14417 | 1.84 | 11.04 | 12.88 |
| 434.1 | **160.0** | **51.46** | 89.95 | 0.02458 | 0.15173 | 1.81 | 11.62 | 13.43 |
| 435.2 | **160.6** | **46.15** | 89.69 | 0.02735 | 0.14902 | 2.01 | 11.38 | 13.40 |
| 436.4 | **160.1** | **50.67** | 89.35 | 0.02499 | 0.15024 | 1.84 | 11.50 | 13.34 |
| 451.9 | **160.3** | **48.60** | 89.02 | 0.02607 | 0.14873 | 1.92 | 11.38 | 13.29 |
| 452.7 | **161.7** | **47.03** | 89.20 | 0.02689 | 0.14843 | 1.98 | 11.34 | 13.32 |

**EXPERIMENT 3 - WGC-B ($Au/Fe_2O_3/Al_2O_3$)**

| | | |
|---|---|---|
| **Pressure** | 2.0 | bar (absolute) |
| **WHSV** | 4.0 | $hr^{-1}$ |
| **S/DG** | 1.0 | mol/mol |

| Time-on-stream (hours) | Temperature (°C) | $X_{CO}$ (%) | C balance (%) | $x_{CO}$ (%) | $x_{CO_2}$ (%) | $F_{CO}$ (ml/min) | $F_{CO_2}$ (ml/min) | $F_{CO+CO_2}$ (ml/min) |
|---|---|---|---|---|---|---|---|---|
| 2.8 | **192.6** | **26.39** | 94.47 | 0.0378 | 0.1502 | 2.75 | 11.36 | 14.11 |
| 6.0 | **192.9** | **25.68** | 95.19 | 0.0381 | 0.1513 | 2.78 | 11.44 | 14.22 |
| 8.7 | **193.1** | **25.09** | 94.82 | 0.0385 | 0.1503 | 2.80 | 11.36 | 14.16 |
| 18.4 | **193.0** | **21.98** | 94.54 | 0.0401 | 0.1484 | 2.91 | 11.21 | 14.12 |
| 20.9 | **193.3** | **20.54** | 95.81 | 0.0409 | 0.1504 | 2.97 | 11.34 | 14.31 |
| 23.2 | **193.0** | **19.26** | 97.81 | 0.0416 | 0.1538 | 3.01 | 11.59 | 14.61 |
| 28.5 | **192.3** | **17.82** | 96.16 | 0.0423 | 0.1499 | 3.07 | 11.29 | 14.36 |
| 34.1 | **192.7** | **17.27** | 95.68 | 0.0426 | 0.1487 | 3.09 | 11.20 | 14.29 |
| 45.3 | **193.1** | **15.81** | 97.10 | 0.0434 | 0.1509 | 3.14 | 11.36 | 14.50 |
| 49.2 | **192.7** | **16.40** | 95.40 | 0.0431 | 0.1478 | 3.12 | 11.13 | 14.25 |
| 53.8 | **194.1** | **14.88** | 97.14 | 0.0439 | 0.1506 | 3.18 | 11.33 | 14.51 |
| 67.6 | **194.1** | **17.00** | 94.18 | 0.0428 | 0.1456 | 3.10 | 10.97 | 14.07 |
| 71.2 | **193.0** | **14.76** | 95.25 | 0.0440 | 0.1468 | 3.18 | 11.04 | 14.22 |
| 74.6 | **193.0** | **16.09** | 93.74 | 0.0433 | 0.1444 | 3.13 | 10.87 | 14.00 |
| 77.4 | **193.0** | **15.07** | 93.73 | 0.0438 | 0.1439 | 3.17 | 10.83 | 14.00 |
| 80.8 | **193.0** | **17.04** | 93.10 | 0.0428 | 0.1435 | 3.10 | 10.81 | 13.90 |
| 90.8 | **183.2** | **14.72** | 93.42 | 0.0440 | 0.1431 | 3.18 | 10.77 | 13.95 |
| 92.3 | **183.7** | **12.02** | 94.12 | 0.0455 | 0.1434 | 3.29 | 10.77 | 14.06 |
| 93.4 | **183.9** | **14.46** | 93.90 | 0.0442 | 0.1440 | 3.19 | 10.83 | 14.02 |
| 94.8 | **183.6** | **12.10** | 94.43 | 0.0454 | 0.1440 | 3.28 | 10.82 | 14.10 |
| 96.1 | **183.9** | **10.49** | 95.66 | 0.0463 | 0.1458 | 3.34 | 10.94 | 14.29 |
| 97.3 | **184.2** | **13.29** | 93.73 | 0.0448 | 0.1432 | 3.24 | 10.76 | 14.00 |
| 98.8 | **184.5** | **12.20** | 94.26 | 0.0454 | 0.1437 | 3.28 | 10.80 | 14.08 |
| 100.0 | **184.2** | **13.23** | 93.13 | 0.0448 | 0.1419 | 3.24 | 10.67 | 13.91 |
| 114.3 | **164.9** | **9.08** | 94.08 | 0.0471 | 0.1421 | 3.40 | 10.66 | 14.05 |
| 115.6 | **164.9** | **8.66** | 94.83 | 0.0473 | 0.1434 | 3.41 | 10.75 | 14.16 |
| 116.8 | **165.0** | **8.79** | 94.67 | 0.0472 | 0.1431 | 3.41 | 10.73 | 14.14 |
| 118.2 | **165.1** | **8.26** | 94.59 | 0.0475 | 0.1427 | 3.43 | 10.70 | 14.13 |
| 119.3 | **164.9** | **8.52** | 95.30 | 0.0474 | 0.1443 | 3.42 | 10.82 | 14.23 |
| 123.0 | **202.8** | **16.50** | 94.14 | 0.0431 | 0.1453 | 3.12 | 10.94 | 14.06 |
| 124.5 | **202.7** | **17.78** | 94.13 | 0.0424 | 0.1459 | 3.07 | 10.99 | 14.06 |
| 125.8 | **203.0** | **16.34** | 94.17 | 0.0431 | 0.1453 | 3.12 | 10.94 | 14.06 |
| 127.1 | **203.2** | **15.44** | 93.50 | 0.0436 | 0.1436 | 3.16 | 10.81 | 13.96 |
| 128.7 | **203.4** | **15.91** | 93.91 | 0.0434 | 0.1446 | 3.14 | 10.88 | 14.02 |
| 129.9 | **203.1** | **17.33** | 93.72 | 0.0426 | 0.1449 | 3.09 | 10.91 | 14.00 |
| 138.5 | **212.8** | **20.53** | 93.48 | 0.0409 | 0.1457 | 2.97 | 10.99 | 13.96 |
| 139.7 | **211.1** | **18.93** | 94.22 | 0.0417 | 0.1465 | 3.03 | 11.04 | 14.07 |
| 140.9 | **211.7** | **18.52** | 94.44 | 0.0420 | 0.1468 | 3.04 | 11.06 | 14.11 |
| 142.2 | **211.5** | **17.61** | 95.93 | 0.0425 | 0.1494 | 3.08 | 11.25 | 14.33 |
| 143.2 | **212.1** | **17.81** | 95.61 | 0.0423 | 0.1488 | 3.07 | 11.21 | 14.28 |
| 146.4 | **221.5** | **19.80** | 94.96 | 0.0413 | 0.1484 | 2.99 | 11.19 | 14.18 |
| 163.0 | **221.6** | **20.26** | 93.58 | 0.0410 | 0.1458 | 2.98 | 11.00 | 13.98 |
| 165.3 | **220.4** | **18.20** | 94.83 | 0.0421 | 0.1474 | 3.05 | 11.11 | 14.16 |
| 166.6 | **221.5** | **17.96** | 94.43 | 0.0423 | 0.1465 | 3.06 | 11.04 | 14.10 |
| 167.8 | **222.1** | **17.90** | 95.12 | 0.0423 | 0.1479 | 3.07 | 11.14 | 14.21 |
| 172.0 | **232.1** | **17.68** | 95.61 | 0.0424 | 0.1488 | 3.07 | 11.21 | 14.28 |

**EXPERIMENT 3 - WGC-B ($Au/Fe_2O_3/Al_2O_3$)**

| | | |
|---|---|---|
| **Pressure** | 2.0 | bar (absolute) |
| **WHSV** | 4.0 | $hr^{-1}$ |
| **S/DG** | 1.0 | mol/mol |

| Time-on-stream (hours) | Temperature (°C) | $X_{CO}$ (%) | C balance (%) | $x_{CO}$ (%) | $x_{CO_2}$ (%) | $F_{CO}$ (ml/min) | $F_{CO_2}$ (ml/min) | $F_{CO+CO_2}$ (ml/min) |
|---|---|---|---|---|---|---|---|---|
| 173.9 | **231.3** | **18.05** | 95.22 | 0.0422 | 0.1481 | 3.06 | 11.16 | 14.22 |
| 175.8 | **231.5** | **17.50** | 94.54 | 0.04252 | 0.14656 | 3.08 | 11.04 | 14.12 |
| 186.5 | **241.0** | **17.00** | 93.71 | 0.04278 | 0.14470 | 3.10 | 10.90 | 14.00 |
| 187.3 | **241.3** | **16.13** | 95.45 | 0.04325 | 0.14778 | 3.13 | 11.12 | 14.26 |
| 191.8 | **251.5** | **16.30** | 95.23 | 0.04316 | 0.14741 | 3.13 | 11.10 | 14.22 |
| 195.1 | **251.4** | **11.72** | 99.89 | 0.04563 | 0.15474 | 3.30 | 11.62 | 14.92 |
| 196.7 | **251.7** | **12.15** | 99.06 | 0.04540 | 0.15327 | 3.28 | 11.51 | 14.79 |
| 215.8 | **251.3** | **8.81** | 98.73 | 0.04720 | 0.15121 | 3.41 | 11.34 | 14.75 |
| 218.8 | **251.5** | **8.34** | 98.85 | 0.04746 | 0.15124 | 3.42 | 11.34 | 14.76 |
| 221.4 | **251.5** | **7.63** | 98.49 | 0.04784 | 0.15023 | 3.45 | 11.26 | 14.71 |
| 226.3 | **251.4** | **9.12** | 97.95 | 0.04703 | 0.14979 | 3.39 | 11.24 | 14.63 |
| 237.1 | **251.3** | **7.48** | 97.70 | 0.04792 | 0.14858 | 3.45 | 11.14 | 14.59 |
| 241.1 | **261.6** | **8.24** | 97.86 | 0.04751 | 0.14924 | 3.43 | 11.19 | 14.62 |
| 242.2 | **261.6** | **7.10** | 97.77 | 0.04813 | 0.14857 | 3.47 | 11.13 | 14.60 |
| 244.8 | **261.6** | **7.76** | 97.97 | 0.04777 | 0.14924 | 3.44 | 11.19 | 14.63 |
| 258.7 | **272.4** | **7.15** | 97.77 | 0.04811 | 0.14859 | 3.47 | 11.13 | 14.60 |
| 259.7 | **272.7** | **6.36** | 98.31 | 0.04853 | 0.14933 | 3.50 | 11.19 | 14.68 |
| 260.8 | **272.7** | **6.91** | 97.56 | 0.04823 | 0.14807 | 3.48 | 11.09 | 14.57 |
| 265.0 | **262.6** | **6.00** | 97.76 | 0.04873 | 0.14809 | 3.51 | 11.09 | 14.60 |
| 266.0 | **262.9** | **3.59** | 98.01 | 0.05004 | 0.14756 | 3.60 | 11.04 | 14.64 |
| 267.1 | **263.0** | **4.02** | 98.18 | 0.04981 | 0.14808 | 3.58 | 11.08 | 14.66 |
| 282.5 | **241.8** | **2.22** | 98.10 | 0.05079 | 0.14716 | 3.65 | 11.00 | 14.65 |
| 283.6 | **242.1** | **2.15** | 98.25 | 0.05083 | 0.14743 | 3.65 | 11.02 | 14.67 |

**EXPERIMENT 4 - WGC-B ($Au/Fe_2O_3/Al_2O_3$)**

| | | |
|---|---|---|
| **Pressure** | 2.0 | bar (absolute) |
| **WHSV** | 4.0 | $hr^{-1}$ |
| **S/DG** | 1.0 | mol/mol |

| Time-on-stream (hours) | Temperature (°C) | $X_{CO}$ (%) | C balance (%) | $x_{CO}$ (%) | $x_{CO_2}$ (%) | $F_{CO}$ (ml/min) | $F_{CO_2}$ (ml/min) | $F_{CO+CO_2}$ (ml/min) |
|---|---|---|---|---|---|---|---|---|
| 19.1 | **185.3** | **21.08** | 89.14 | 0.0406 | 0.1374 | 2.95 | 10.37 | 13.31 |
| 21.8 | **185.9** | **19.66** | 89.66 | 0.0414 | 0.1378 | 3.00 | 10.39 | 13.39 |
| 23.9 | **185.9** | **19.39** | 89.97 | 0.0415 | 0.1383 | 3.01 | 10.43 | 13.44 |
| 26.1 | **185.9** | **19.29** | 89.83 | 0.0416 | 0.1380 | 3.01 | 10.40 | 13.42 |
| 45.1 | **186.1** | **17.84** | 89.23 | 0.0423 | 0.1362 | 3.07 | 10.26 | 13.33 |
| 46.2 | **185.9** | **18.81** | 88.86 | 0.0418 | 0.1358 | 3.03 | 10.24 | 13.27 |
| 48.9 | **186.1** | **16.76** | 90.06 | 0.0429 | 0.1374 | 3.11 | 10.34 | 13.45 |
| 50.2 | **186.3** | **16.63** | 89.38 | 0.0430 | 0.1359 | 3.11 | 10.24 | 13.35 |
| 52.3 | **185.9** | **17.55** | 88.90 | 0.0425 | 0.1354 | 3.08 | 10.20 | 13.28 |
| 57.9 | **186.2** | **17.87** | 88.26 | 0.0423 | 0.1343 | 3.07 | 10.11 | 13.18 |
| 66.9 | **186.0** | **16.98** | 89.10 | 0.0428 | 0.1355 | 3.10 | 10.21 | 13.31 |

**EXPERIMENT 4 - WGC-B ($Au/Fe_2O_3/Al_2O_3$)**

| | | |
|---|---|---|
| **Pressure** | 2.0 | bar (absolute) |
| **WHSV** | **8.0** | **$hr^{-1}$** |
| **S/DG** | 1.0 | mol/mol |

| Time-on-stream (hours) | Temperature (°C) | $X_{CO}$ (%) | C balance (%) | $x_{CO}$ (%) | $x_{CO_2}$ (%) | $F_{CO}$ (ml/min) | $F_{CO_2}$ (ml/min) | $F_{CO+CO_2}$ (ml/min) |
|---|---|---|---|---|---|---|---|---|
| 70.1 | **185.4** | **10.53** | 100.85 | 0.0463 | 0.1561 | 3.34 | 11.72 | 15.06 |
| 71.3 | **185.6** | **8.96** | 92.78 | 0.0471 | 0.1394 | 3.40 | 10.46 | 13.86 |
| 74.0 | **185.2** | **9.05** | 92.48 | 0.0471 | 0.1389 | 3.40 | 10.42 | 13.81 |
| 74.7 | **185.8** | **9.04** | 91.84 | 0.0471 | 0.1376 | 3.40 | 10.32 | 13.72 |
| 76.1 | **185.4** | **9.23** | 92.01 | 0.0470 | 0.1380 | 3.39 | 10.35 | 13.74 |
| 77.2 | **185.3** | **9.08** | 91.97 | 0.0471 | 0.1379 | 3.40 | 10.34 | 13.74 |

**EXPERIMENT 4 - WGC-B ($Au/Fe_2O_3/Al_2O_3$)**

| | | |
|---|---|---|
| **Pressure** | 2.0 | bar (absolute) |
| **WHSV** | **4.0** | **$hr^{-1}$** |
| **S/DG** | 1.0 | mol/mol |

| Time-on-stream (hours) | Temperature (°C) | $X_{CO}$ (%) | C balance (%) | $x_{CO}$ (%) | $x_{CO_2}$ (%) | $F_{CO}$ (ml/min) | $F_{CO_2}$ (ml/min) | $F_{CO+CO_2}$ (ml/min) |
|---|---|---|---|---|---|---|---|---|
| 89.7 | **186.0** | **15.33** | 88.98 | 0.0437 | 0.1346 | 3.16 | 10.13 | 13.29 |
| 90.7 | **186.2** | **15.65** | 89.42 | 0.0435 | 0.1356 | 3.15 | 10.21 | 13.35 |
| 91.8 | **186.5** | **15.04** | 90.72 | 0.0438 | 0.1379 | 3.17 | 10.38 | 13.55 |

**EXPERIMENT 4 - WGC-B ($Au/Fe_2O_3/Al_2O_3$)**

| | | |
|---|---|---|
| **Pressure** | 2.0 | bar (absolute) |
| **WHSV** | **2.0** | **$hr^{-1}$** |
| **S/DG** | 1.0 | mol/mol |

| Time-on-stream (hours) | Temperature (°C) | $X_{CO}$ (%) | C balance (%) | $x_{CO}$ (%) | $x_{CO_2}$ (%) | $F_{CO}$ (ml/min) | $F_{CO_2}$ (ml/min) | $F_{CO+CO_2}$ (ml/min) |
|---|---|---|---|---|---|---|---|---|
| 96.5 | **187.3** | **23.48** | 88.50 | 0.0393 | 0.1371 | 2.86 | 10.36 | 13.22 |
| 97.6 | **187.3** | **22.40** | 87.42 | 0.0399 | 0.1345 | 2.90 | 10.16 | 13.06 |
| 98.7 | **186.3** | **22.90** | 87.33 | 0.0396 | 0.1346 | 2.88 | 10.16 | 13.04 |

**EXPERIMENT 4 - WGC-B ($Au/Fe_2O_3/Al_2O_3$)**

| | | |
|---|---|---|
| **Pressure** | 2.0 | bar (absolute) |
| **WHSV** | **4.0** | **$hr^{-1}$** |
| **S/DG** | 1.0 | mol/mol |

| Time-on-stream (hours) | Temperature (°C) | $X_{CO}$ (%) | C balance (%) | $x_{CO}$ (%) | $x_{CO_2}$ (%) | $F_{CO}$ (ml/min) | $F_{CO_2}$ (ml/min) | $F_{CO+CO_2}$ (ml/min) |
|---|---|---|---|---|---|---|---|---|
| 113.7 | **186.0** | **15.50** | 89.36 | 0.0436 | 0.1354 | 3.16 | 10.19 | 13.35 |
| 114.8 | **186.1** | **14.88** | 89.16 | 0.0439 | 0.1348 | 3.18 | 10.14 | 13.32 |

**EXPERIMENT 4 - WGC-B ($Au/Fe_2O_3/Al_2O_3$)**

| | | |
|---|---|---|
| **Pressure** | 2.0 | bar (absolute) |
| **WHSV** | 4.0 | $hr^{-1}$ |
| **S/DG** | **2.0** | **mol/mol** |

| Time-on-stream (hours) | Temperature (°C) | $X_{CO}$ (%) | C balance (%) | $x_{CO}$ (%) | $x_{CO_2}$ (%) | $F_{CO}$ (ml/min) | $F_{CO_2}$ (ml/min) | $F_{CO+CO_2}$ (ml/min) |
|---|---|---|---|---|---|---|---|---|
| 119.3 | **186.6** | **15.22** | 89.39 | 0.0437 | 0.1354 | 3.17 | 10.18 | 13.35 |
| 120.4 | **186.7** | **15.20** | 89.87 | 0.0437 | 0.1363 | 3.17 | 10.26 | 13.42 |
| 121.5 | **186.7** | **15.07** | 89.81 | 0.0438 | 0.1361 | 3.17 | 10.24 | 13.41 |
| 122.3 | **186.8** | **15.13** | 90.11 | 0.0438 | 0.1368 | 3.17 | 10.29 | 13.46 |

**EXPERIMENT 4 - WGC-B ($Au/Fe_2O_3/Al_2O_3$)**

| | | |
|---|---|---|
| **Pressure** | 2.0 | bar (absolute) |
| **WHSV** | 4.0 | $hr^{-1}$ |
| **S/DG** | **1.0** | **mol/mol** |

| Time-on-stream (hours) | Temperature (°C) | $X_{CO}$ (%) | C balance (%) | $x_{CO}$ (%) | $x_{CO_2}$ (%) | $F_{CO}$ (ml/min) | $F_{CO_2}$ (ml/min) | $F_{CO+CO_2}$ (ml/min) |
|---|---|---|---|---|---|---|---|---|
| 127.0 | **185.4** | **14.90** | 89.18 | 0.0439 | 0.1348 | 3.18 | 10.14 | 13.32 |
| 128.0 | **185.5** | **15.07** | 88.64 | 0.0438 | 0.1338 | 3.17 | 10.07 | 13.24 |

**EXPERIMENT 4 - WGC-B ($Au/Fe_2O_3/Al_2O_3$)**

| | | |
|---|---|---|
| **Pressure** | 2.0 | bar (absolute) |
| **WHSV** | 4.0 | $hr^{-1}$ |
| **S/DG** | **0.5** | **mol/mol** |

| Time-on-stream (hours) | Temperature (°C) | $X_{CO}$ (%) | C balance (%) | $x_{CO}$ (%) | $x_{CO_2}$ (%) | $F_{CO}$ (ml/min) | $F_{CO_2}$ (ml/min) | $F_{CO+CO_2}$ (ml/min) |
|---|---|---|---|---|---|---|---|---|
| 138.7 | **186.7** | **12.80** | 89.84 | 0.0450 | 0.1352 | 3.26 | 10.16 | 13.42 |
| 140.4 | **186.7** | **12.07** | 89.87 | 0.0454 | 0.1350 | 3.28 | 10.14 | 13.42 |
| 141.4 | **187.3** | **12.15** | 90.38 | 0.0454 | 0.1360 | 3.28 | 10.22 | 13.50 |

**EXPERIMENT 4 - WGC-B ($Au/Fe_2O_3/Al_2O_3$)**

| | | |
|---|---|---|
| **Pressure** | 2.0 | bar (absolute) |
| **WHSV** | 4.0 | $hr^{-1}$ |
| **S/DG** | **1.0** | **mol/mol** |

| Time-on-stream (hours) | Temperature (°C) | $X_{CO}$ (%) | C balance (%) | $x_{CO}$ (%) | $x_{CO_2}$ (%) | $F_{CO}$ (ml/min) | $F_{CO_2}$ (ml/min) | $F_{CO+CO_2}$ (ml/min) |
|---|---|---|---|---|---|---|---|---|
| 144.6 | **185.1** | **13.66** | 90.10 | 0.0446 | 0.1361 | 3.22 | 10.23 | 13.46 |
| 145.8 | **185.1** | **13.47** | 89.99 | 0.0447 | 0.1358 | 3.23 | 10.21 | 13.44 |
| 146.9 | **185.2** | **13.89** | 90.11 | 0.0445 | 0.1362 | 3.22 | 10.24 | 13.46 |

**EXPERIMENT 4 - WGC-B ($Au/Fe_2O_3/Al_2O_3$)**

| | | |
|---|---|---|
| **Pressure** | **4.0** | **bar (absolute)** |
| **WHSV** | 4.0 | $hr^{-1}$ |
| **S/DG** | 1.0 | mol/mol |

| Time-on-stream (hours) | Temperature (°C) | $X_{CO}$ (%) | C balance (%) | $x_{CO}$ (%) | $x_{CO_2}$ (%) | $F_{CO}$ (ml/min) | $F_{CO_2}$ (ml/min) | $F_{CO+CO_2}$ (ml/min) |
|---|---|---|---|---|---|---|---|---|
| 161.7 | **187.5** | **19.94** | 89.07 | 0.0412 | 0.1368 | 2.99 | 10.31 | 13.30 |
| 163.0 | **187.4** | **19.66** | 88.97 | 0.0414 | 0.1364 | 3.00 | 10.29 | 13.29 |
| 164.3 | **187.0** | **19.32** | 89.05 | 0.0415 | 0.1364 | 3.01 | 10.29 | 13.30 |
| 165.4 | **187.4** | **19.20** | 89.16 | 0.0416 | 0.1366 | 3.02 | 10.30 | 13.32 |

**EXPERIMENT 4 - WGC-B ($Au/Fe_2O_3/Al_2O_3$)**

| | | |
|---|---|---|
| **Pressure** | **2.0** | **bar (absolute)** |
| **WHSV** | 4.0 | $hr^{-1}$ |
| **S/DG** | 1.0 | mol/mol |

| Time-on-stream (hours) | Temperature (°C) | $X_{CO}$ (%) | C balance (%) | $x_{CO}$ (%) | $x_{CO_2}$ (%) | $F_{CO}$ (ml/min) | $F_{CO_2}$ (ml/min) | $F_{CO+CO_2}$ (ml/min) |
|---|---|---|---|---|---|---|---|---|
| 168.5 | **185.9** | **12.98** | 89.40 | 0.0449 | 0.1344 | 3.25 | 10.10 | 13.35 |
| 171.2 | **185.9** | **12.77** | 89.46 | 0.0451 | 0.1344 | 3.26 | 10.10 | 13.36 |
| 178.1 | **184.9** | **14.48** | 87.32 | 0.0441 | 0.1309 | 3.19 | 9.85 | 13.04 |
| 186.7 | **185.9** | **13.12** | 88.78 | 0.0449 | 0.1333 | 3.24 | 10.02 | 13.26 |
| 187.7 | **186.8** | **12.95** | 89.29 | 0.0450 | 0.1342 | 3.25 | 10.08 | 13.34 |

**EXPERIMENT 4 - WGC-B ($Au/Fe_2O_3/Al_2O_3$)**

| | | |
|---|---|---|
| **Pressure** | **8.0** | **bar (absolute)** |
| **WHSV** | 4.0 | $hr^{-1}$ |
| **S/DG** | 1.0 | mol/mol |

| Time-on-stream (hours) | Temperature (°C) | $X_{CO}$ (%) | C balance (%) | $x_{CO}$ (%) | $x_{CO_2}$ (%) | $F_{CO}$ (ml/min) | $F_{CO_2}$ (ml/min) | $F_{CO+CO_2}$ (ml/min) |
|---|---|---|---|---|---|---|---|---|
| 191.1 | **188.8** | **25.73** | 88.28 | 0.0381 | 0.1377 | 2.77 | 10.41 | 13.18 |
| 192.2 | **188.8** | **24.43** | 92.33 | 0.0388 | 0.1451 | 2.82 | 10.97 | 13.79 |
| 193.1 | **189.0** | **24.41** | 94.26 | 0.0388 | 0.1489 | 2.82 | 11.26 | 14.08 |
| 194.1 | **188.8** | **23.14** | 91.53 | 0.0395 | 0.1430 | 2.87 | 10.80 | 13.67 |

**EXPERIMENT 4 - WGC-B ($Au/Fe_2O_3/Al_2O_3$)**

| | | |
|---|---|---|
| **Pressure** | **2.0** | **bar (absolute)** |
| **WHSV** | 4.0 | $hr^{-1}$ |
| **S/DG** | 1.0 | mol/mol |

| Time-on-stream (hours) | Temperature (°C) | $X_{CO}$ (%) | C balance (%) | $x_{CO}$ (%) | $x_{CO_2}$ (%) | $F_{CO}$ (ml/min) | $F_{CO_2}$ (ml/min) | $F_{CO+CO_2}$ (ml/min) |
|---|---|---|---|---|---|---|---|---|
| 213.7 | **185.9** | **10.66** | 89.39 | 0.0462 | 0.1334 | 3.34 | 10.02 | 13.35 |
| 214.8 | **185.7** | **12.53** | 100.08 | 0.0452 | 0.1555 | 3.27 | 11.68 | 14.95 |
| 219.2 | **185.6** | **10.47** | 91.68 | 0.0463 | 0.1379 | 3.34 | 10.35 | 13.69 |
| 220.1 | **185.6** | **10.89** | 90.40 | 0.0461 | 0.1355 | 3.33 | 10.17 | 13.50 |

**EXPERIMENT 4 - WGC-B ($Au/Fe_2O_3/Al_2O_3$)**

| | | |
|---|---|---|
| **Pressure** | 2.0 | bar (absolute) |
| **WHSV** | 4.0 | $hr^{-1}$ |
| **S/DG** | 1.0 | mol/mol |

| Time-on-stream (hours) | Temperature (°C) | $X_{CO}$ (%) | C balance (%) | $x_{CO}$ (%) | $x_{CO_2}$ (%) | $F_{CO}$ (ml/min) | $F_{CO_2}$ (ml/min) | $F_{CO+CO_2}$ (ml/min) |
|---|---|---|---|---|---|---|---|---|
| 236.9 | **127.8** | **6.93** | 89.22 | 0.0482 | 0.1315 | 3.48 | 9.85 | 13.33 |
| 240.0 | **127.5** | **7.33** | 89.70 | 0.0480 | 0.1326 | 3.46 | 9.94 | 13.40 |
| 241.9 | **127.9** | **6.99** | 90.00 | 0.0482 | 0.1330 | 3.47 | 9.97 | 13.44 |
| 259.0 | **204.6** | **11.24** | 91.00 | 0.0459 | 0.1369 | 3.31 | 10.28 | 13.59 |
| 260.1 | **204.8** | **11.67** | 90.78 | 0.0457 | 0.1366 | 3.30 | 10.26 | 13.56 |
| 261.1 | **205.3** | **9.95** | 91.56 | 0.0466 | 0.1374 | 3.36 | 10.31 | 13.67 |
| 264.4 | **214.6** | **11.85** | 91.35 | 0.0456 | 0.1378 | 3.29 | 10.35 | 13.64 |
| 265.5 | **214.8** | **11.18** | 91.03 | 0.0459 | 0.1369 | 3.32 | 10.28 | 13.60 |
| 266.5 | **214.6** | **11.06** | 90.78 | 0.0460 | 0.1363 | 3.32 | 10.24 | 13.56 |
| 281.9 | **224.3** | **10.61** | 91.71 | 0.0462 | 0.1380 | 3.34 | 10.36 | 13.70 |
| 283.4 | **224.2** | **11.05** | 90.80 | 0.0460 | 0.1364 | 3.32 | 10.24 | 13.56 |
| 285.6 | **224.2** | **10.86** | 90.73 | 0.0461 | 0.1362 | 3.33 | 10.22 | 13.55 |

**EXPERIMENT 5 - WGC-C ($Au/Fe_2O_3$)**

| | | |
|---|---|---|
| **Pressure** | 2.0 | bar (absolute) |
| **WHSV** | 4.0 | $hr^{-1}$ |
| **S/DG** | 1.0 | mol/mol |

| Time-on-stream (hours) | Temperature (°C) | $X_{CO}$ (%) | C balance (%) | $x_{CO}$ (%) | $x_{CO_2}$ (%) | $F_{CO}$ (ml/min) | $F_{CO_2}$ (ml/min) | $F_{CO+CO_2}$ (ml/min) |
|---|---|---|---|---|---|---|---|---|
| 2.2 | **191.3** | **97.6** | 98.3 | 0.0012 | 0.1862 | 0.09 | 14.58 | 14.67 |
| 4.3 | **191.3** | **97.1** | 97.8 | 0.0014 | 0.1852 | 0.11 | 14.50 | 14.60 |
| 8.8 | **190.4** | **97.3** | 97.5 | 0.0013 | 0.1847 | 0.10 | 14.46 | 14.56 |
| 21.5 | **190.8** | **94.6** | 97.3 | 0.0027 | 0.1832 | 0.20 | 14.33 | 14.53 |
| 23.7 | **191.0** | **92.2** | 97.9 | 0.0039 | 0.1835 | 0.29 | 14.33 | 14.62 |
| 25.9 | **191.1** | **92.2** | 98.0 | 0.0039 | 0.1836 | 0.29 | 14.34 | 14.63 |
| 28.0 | **191.1** | **90.7** | 98.4 | 0.0046 | 0.1838 | 0.35 | 14.35 | 14.69 |
| 44.7 | **191.0** | **88.4** | 96.7 | 0.0058 | 0.1797 | 0.43 | 14.01 | 14.45 |
| 47.6 | **191.2** | **86.5** | 97.3 | 0.0067 | 0.1800 | 0.50 | 14.03 | 14.53 |
| 49.6 | **191.5** | **84.3** | 97.0 | 0.0078 | 0.1786 | 0.59 | 13.90 | 14.48 |
| 51.4 | **191.3** | **84.1** | 98.0 | 0.0079 | 0.1806 | 0.59 | 14.05 | 14.64 |
| 53.6 | **191.5** | **83.4** | 98.7 | 0.0083 | 0.1814 | 0.62 | 14.11 | 14.73 |
| 69.6 | **190.9** | **81.5** | 96.6 | 0.0092 | 0.1769 | 0.69 | 13.74 | 14.43 |
| 71.6 | **191.0** | **80.7** | 93.7 | 0.0096 | 0.1708 | 0.72 | 13.27 | 13.99 |
| 73.2 | **191.1** | **80.1** | 98.1 | 0.0099 | 0.1791 | 0.74 | 13.91 | 14.65 |
| 75.0 | **191.0** | **78.9** | 100.5 | 0.0106 | 0.1832 | 0.79 | 14.22 | 15.01 |
| 77.5 | **191.2** | **78.1** | 100.4 | 0.0109 | 0.1826 | 0.82 | 14.17 | 14.99 |
| 82.8 | **191.1** | **76.9** | 99.1 | 0.0116 | 0.1798 | 0.86 | 13.94 | 14.81 |
| 92.1 | **191.2** | **74.4** | 99.5 | 0.0128 | 0.1795 | 0.95 | 13.90 | 14.86 |
| 95.5 | **191.0** | **72.9** | 100.3 | 0.0136 | 0.1806 | 1.01 | 13.97 | 14.98 |
| 98.4 | **191.0** | **71.6** | 100.9 | 0.0143 | 0.1812 | 1.06 | 14.01 | 15.08 |
| 99.5 | **191.2** | **70.5** | 100.4 | 0.0148 | 0.1798 | 1.10 | 13.90 | 15.00 |
| 100.4 | **191.2** | **68.9** | 97.2 | 0.0156 | 0.1729 | 1.16 | 13.36 | 14.52 |
| 102.7 | **191.2** | **69.1** | 100.3 | 0.0155 | 0.1789 | 1.15 | 13.82 | 14.98 |
| 104.7 | **191.2** | **67.7** | 100.5 | 0.0162 | 0.1788 | 1.21 | 13.80 | 15.01 |
| 118.0 | **191.2** | **69.3** | 99.7 | 0.0154 | 0.1780 | 1.15 | 13.75 | 14.90 |
| 121.3 | **191.4** | **67.2** | 101.3 | 0.0165 | 0.1801 | 1.23 | 13.90 | 15.13 |
| 124.5 | **191.4** | **66.1** | 100.6 | 0.0171 | 0.1783 | 1.27 | 13.76 | 15.02 |
| 127.9 | **191.3** | **65.8** | 100.0 | 0.0172 | 0.1771 | 1.28 | 13.66 | 14.94 |
| 130.4 | **191.1** | **65.0** | 100.5 | 0.0176 | 0.1778 | 1.31 | 13.71 | 15.01 |
| 141.4 | **191.1** | **62.9** | 99.0 | 0.0187 | 0.1741 | 1.38 | 13.41 | 14.79 |
| 143.4 | **191.4** | **62.2** | 99.5 | 0.0191 | 0.1747 | 1.41 | 13.45 | 14.86 |
| 148.8 | **191.4** | **61.5** | 100.5 | 0.0194 | 0.1764 | 1.44 | 13.57 | 15.01 |
| 151.5 | **189.5** | **59.9** | 98.2 | 0.0202 | 0.1713 | 1.50 | 13.17 | 14.67 |
| 154.3 | **190.5** | **60.3** | 98.3 | 0.0200 | 0.1716 | 1.48 | 13.20 | 14.68 |
| 165.2 | **190.2** | **58.0** | 99.1 | 0.0212 | 0.1722 | 1.57 | 13.23 | 14.80 |
| 167.8 | **191.5** | **57.5** | 99.5 | 0.0215 | 0.1728 | 1.59 | 13.28 | 14.86 |
| 170.3 | **191.4** | **57.3** | 99.6 | 0.0215 | 0.1730 | 1.59 | 13.29 | 14.88 |
| 173.4 | **191.4** | **56.6** | 99.7 | 0.0219 | 0.1727 | 1.62 | 13.26 | 14.89 |
| 176.9 | **191.4** | **56.3** | 98.5 | 0.0221 | 0.1705 | 1.63 | 13.09 | 14.72 |
| 188.4 | **191.3** | **54.2** | 98.0 | 0.0232 | 0.1686 | 1.71 | 12.93 | 14.64 |
| 190.4 | **191.3** | **52.0** | 99.3 | 0.0243 | 0.1703 | 1.79 | 13.05 | 14.84 |
| 192.5 | **190.8** | **49.4** | 99.6 | 0.0256 | 0.1697 | 1.89 | 12.98 | 14.87 |
| 194.7 | **191.0** | **48.2** | 99.4 | 0.0263 | 0.1688 | 1.94 | 12.91 | 14.84 |

**EXPERIMENT 6 - WGC-C ($Au/Fe_2O_3$)**

| | | |
|---|---|---|
| **Pressure** | 2.0 | bar (absolute) |
| **WHSV** | 4.0 | $hr^{-1}$ |
| **S/DG** | 1.0 | mol/mol |

| Time-on-stream (hours) | Temperature (°C) | $X_{CO}$ (%) | C balance (%) | $x_{CO}$ (%) | $x_{CO_2}$ (%) | $F_{CO}$ (ml/min) | $F_{CO_2}$ (ml/min) | $F_{CO+CO_2}$ (ml/min) |
|---|---|---|---|---|---|---|---|---|
| 2.9 | **195.6** | **97.3** | 90.0 | 0.0013 | 0.1705 | 0.10 | 13.35 | 13.45 |
| 4.9 | **195.3** | **98.0** | 91.6 | 0.0010 | 0.1736 | 0.07 | 13.60 | 13.68 |
| 8.7 | **195.4** | **97.5** | 90.3 | 0.0012 | 0.1711 | 0.09 | 13.40 | 13.49 |
| 19.6 | **195.5** | **94.0** | 93.4 | 0.0030 | 0.1756 | 0.22 | 13.73 | 13.95 |
| 22.5 | **195.4** | **93.9** | 91.1 | 0.0030 | 0.1712 | 0.23 | 13.38 | 13.61 |
| 24.8 | **195.6** | **92.7** | 99.0 | 0.0036 | 0.1857 | 0.27 | 14.51 | 14.78 |
| 27.2 | **195.5** | **91.4** | 94.8 | 0.0042 | 0.1773 | 0.32 | 13.85 | 14.16 |
| 44.8 | **195.5** | **87.6** | 91.0 | 0.0062 | 0.1685 | 0.46 | 13.13 | 13.59 |
| 46.9 | **194.9** | **86.4** | 90.8 | 0.0068 | 0.1675 | 0.51 | 13.05 | 13.56 |
| 48.7 | **194.7** | **85.9** | 90.9 | 0.0070 | 0.1676 | 0.53 | 13.05 | 13.58 |
| 52.2 | **194.7** | **85.9** | 91.0 | 0.0070 | 0.1678 | 0.53 | 13.07 | 13.59 |
| 55.9 | **194.2** | **83.7** | 90.4 | 0.0081 | 0.1657 | 0.61 | 12.89 | 13.50 |
| 69.0 | **195.3** | **82.5** | 91.6 | 0.0087 | 0.1675 | 0.65 | 13.02 | 13.68 |
| 71.5 | **195.5** | **81.4** | 92.3 | 0.0093 | 0.1685 | 0.70 | 13.10 | 13.79 |
| 73.6 | **195.4** | **81.3** | 92.0 | 0.0093 | 0.1678 | 0.70 | 13.04 | 13.74 |
| 75.3 | **195.3** | **80.4** | 91.9 | 0.0098 | 0.1673 | 0.73 | 13.00 | 13.73 |
| 77.4 | **195.0** | **80.2** | 91.7 | 0.0099 | 0.1669 | 0.74 | 12.96 | 13.70 |
| 78.4 | **195.1** | **79.4** | 91.7 | 0.0103 | 0.1665 | 0.77 | 12.93 | 13.69 |
| 79.5 | **195.1** | **79.0** | 91.0 | 0.0105 | 0.1650 | 0.78 | 12.80 | 13.59 |
| 91.5 | **194.7** | **77.4** | 91.7 | 0.0113 | 0.1656 | 0.84 | 12.84 | 13.69 |
| 92.6 | **195.1** | **77.4** | 91.1 | 0.0113 | 0.1646 | 0.85 | 12.76 | 13.61 |
| 93.6 | **195.0** | **77.2** | 91.7 | 0.0114 | 0.1657 | 0.85 | 12.85 | 13.70 |
| 96.9 | **135.7** | **19.5** | 91.5 | 0.0414 | 0.1415 | 3.00 | 10.67 | 13.67 |
| 97.9 | **135.7** | **19.5** | 91.4 | 0.0414 | 0.1412 | 3.00 | 10.64 | 13.65 |
| 99.2 | **135.0** | **18.4** | 91.8 | 0.0420 | 0.1415 | 3.05 | 10.66 | 13.71 |
| 102.4 | **129.9** | **15.9** | 91.4 | 0.0434 | 0.1396 | 3.14 | 10.51 | 13.64 |
| 103.5 | **128.9** | **16.3** | 90.3 | 0.0432 | 0.1376 | 3.13 | 10.36 | 13.49 |
| 105.0 | **129.1** | **16.7** | 90.0 | 0.0429 | 0.1373 | 3.11 | 10.34 | 13.45 |
| 106.0 | **129.0** | **16.8** | 90.4 | 0.0429 | 0.1381 | 3.10 | 10.40 | 13.50 |
| 115.0 | **142.3** | **25.8** | 91.3 | 0.0381 | 0.1437 | 2.77 | 10.87 | 13.64 |
| 116.0 | **141.9** | **25.9** | 90.9 | 0.0380 | 0.1429 | 2.77 | 10.81 | 13.58 |
| 117.0 | **142.0** | **25.2** | 91.7 | 0.0384 | 0.1443 | 2.79 | 10.91 | 13.70 |
| 120.1 | **153.5** | **38.6** | 91.5 | 0.0313 | 0.1494 | 2.29 | 11.37 | 13.66 |
| 121.1 | **153.6** | **38.4** | 91.7 | 0.0314 | 0.1497 | 2.30 | 11.39 | 13.69 |
| 122.1 | **153.6** | **37.9** | 92.0 | 0.0317 | 0.1501 | 2.32 | 11.42 | 13.74 |
| 125.8 | **164.8** | **53.0** | 91.5 | 0.0238 | 0.1553 | 1.75 | 11.91 | 13.66 |
| 127.0 | **165.9** | **55.3** | 90.9 | 0.0226 | 0.1551 | 1.67 | 11.90 | 13.57 |
| 127.9 | **165.7** | **54.8** | 90.9 | 0.0228 | 0.1549 | 1.69 | 11.89 | 13.57 |
| 139.9 | **175.3** | **64.0** | 91.4 | 0.0181 | 0.1597 | 1.35 | 12.31 | 13.65 |
| 141.0 | **174.8** | **63.1** | 91.5 | 0.0186 | 0.1595 | 1.38 | 12.29 | 13.66 |
| 142.0 | **175.1** | **63.5** | 91.7 | 0.0184 | 0.1601 | 1.36 | 12.33 | 13.70 |
| 145.1 | **184.6** | **70.5** | 93.8 | 0.0148 | 0.1670 | 1.10 | 12.91 | 14.01 |
| 146.2 | **185.1** | **70.6** | 91.8 | 0.0147 | 0.1632 | 1.10 | 12.62 | 13.71 |
| 147.6 | **185.2** | **71.0** | 91.1 | 0.0145 | 0.1620 | 1.08 | 12.52 | 13.61 |
| 162.8 | **194.4** | **74.1** | 89.3 | 0.0130 | 0.1597 | 0.97 | 12.37 | 13.34 |
| 163.9 | **194.9** | **74.0** | 90.6 | 0.0130 | 0.1622 | 0.97 | 12.56 | 13.53 |

**EXPERIMENT 6 - WGC-C ($Au/Fe_2O_3$)**

| | | |
|---|---|---|
| **Pressure** | 2.0 | bar (absolute) |
| **WHSV** | 4.0 | $hr^{-1}$ |
| **S/DG** | 1.0 | mol/mol |

| Time-on-stream (hours) | Temperature (°C) | $X_{CO}$ (%) | C balance (%) | $x_{CO}$ (%) | $x_{CO_2}$ (%) | $F_{CO}$ (ml/min) | $F_{CO_2}$ (ml/min) | $F_{CO+CO_2}$ (ml/min) |
|---|---|---|---|---|---|---|---|---|
| 164.9 | **194.9** | **73.8** | 90.6 | 0.0131 | 0.1620 | 0.98 | 12.55 | 13.53 |
| 168.3 | **204.9** | **75.8** | 91.1 | 0.0121 | 0.1638 | 0.90 | 12.70 | 13.60 |
| 169.3 | **205.0** | **75.8** | 106.6 | 0.0121 | 0.1938 | 0.91 | 15.02 | 15.93 |
| 170.3 | **204.9** | **75.6** | 92.5 | 0.0122 | 0.1665 | 0.91 | 12.90 | 13.81 |
| 173.4 | **215.0** | **76.0** | 90.2 | 0.0120 | 0.1623 | 0.90 | 12.58 | 13.47 |
| 174.4 | **215.0** | **75.3** | 90.5 | 0.0124 | 0.1625 | 0.92 | 12.59 | 13.51 |
| 175.5 | **215.0** | **75.3** | 90.1 | 0.0124 | 0.1618 | 0.92 | 12.54 | 13.46 |
| 186.9 | **224.7** | **72.8** | 89.5 | 0.0137 | 0.1597 | 1.02 | 12.36 | 13.37 |
| 187.9 | **224.7** | **71.6** | 90.5 | 0.0142 | 0.1611 | 1.06 | 12.46 | 13.52 |
| 189.0 | **224.5** | **71.9** | 90.5 | 0.0141 | 0.1612 | 1.05 | 12.47 | 13.52 |
| 192.2 | **235.1** | **68.2** | 90.7 | 0.0160 | 0.1600 | 1.19 | 12.35 | 13.54 |
| 193.7 | **234.8** | **70.6** | 91.4 | 0.0147 | 0.1624 | 1.10 | 12.55 | 13.65 |
| 194.8 | **234.5** | **70.3** | 91.6 | 0.0149 | 0.1626 | 1.11 | 12.57 | 13.68 |
| 213.4 | **193.9** | **61.6** | 89.5 | 0.0194 | 0.1550 | 1.43 | 11.93 | 13.37 |
| 214.4 | **194.2** | **58.1** | 89.4 | 0.0212 | 0.1534 | 1.56 | 11.79 | 13.36 |
| 218.9 | **175.3** | **46.3** | 89.9 | 0.0273 | 0.1495 | 2.00 | 11.42 | 13.42 |

**EXPERIMENT 7 - WGC-C ($Au/Fe_2O_3$)**

| | | |
|---|---|---|
| **Pressure** | 2.0 | bar (absolute) |
| **WHSV** | 4.0 | $hr^{-1}$ |
| **S/DG** | 1.0 | mol/mol |

| Time-on-stream (hours) | Temperature (°C) | $X_{CO}$ (%) | C balance (%) | $x_{CO}$ (%) | $x_{CO_2}$ (%) | $F_{CO}$ (ml/min) | $F_{CO_2}$ (ml/min) | $F_{CO+CO_2}$ (ml/min) |
|---|---|---|---|---|---|---|---|---|
| 2.1 | **191.2** | **98.0** | 97.4 | 0.0010 | 0.1847 | 0.08 | 14.47 | 14.55 |
| 6.4 | **191.3** | **97.1** | 98.2 | 0.0015 | 0.1860 | 0.11 | 14.56 | 14.67 |
| 18.4 | **190.2** | **91.2** | 101.1 | 0.0044 | 0.1892 | 0.33 | 14.77 | 15.10 |
| 21.1 | **190.6** | **90.0** | 103.3 | 0.0050 | 0.1928 | 0.37 | 15.05 | 15.42 |
| 23.8 | **190.5** | **88.3** | 104.7 | 0.0058 | 0.1950 | 0.44 | 15.20 | 15.64 |
| 30.3 | **190.8** | **86.2** | 96.6 | 0.0069 | 0.1786 | 0.52 | 13.91 | 14.43 |
| 43.2 | **190.2** | **77.0** | 98.0 | 0.0115 | 0.1777 | 0.86 | 13.78 | 14.64 |
| 45.7 | **190.2** | **76.3** | 98.8 | 0.0119 | 0.1789 | 0.89 | 13.87 | 14.75 |
| 48.2 | **190.0** | **76.2** | 99.0 | 0.0119 | 0.1793 | 0.89 | 13.90 | 14.79 |
| 52.4 | **190.1** | **77.1** | 98.8 | 0.0114 | 0.1793 | 0.85 | 13.91 | 14.76 |
| 55.1 | **190.0** | **76.4** | 97.2 | 0.0118 | 0.1759 | 0.88 | 13.64 | 14.52 |
| 67.0 | **190.3** | **71.9** | 98.2 | 0.0141 | 0.1761 | 1.05 | 13.62 | 14.67 |
| 69.8 | **190.0** | **70.7** | 97.7 | 0.0147 | 0.1747 | 1.09 | 13.51 | 14.60 |
| 72.8 | **189.9** | **69.1** | 98.3 | 0.0155 | 0.1752 | 1.16 | 13.53 | 14.69 |
| 76.1 | **190.1** | **68.7** | 98.2 | 0.0157 | 0.1747 | 1.17 | 13.49 | 14.66 |
| 79.2 | **190.2** | **68.0** | 96.9 | 0.0161 | 0.1720 | 1.19 | 13.28 | 14.48 |
| 90.1 | **190.2** | **63.6** | 97.3 | 0.0183 | 0.1711 | 1.36 | 13.18 | 14.54 |
| 94.2 | **165.4** | **40.5** | 97.7 | 0.0303 | 0.1624 | 2.22 | 12.37 | 14.59 |
| 95.4 | **164.9** | **40.6** | 97.4 | 0.0303 | 0.1618 | 2.22 | 12.33 | 14.55 |
| 96.7 | **165.1** | **40.6** | 97.6 | 0.0302 | 0.1622 | 2.22 | 12.36 | 14.58 |

**EXPERIMENT 7 - WGC-C ($Au/Fe_2O_3$)**

| | | |
|---|---|---|
| **Pressure** | **4.0** | **bar (absolute)** |
| **WHSV** | 4.0 | $hr^{-1}$ |
| **S/DG** | 1.0 | mol/mol |

| Time-on-stream (hours) | Temperature (°C) | $X_{CO}$ (%) | C balance (%) | $x_{CO}$ (%) | $x_{CO_2}$ (%) | $F_{CO}$ (ml/min) | $F_{CO_2}$ (ml/min) | $F_{CO+CO_2}$ (ml/min) |
|---|---|---|---|---|---|---|---|---|
| 100.1 | **166.7** | **52.6** | 97.4 | 0.0240 | 0.1668 | 1.77 | 12.78 | 14.55 |
| 101.8 | **167.0** | **52.9** | 97.3 | 0.0238 | 0.1667 | 1.76 | 12.77 | 14.53 |
| 103.8 | **167.1** | **53.0** | 97.0 | 0.0238 | 0.1660 | 1.76 | 12.72 | 14.48 |

**EXPERIMENT 7 - WGC-C ($Au/Fe_2O_3$)**

| | | |
|---|---|---|
| **Pressure** | **2.0** | **bar (absolute)** |
| **WHSV** | 4.0 | $hr^{-1}$ |
| **S/DG** | 1.0 | mol/mol |

| Time-on-stream (hours) | Temperature (°C) | $X_{CO}$ (%) | C balance (%) | $x_{CO}$ (%) | $x_{CO_2}$ (%) | $F_{CO}$ (ml/min) | $F_{CO_2}$ (ml/min) | $F_{CO+CO_2}$ (ml/min) |
|---|---|---|---|---|---|---|---|---|
| 113.3 | **165.1** | **38.2** | 96.8 | 0.0315 | 0.1597 | 2.31 | 12.15 | 14.46 |
| 114.4 | **164.9** | **38.0** | 97.3 | 0.0316 | 0.1606 | 2.32 | 12.22 | 14.54 |

**EXPERIMENT 7 - WGC-C ($Au/Fe_2O_3$)**

| | | |
|---|---|---|
| **Pressure** | **8.0** | **bar (absolute)** |
| **WHSV** | 4.0 | $hr^{-1}$ |
| **S/DG** | 1.0 | mol/mol |

| Time-on-stream (hours) | Temperature (°C) | $X_{CO}$ (%) | C balance (%) | $x_{CO}$ (%) | $x_{CO_2}$ (%) | $F_{CO}$ (ml/min) | $F_{CO_2}$ (ml/min) | $F_{CO+CO_2}$ (ml/min) |
|---|---|---|---|---|---|---|---|---|
| 117.8 | **168.0** | **56.7** | 96.0 | 0.0219 | 0.1657 | 1.62 | 12.72 | 14.34 |
| 118.9 | **168.5** | **53.5** | 97.3 | 0.0235 | 0.1668 | 1.74 | 12.79 | 14.53 |
| 120.1 | **168.8** | **52.5** | 96.8 | 0.0240 | 0.1655 | 1.77 | 12.68 | 14.45 |

**EXPERIMENT 7 - WGC-C ($Au/Fe_2O_3$)**

| | | |
|---|---|---|
| **Pressure** | **2.0** | **bar (absolute)** |
| **WHSV** | 4.0 | $hr^{-1}$ |
| **S/DG** | 1.0 | mol/mol |

| Time-on-stream (hours) | Temperature (°C) | $X_{CO}$ (%) | C balance (%) | $x_{CO}$ (%) | $x_{CO_2}$ (%) | $F_{CO}$ (ml/min) | $F_{CO_2}$ (ml/min) | $F_{CO+CO_2}$ (ml/min) |
|---|---|---|---|---|---|---|---|---|
| 123.6 | **164.8** | **31.9** | 97.4 | 0.0348 | 0.1582 | 2.54 | 12.00 | 14.54 |
| 127.8 | **165.4** | **34.3** | 95.4 | 0.0335 | 0.1552 | 2.45 | 11.79 | 14.24 |
| 137.6 | **165.1** | **32.7** | 95.6 | 0.0344 | 0.1549 | 2.51 | 11.76 | 14.27 |

**EXPERIMENT 7 - WGC-C ($Au/Fe_2O_3$)**

| | | |
|---|---|---|
| **Pressure** | 2.0 | bar (absolute) |
| **WHSV** | **8.0** | **$hr^{-1}$** |
| **S/DG** | 1.0 | mol/mol |

| Time-on-stream (hours) | Temperature (°C) | $X_{CO}$ (%) | C balance (%) | $x_{CO}$ (%) | $x_{CO_2}$ (%) | $F_{CO}$ (ml/min) | $F_{CO_2}$ (ml/min) | $F_{CO+CO_2}$ (ml/min) |
|---|---|---|---|---|---|---|---|---|
| 140.8 | **164.2** | **14.6** | 99.1 | 0.0441 | 0.1545 | 3.19 | 11.62 | 14.81 |
| 141.8 | **163.8** | **14.0** | 99.6 | 0.0444 | 0.1552 | 3.21 | 11.67 | 14.88 |
| 143.0 | **164.1** | **13.5** | 99.7 | 0.0447 | 0.1551 | 3.23 | 11.66 | 14.89 |

**EXPERIMENT 7 - WGC-C ($Au/Fe_2O_3$)**

| | | |
|---|---|---|
| **Pressure** | 2.0 | bar (absolute) |
| **WHSV** | **4.0** | **$hr^{-1}$** |
| **S/DG** | 1.0 | mol/mol |

| Time-on-stream (hours) | Temperature (°C) | $X_{CO}$ (%) | C balance (%) | $x_{CO}$ (%) | $x_{CO_2}$ (%) | $F_{CO}$ (ml/min) | $F_{CO_2}$ (ml/min) | $F_{CO+CO_2}$ (ml/min) |
|---|---|---|---|---|---|---|---|---|
| 146.3 | **164.6** | **29.6** | 97.4 | 0.0360 | 0.1572 | 2.63 | 11.91 | 14.54 |
| 147.9 | **165.2** | **31.0** | 97.0 | 0.0353 | 0.1571 | 2.58 | 11.91 | 14.49 |

**EXPERIMENT 7 - WGC-C ($Au/Fe_2O_3$)**

| | | |
|---|---|---|
| **Pressure** | 2.0 | bar (absolute) |
| **WHSV** | **2.0** | **$hr^{-1}$** |
| **S/DG** | 1.0 | mol/mol |

| Time-on-stream (hours) | Temperature (°C) | $X_{CO}$ (%) | C balance (%) | $x_{CO}$ (%) | $x_{CO_2}$ (%) | $F_{CO}$ (ml/min) | $F_{CO_2}$ (ml/min) | $F_{CO+CO_2}$ (ml/min) |
|---|---|---|---|---|---|---|---|---|
| 161.4 | **165.9** | **45.1** | 94.5 | 0.0279 | 0.1579 | 2.05 | 12.06 | 14.11 |
| 162.4 | **165.6** | **46.1** | 94.5 | 0.0274 | 0.1584 | 2.01 | 12.10 | 14.12 |
| 163.5 | **165.0** | **44.6** | 94.1 | 0.0282 | 0.1570 | 2.07 | 11.98 | 14.05 |

**EXPERIMENT 7 - WGC-C ($Au/Fe_2O_3$)**

| | | |
|---|---|---|
| **Pressure** | 2.0 | bar (absolute) |
| **WHSV** | **4.0** | **$hr^{-1}$** |
| **S/DG** | 1.0 | mol/mol |

| Time-on-stream (hours) | Temperature (°C) | $X_{CO}$ (%) | C balance (%) | $x_{CO}$ (%) | $x_{CO_2}$ (%) | $F_{CO}$ (ml/min) | $F_{CO_2}$ (ml/min) | $F_{CO+CO_2}$ (ml/min) |
|---|---|---|---|---|---|---|---|---|
| 166.8 | **165.8** | **29.9** | 97.3 | 0.0359 | 0.1571 | 2.62 | 11.91 | 14.53 |
| 167.9 | **165.9** | **28.1** | 96.8 | 0.0369 | 0.1554 | 2.69 | 11.77 | 14.46 |
| 169.0 | **165.2** | **29.1** | 97.4 | 0.0363 | 0.1571 | 2.65 | 11.90 | 14.55 |

**EXPERIMENT 7 - WGC-C ($Au/Fe_2O_3$)**

| | | |
|---|---|---|
| **Pressure** | 2.0 | bar (absolute) |
| **WHSV** | 4.0 | $hr^{-1}$ |
| **S/DG** | **2.0** | **mol/mol** |

| Time-on-stream (hours) | Temperature (°C) | $X_{CO}$ (%) | C balance (%) | $x_{CO}$ (%) | $x_{CO_2}$ (%) | $F_{CO}$ (ml/min) | $F_{CO_2}$ (ml/min) | $F_{CO+CO_2}$ (ml/min) |
|---|---|---|---|---|---|---|---|---|
| 172.5 | **166.2** | **29.8** | 96.8 | 0.0359 | 0.1562 | 2.62 | 11.84 | 14.46 |
| 173.6 | **165.7** | **29.7** | 96.0 | 0.0360 | 0.1545 | 2.63 | 11.71 | 14.33 |
| 175.5 | **165.2** | **30.0** | 95.5 | 0.0359 | 0.1536 | 2.62 | 11.64 | 14.26 |

**EXPERIMENT 7 - WGC-C ($Au/Fe_2O_3$)**

| | | |
|---|---|---|
| **Pressure** | 2.0 | bar (absolute) |
| **WHSV** | 4.0 | $hr^{-1}$ |
| **S/DG** | **1.0** | **mol/mol** |

| Time-on-stream (hours) | Temperature (°C) | $X_{CO}$ (%) | C balance (%) | $x_{CO}$ (%) | $x_{CO_2}$ (%) | $F_{CO}$ (ml/min) | $F_{CO_2}$ (ml/min) | $F_{CO+CO_2}$ (ml/min) |
|---|---|---|---|---|---|---|---|---|
| 185.2 | **165.4** | **28.6** | 96.4 | 0.0366 | 0.1548 | 2.67 | 11.73 | 14.39 |
| 186.3 | **165.4** | **28.9** | 96.7 | 0.0365 | 0.1555 | 2.66 | 11.78 | 14.44 |
| 189.7 | **168.0** | **22.0** | 95.2 | 0.0401 | 0.1498 | 2.91 | 11.31 | 14.22 |

**EXPERIMENT 7 - WGC-C ($Au/Fe_2O_3$)**

| | | |
|---|---|---|
| **Pressure** | 2.0 | bar (absolute) |
| **WHSV** | 4.0 | $hr^{-1}$ |
| **S/DG** | **0.5** | **mol/mol** |

| **Time-on-stream** (hours) | **Temperature** (°C) | **$X_{CO}$** (%) | **C balance** (%) | **$x_{CO}$** (%) | **$x_{CO_2}$** (%) | **$F_{CO}$** (ml/min) | **$F_{CO_2}$** (ml/min) | **$F_{CO+CO_2}$** (ml/min) |
|---|---|---|---|---|---|---|---|---|
| 191.8 | **173.5** | **14.8** | 96.1 | 0.0440 | 0.1484 | 3.18 | 11.16 | 14.35 |

**EXPERIMENT 8 - WGC-A ($Au/TiO_2$)**

| | | |
|---|---|---|
| **Pressure** | 2.0 | bar (absolute) |
| **WHSV** | 4.0 | $hr^{-1}$ |
| **S/DG** | 1.0 | mol/mol |

| Time-on-stream (hours) | Temperature (°C) | $X_{CO}$ (%) | C balance (%) | $x_{CO}$ (%) | $x_{CO_2}$ (%) | $F_{CO}$ (ml/min) | $F_{CO_2}$ (ml/min) | $F_{CO+CO_2}$ (ml/min) |
|---|---|---|---|---|---|---|---|---|
| 2.1 | **192.5** | **23.2** | 96.4 | 0.0394 | 0.1527 | 2.87 | 11.53 | 14.40 |
| 4.5 | **192.4** | **21.8** | 96.3 | 0.0402 | 0.1518 | 2.92 | 11.46 | 14.38 |
| 6.9 | **192.4** | **22.1** | 94.2 | 0.0401 | 0.1478 | 2.91 | 11.16 | 14.07 |
| 16.4 | **191.9** | **18.4** | 94.4 | 0.0420 | 0.1467 | 3.05 | 11.06 | 14.10 |
| 19.1 | **192.4** | **18.5** | 94.8 | 0.0420 | 0.1474 | 3.04 | 11.11 | 14.15 |
| 21.8 | **192.0** | **16.0** | 95.1 | 0.0433 | 0.1471 | 3.14 | 11.07 | 14.21 |
| 25.0 | **192.1** | **15.5** | 94.4 | 0.0436 | 0.1454 | 3.16 | 10.94 | 14.10 |
| 31.5 | **192.2** | **15.3** | 93.6 | 0.0437 | 0.1438 | 3.16 | 10.82 | 13.98 |
| 41.0 | **192.3** | **14.6** | 94.2 | 0.0441 | 0.1445 | 3.19 | 10.87 | 14.06 |
| 43.5 | **191.9** | **12.6** | 94.5 | 0.0451 | 0.1444 | 3.26 | 10.85 | 14.11 |
| 46.1 | **192.4** | **12.7** | 95.1 | 0.0451 | 0.1457 | 3.26 | 10.95 | 14.21 |
| 49.3 | **191.9** | **12.5** | 94.7 | 0.0452 | 0.1447 | 3.27 | 10.87 | 14.14 |
| 51.5 | **192.6** | **12.8** | 94.7 | 0.0450 | 0.1449 | 3.26 | 10.89 | 14.14 |
| 53.8 | **191.5** | **12.8** | 93.6 | 0.0450 | 0.1428 | 3.26 | 10.73 | 13.99 |
| 64.0 | **191.1** | **12.5** | 93.6 | 0.0452 | 0.1426 | 3.27 | 10.71 | 13.98 |
| 66.5 | **192.0** | **12.3** | 94.3 | 0.0453 | 0.1440 | 3.27 | 10.82 | 14.09 |
| 69.3 | **192.9** | **12.9** | 95.0 | 0.0450 | 0.1454 | 3.25 | 10.93 | 14.18 |
| 72.4 | **192.3** | **10.6** | 94.9 | 0.0462 | 0.1443 | 3.34 | 10.83 | 14.17 |
| 75.7 | **173.5** | **7.5** | 98.6 | 0.0479 | 0.1504 | 3.45 | 11.27 | 14.73 |
| 76.8 | **173.6** | **8.1** | 94.3 | 0.0476 | 0.1421 | 3.43 | 10.65 | 14.09 |
| 77.9 | **173.8** | **8.8** | 94.5 | 0.0472 | 0.1429 | 3.41 | 10.71 | 14.12 |
| 88.6 | **154.5** | **6.4** | 93.8 | 0.0485 | 0.1404 | 3.49 | 10.51 | 14.01 |
| 89.8 | **154.7** | **5.6** | 93.7 | 0.0489 | 0.1399 | 3.52 | 10.48 | 14.00 |
| 91.5 | **154.6** | **5.6** | 95.5 | 0.0489 | 0.1433 | 3.52 | 10.73 | 14.26 |
| 95.1 | **193.2** | **12.6** | 94.6 | 0.0452 | 0.1446 | 3.26 | 10.87 | 14.13 |
| 96.4 | **192.6** | **12.6** | 94.2 | 0.0452 | 0.1439 | 3.26 | 10.81 | 14.08 |
| 112.9 | **191.8** | **11.7** | 76.0 | 0.0456 | 0.1073 | 3.30 | 8.06 | 11.36 |
| 116.6 | **193.0** | **11.1** | 96.2 | 0.0460 | 0.1472 | 3.32 | 11.05 | 14.37 |
| 119.9 | **202.9** | **12.5** | 96.1 | 0.0452 | 0.1476 | 3.27 | 11.09 | 14.36 |
| 121.1 | **202.7** | **12.7** | 95.8 | 0.0451 | 0.1470 | 3.26 | 11.04 | 14.30 |
| 122.3 | **202.8** | **14.1** | 96.2 | 0.0443 | 0.1485 | 3.21 | 11.16 | 14.37 |
| 124.5 | **202.1** | **14.1** | 94.9 | 0.0444 | 0.1459 | 3.21 | 10.97 | 14.18 |
| 125.7 | **202.0** | **15.4** | 94.9 | 0.0436 | 0.1464 | 3.16 | 11.01 | 14.17 |
| 138.3 | **202.0** | **16.0** | 95.3 | 0.0433 | 0.1474 | 3.14 | 11.09 | 14.23 |
| 140.2 | **202.2** | **14.9** | 96.2 | 0.0439 | 0.1488 | 3.18 | 11.19 | 14.37 |
| 143.4 | **210.7** | **15.7** | 97.5 | 0.0435 | 0.1518 | 3.15 | 11.42 | 14.57 |
| 145.0 | **210.9** | **17.3** | 97.1 | 0.0426 | 0.1516 | 3.09 | 11.42 | 14.51 |
| 147.4 | **210.4** | **16.9** | 96.0 | 0.0428 | 0.1492 | 3.10 | 11.24 | 14.34 |
| 150.4 | **211.3** | **18.6** | 95.4 | 0.0419 | 0.1488 | 3.04 | 11.21 | 14.25 |
| 160.2 | **210.7** | **18.3** | 96.0 | 0.0421 | 0.1498 | 3.05 | 11.29 | 14.34 |
| 162.2 | **211.4** | **18.8** | 96.6 | 0.0418 | 0.1511 | 3.03 | 11.39 | 14.42 |
| 166.4 | **231.8** | **25.8** | 97.7 | 0.0381 | 0.1563 | 2.77 | 11.82 | 14.60 |
| 168.0 | **232.4** | **26.2** | 97.2 | 0.0379 | 0.1555 | 2.76 | 11.76 | 14.52 |
| 171.4 | **231.4** | **28.4** | 96.3 | 0.0367 | 0.1545 | 2.67 | 11.70 | 14.38 |
| 174.3 | **231.6** | **29.9** | 95.6 | 0.0359 | 0.1539 | 2.62 | 11.66 | 14.28 |
| 183.8 | **231.9** | **31.5** | 96.4 | 0.0351 | 0.1561 | 2.56 | 11.84 | 14.40 |

**EXPERIMENT 8 - WGC-A ($Au/TiO_2$)**

| | | |
|---|---|---|
| **Pressure** | 2.0 | bar (absolute) |
| **WHSV** | 4.0 | $hr^{-1}$ |
| **S/DG** | 1.0 | mol/mol |

| Time-on-stream (hours) | Temperature (°C) | $X_{CO}$ (%) | C balance (%) | $x_{CO}$ (%) | $x_{CO2}$ (%) | $F_{CO}$ (ml/min) | $F_{CO2}$ (ml/min) | $F_{CO+CO2}$ (ml/min) |
|---|---|---|---|---|---|---|---|---|
| 185.2 | **232.3** | **31.6** | 96.4 | 0.0350 | 0.1562 | 2.55 | 11.85 | 14.40 |
| 187.1 | **232.0** | **31.7** | 96.5 | 0.0349 | 0.1564 | 2.55 | 11.87 | 14.42 |
| 209.2 | **251.1** | **46.3** | 96.0 | 0.0273 | 0.1615 | 2.00 | 12.34 | 14.34 |
| 211.9 | **252.8** | **48.0** | 96.3 | 0.0264 | 0.1626 | 1.94 | 12.44 | 14.38 |
| 218.2 | **252.0** | **46.3** | 96.1 | 0.0273 | 0.1616 | 2.01 | 12.35 | 14.35 |
| 221.9 | **250.5** | **48.3** | 95.5 | 0.0262 | 0.1613 | 1.93 | 12.33 | 14.26 |
| 231.8 | **272.9** | **58.3** | 95.9 | 0.0211 | 0.1661 | 1.56 | 12.77 | 14.32 |
| 234.0 | **272.9** | **58.5** | 96.2 | 0.0209 | 0.1668 | 1.55 | 12.82 | 14.37 |
| 237.7 | **273.4** | **58.2** | 96.3 | 0.0211 | 0.1669 | 1.56 | 12.83 | 14.39 |
| 239.8 | **273.5** | **58.4** | 96.5 | 0.0210 | 0.1673 | 1.55 | 12.86 | 14.41 |
| 244.6 | **294.0** | **69.9** | 95.0 | 0.0151 | 0.1690 | 1.13 | 13.06 | 14.19 |
| 246.7 | **294.0** | **70.1** | 94.8 | 0.0150 | 0.1688 | 1.12 | 13.04 | 14.16 |
| 255.6 | **294.1** | **71.0** | 95.6 | 0.0145 | 0.1707 | 1.08 | 13.20 | 14.28 |
| 257.3 | **294.3** | **70.8** | 95.4 | 0.0146 | 0.1701 | 1.09 | 13.15 | 14.24 |
| 261.1 | **314.3** | **76.8** | 97.6 | 0.0116 | 0.1768 | 0.87 | 13.71 | 14.58 |
| 263.4 | **314.7** | **77.0** | 97.2 | 0.0115 | 0.1761 | 0.86 | 13.66 | 14.52 |
| 267.3 | **314.4** | **77.3** | 96.5 | 0.0113 | 0.1749 | 0.85 | 13.57 | 14.41 |
| 271.0 | **313.3** | **77.3** | 95.0 | 0.0113 | 0.1720 | 0.85 | 13.34 | 14.19 |
| 281.4 | **252.9** | **55.3** | 94.7 | 0.0226 | 0.1626 | 1.67 | 12.48 | 14.14 |
| 283.9 | **252.7** | **54.5** | 95.3 | 0.0230 | 0.1634 | 1.70 | 12.53 | 14.23 |
| 288.4 | **253.0** | **54.5** | 96.5 | 0.0230 | 0.1658 | 1.70 | 12.72 | 14.42 |
| 291.5 | **252.3** | **54.8** | 95.1 | 0.0229 | 0.1632 | 1.69 | 12.52 | 14.21 |
| 305.9 | **253.0** | **54.5** | 94.5 | 0.0230 | 0.1618 | 1.70 | 12.41 | 14.11 |

**EXPERIMENT 8 - WGC-A ($Au/TiO_2$)**

| | | |
|---|---|---|
| **Pressure** | 2.0 | bar (absolute) |
| **WHSV** | **8.0** | **$hr^{-1}$** |
| **S/DG** | 1.0 | mol/mol |

| Time-on-stream (hours) | Temperature (°C) | $X_{CO}$ (%) | C balance (%) | $x_{CO}$ (%) | $x_{CO2}$ (%) | $F_{CO}$ (ml/min) | $F_{CO2}$ (ml/min) | $F_{CO+CO2}$ (ml/min) |
|---|---|---|---|---|---|---|---|---|
| 312.0 | **253.2** | **33.7** | 101.9 | 0.0339 | 0.1677 | 2.48 | 12.74 | 15.21 |
| 314.3 | **253.1** | **34.4** | 97.2 | 0.0335 | 0.1589 | 2.45 | 12.07 | 14.52 |
| 316.4 | **253.1** | **34.3** | 96.7 | 0.0336 | 0.1578 | 2.45 | 11.98 | 14.44 |

**EXPERIMENT 8 - WGC-A ($Au/TiO_2$)**

| | | |
|---|---|---|
| **Pressure** | 2.0 | bar (absolute) |
| **WHSV** | **4.0** | **$hr^{-1}$** |
| **S/DG** | 1.0 | mol/mol |

| Time-on-stream (hours) | Temperature (°C) | $X_{CO}$ (%) | C balance (%) | $x_{CO}$ (%) | $x_{CO_2}$ (%) | $F_{CO}$ (ml/min) | $F_{CO_2}$ (ml/min) | $F_{CO+CO_2}$ (ml/min) |
|---|---|---|---|---|---|---|---|---|
| 328.1 | **252.1** | **53.7** | 97.9 | 0.0234 | 0.1682 | 1.73 | 12.90 | 14.62 |
| 329.5 | **252.7** | **52.4** | 94.4 | 0.0241 | 0.1607 | 1.78 | 12.32 | 14.09 |

**EXPERIMENT 8 - WGC-A ($Au/TiO_2$)**

| | | |
|---|---|---|
| **Pressure** | 2.0 | bar (absolute) |
| **WHSV** | **2.0** | **$hr^{-1}$** |
| **S/DG** | 1.0 | mol/mol |

| Time-on-stream (hours) | Temperature (°C) | $X_{CO}$ (%) | C balance (%) | $x_{CO}$ (%) | $x_{CO_2}$ (%) | $F_{CO}$ (ml/min) | $F_{CO_2}$ (ml/min) | $F_{CO+CO_2}$ (ml/min) |
|---|---|---|---|---|---|---|---|---|
| 333.1 | **253.1** | **72.3** | 92.8 | 0.0139 | 0.1659 | 1.03 | 12.83 | 13.87 |
| 335.1 | **253.1** | **72.9** | 92.7 | 0.0136 | 0.1658 | 1.01 | 12.83 | 13.84 |
| 336.7 | **253.0** | **72.2** | 93.1 | 0.0139 | 0.1663 | 1.04 | 12.87 | 13.90 |

**EXPERIMENT 8 - WGC-A ($Au/TiO_2$)**

| | | |
|---|---|---|
| **Pressure** | 2.0 | bar (absolute) |
| **WHSV** | **4.0** | **$hr^{-1}$** |
| **S/DG** | 1.0 | mol/mol |

| Time-on-stream (hours) | Temperature (°C) | $X_{CO}$ (%) | C balance (%) | $x_{CO}$ (%) | $x_{CO_2}$ (%) | $F_{CO}$ (ml/min) | $F_{CO_2}$ (ml/min) | $F_{CO+CO_2}$ (ml/min) |
|---|---|---|---|---|---|---|---|---|
| 339.8 | **251.9** | **52.2** | 96.2 | 0.0242 | 0.1642 | 1.79 | 12.58 | 14.36 |
| 342.3 | **252.0** | **54.2** | 93.3 | 0.0232 | 0.1594 | 1.71 | 12.23 | 13.94 |

**EXPERIMENT 8 - WGC-A ($Au/TiO_2$)**

| | | |
|---|---|---|
| **Pressure** | 2.0 | bar (absolute) |
| **WHSV** | 4.0 | $hr^{-1}$ |
| **S/DG** | **2.0** | **mol/mol** |

| Time-on-stream (hours) | Temperature (°C) | $X_{CO}$ (%) | C balance (%) | $x_{CO}$ (%) | $x_{CO_2}$ (%) | $F_{CO}$ (ml/min) | $F_{CO_2}$ (ml/min) | $F_{CO+CO_2}$ (ml/min) |
|---|---|---|---|---|---|---|---|---|
| 352.2 | **251.7** | **42.7** | 93.8 | 0.0291 | 0.1556 | 2.14 | 11.87 | 14.00 |
| 353.4 | **251.1** | **41.4** | 94.2 | 0.0298 | 0.1559 | 2.19 | 11.88 | 14.07 |
| 354.6 | **251.1** | **43.6** | 94.4 | 0.0287 | 0.1571 | 2.10 | 11.99 | 14.09 |

**EXPERIMENT 8 - WGC-A ($Au/TiO_2$)**

| | | |
|---|---|---|
| **Pressure** | 2.0 | bar (absolute) |
| **WHSV** | 4.0 | $hr^{-1}$ |
| **S/DG** | **1.0** | **mol/mol** |

| Time-on-stream (hours) | Temperature (°C) | $X_{CO}$ (%) | C balance (%) | $x_{CO}$ (%) | $x_{CO_2}$ (%) | $F_{CO}$ (ml/min) | $F_{CO_2}$ (ml/min) | $F_{CO+CO_2}$ (ml/min) |
|---|---|---|---|---|---|---|---|---|
| 357.9 | **252.3** | **52.2** | 94.7 | 0.0242 | 0.1613 | 1.79 | 12.36 | 14.15 |
| 359.1 | **252.4** | **49.0** | 92.2 | 0.0259 | 0.1551 | 1.90 | 11.87 | 13.77 |
| 360.3 | **251.8** | **51.4** | 95.3 | 0.0246 | 0.1622 | 1.82 | 12.42 | 14.24 |

**EXPERIMENT 8 - WGC-A ($Au/TiO_2$)**

| | | |
|---|---|---|
| **Pressure** | 2.0 | bar (absolute) |
| **WHSV** | 4.0 | $hr^{-1}$ |
| **S/DG** | **0.5** | **mol/mol** |

| Time-on-stream (hours) | Temperature (°C) | $X_{CO}$ (%) | C balance (%) | $x_{CO}$ (%) | $x_{CO_2}$ (%) | $F_{CO}$ (ml/min) | $F_{CO_2}$ (ml/min) | $F_{CO+CO_2}$ (ml/min) |
|---|---|---|---|---|---|---|---|---|
| 363.7 | **252.3** | **53.5** | 94.8 | 0.0235 | 0.1621 | 1.74 | 12.43 | 14.16 |
| 364.9 | **252.7** | **54.1** | 94.1 | 0.0232 | 0.1609 | 1.71 | 12.34 | 14.05 |
| 366.2 | **252.5** | **53.6** | 93.9 | 0.0235 | 0.1604 | 1.73 | 12.30 | 14.03 |

**EXPERIMENT 8 - WGC-A ($Au/TiO_2$)**

| | | |
|---|---|---|
| **Pressure** | 2.0 | bar (absolute) |
| **WHSV** | 4.0 | $hr^{-1}$ |
| **S/DG** | **1.0** | **mol/mol** |

| Time-on-stream (hours) | Temperature (°C) | $X_{CO}$ (%) | C balance (%) | $x_{CO}$ (%) | $x_{CO_2}$ (%) | $F_{CO}$ (ml/min) | $F_{CO_2}$ (ml/min) | $F_{CO+CO_2}$ (ml/min) |
|---|---|---|---|---|---|---|---|---|
| 375.8 | **252.0** | **49.4** | 93.4 | 0.0256 | 0.1577 | 1.89 | 12.06 | 13.95 |
| 377.0 | **252.1** | **50.0** | 93.5 | 0.0253 | 0.1581 | 1.87 | 12.10 | 13.97 |

**EXPERIMENT 8 - WGC-A ($Au/TiO_2$)**

| | | |
|---|---|---|
| **Pressure** | **4.0** | **bar (absolute)** |
| **WHSV** | 4.0 | $hr^{-1}$ |
| **S/DG** | 1.0 | mol/mol |

| Time-on-stream (hours) | Temperature (°C) | $X_{CO}$ (%) | C balance (%) | $x_{CO}$ (%) | $x_{CO_2}$ (%) | $F_{CO}$ (ml/min) | $F_{CO_2}$ (ml/min) | $F_{CO+CO_2}$ (ml/min) |
|---|---|---|---|---|---|---|---|---|
| 380.9 | **253.4** | **64.5** | 94.3 | 0.0179 | 0.1655 | 1.33 | 12.75 | 14.08 |
| 382.3 | **253.4** | **64.3** | 94.1 | 0.0180 | 0.1651 | 1.33 | 12.73 | 14.06 |
| 383.7 | **253.3** | **65.3** | 95.9 | 0.0175 | 0.1689 | 1.30 | 13.03 | 14.32 |

**EXPERIMENT 8 - WGC-A ($Au/TiO_2$)**

| | | |
|---|---|---|
| **Pressure** | **2.0** | **bar (absolute)** |
| **WHSV** | 4.0 | $hr^{-1}$ |
| **S/DG** | 1.0 | mol/mol |

| Time-on-stream (hours) | Temperature (°C) | $X_{CO}$ (%) | C balance (%) | $x_{CO}$ (%) | $x_{CO_2}$ (%) | $F_{CO}$ (ml/min) | $F_{CO_2}$ (ml/min) | $F_{CO+CO_2}$ (ml/min) |
|---|---|---|---|---|---|---|---|---|
| 387.3 | **251.8** | **47.1** | 94.9 | 0.0268 | 0.1596 | 1.97 | 12.20 | 14.17 |
| 388.8 | **252.5** | **50.9** | 93.8 | 0.0249 | 0.1590 | 1.84 | 12.18 | 14.01 |

**EXPERIMENT 8 - WGC-A ($Au/TiO_2$)**

| | | |
|---|---|---|
| **Pressure** | **8.0** | **bar (absolute)** |
| **WHSV** | 4.0 | $hr^{-1}$ |
| **S/DG** | 1.0 | mol/mol |

| Time-on-stream (hours) | Temperature (°C) | $X_{CO}$ (%) | C balance (%) | $x_{CO}$ (%) | $x_{CO_2}$ (%) | $F_{CO}$ (ml/min) | $F_{CO_2}$ (ml/min) | $F_{CO+CO_2}$ (ml/min) |
|---|---|---|---|---|---|---|---|---|
| 400.2 | **254.7** | **73.2** | 93.6 | 0.0134 | 0.1676 | 1.00 | 12.98 | 13.98 |
| 401.6 | **255.1** | **73.0** | 93.9 | 0.0135 | 0.1682 | 1.01 | 13.02 | 14.03 |
| 403.4 | **254.8** | **74.3** | 94.4 | 0.0129 | 0.1696 | 0.96 | 13.13 | 14.10 |

**EXPERIMENT 8 - WGC-A ($Au/TiO_2$)**

| | | |
|---|---|---|
| **Pressure** | **2.0** | **bar (absolute)** |
| **WHSV** | 4.0 | $hr^{-1}$ |
| **S/DG** | 1.0 | mol/mol |

| Time-on-stream (hours) | Temperature (°C) | $X_{CO}$ (%) | C balance (%) | $x_{CO}$ (%) | $x_{CO_2}$ (%) | $F_{CO}$ (ml/min) | $F_{CO_2}$ (ml/min) | $F_{CO+CO_2}$ (ml/min) |
|---|---|---|---|---|---|---|---|---|
| 406.7 | **253.5** | **45.2** | 96.0 | 0.0278 | 0.1610 | 2.05 | 12.29 | 14.34 |
| 407.9 | **252.9** | **46.1** | 95.6 | 0.0274 | 0.1606 | 2.01 | 12.27 | 14.28 |

# APPENDIX III

# GOLD REFERENCE CATALYST DATA SHEETS

WORLD GOLD COUNCIL

45 Pall Mall, London SW1Y 5JG
Tel: +44 (0)20 7930 5171, Fax: +44 (0)20 7839 6561
www.gold.org

# GOLD REFERENCE CATALYST DATA SHEET

1. Catalyst Type: **TYPE A** 1.5 wt% $Au/TiO_2$
2. Lot No. $Au\text{-}TiO_2$ #02-4
3. Preparation Method Deposition Precipitation

**Results of characterizations**

4. Elemental analysis by ICP

   Au / wt% 1.51

   Na / wt% 0.042

5. Diameter of Gold particles measured by TEM observation

   Average / nm 3.8; $\sigma$ / nm 1.50

6. Catalytic activity measured by fixed bed flow reactor

   Temperature at 50% conversion for CO oxidation / °C: - 45

   Temperature at 50% conversion for $H_2$ oxidation / °C: 43

*Note: It may be that catalytic activities will vary from the above values, depending on storage and/or pretreatment conditions. If significantly different results are obtained in testing, please advise Dr Richard Holliday, World Gold Council (email: Richard.holliday@gold.org) and Dr Susumu Tsubota, AIST, Japan (susumu-tsubota@aist.go.jp)*



Characterizations performed by:
The Environmental Catalysis Research Group,
Special Division of Green Life Technology, AIST.
Corresponding person: Dr. Susumu TSUBOTA:
susumu-tsubota@aist.go.jp

WORLD GOLD COUNCIL

45 Pall Mall, London SW1Y 5JG
Tel: +44 (0)20 7930 5171, Fax: +44 (0)20 7839 6561
www.gold.org

# GOLD REFERENCE CATALYST DATA SHEET

1. Catalyst Type: **TYPE B.** 0.3 wt% $Au/Fe_2O_3$ on alumina beads
2. Lot No. AUS #02-3
3. Preparation Method Deposition Precipitation

**Results of characterizations**

4. Elemental analysis by ICP

| | |
|---|---|
| Au / wt% | 0.28 |
| Fe / wt% | 11.6 |
| Na / wt% | 0.075 |

5. Catalytic activity measured by fixed bed flow reactor

Temperature at 50% conversion for CO oxidation / °C 38 ( dry condition)

100% conversion at 0 °C in wet condition

Temperature at 50% conversion for $H_2$ oxidation / °C 58

*Note: It may be that catalytic activities will vary from the above values, depending on storage and/or pretreatment conditions. If significantly different results are obtained in testing, please advise Dr Richard Holliday, World Gold Council (email: Richard.holliday@gold.org) and Dr Susumu Tsubota, AIST, Japan (susumu-tsubota@aist.go.jp)*

Characterizations performed by:
The Environmental Catalysis Research Group,
Special Division of Green Life Technology, AIST.
Corresponding person: Dr Susumu TSUBOTA:
susumu-tsubota@aist.go.jp

WORLD GOLD COUNCIL

45 Pall Mall, London SW1Y 5JG
Tel: +44 (0)20 7930 5171, Fax: +44 (0)20 7839 6561
www.gold.org

# GOLD REFERENCE CATALYST DATA SHEET

1. Catalyst Type: **TYPE C** 5wt% $Au/Fe_2O_3$
2. Lot No. $Au\text{-}Fe_2O_3$ #02-3
3. Preparation Method Coprecipitation

**Results of characterizations**

4. Elemental analysis by ICP

   Au / wt% 4.48

   Na / wt% 0.0190

7. Diameter of Gold particles measured by TEM observation

   Average / nm 3.7; $\sigma$ / nm 0.93

8. Catalytic activity measured by fixed bed flow reactor

   Temperature at 50% conversion for CO oxidation / °C: - 40

   Temperature at 50% conversion for $H_2$ oxidation / °C: 44



*Note: It may be that catalytic activities will vary from the above values, depending on storage and/or pretreatment conditions. If significantly different results are obtained in testing, please advise Dr Richard Holliday, World Gold Council (email: Richard.holliday@gold.org) and Dr Susumu Tsubota, AIST, Japan (susumu-tsubota@aist.go.jp)*

Characterizations performed by:
The Environmental Catalysis Research Group,
Special Division of Green Life Technology, AIST.
Corresponding person: Dr. Susumu TSUBOTA:
susumu-tsubota@aist.go.jp

# APPENDIX IV

# ACTIVATION ENERGY GRAPHS

# Determination of Activation Energy for C18-7

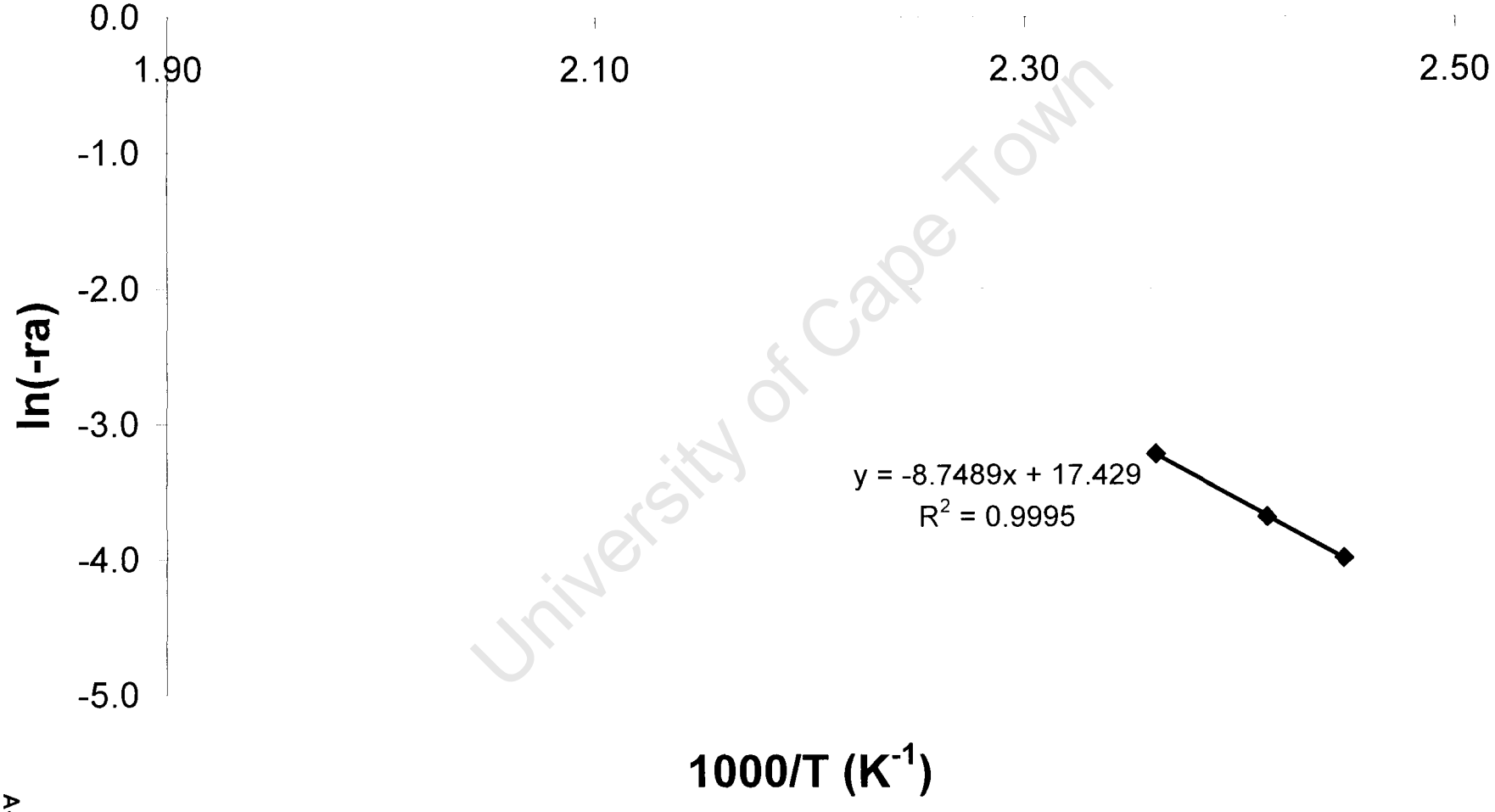

## Determination of Activation Energy for WGC-A

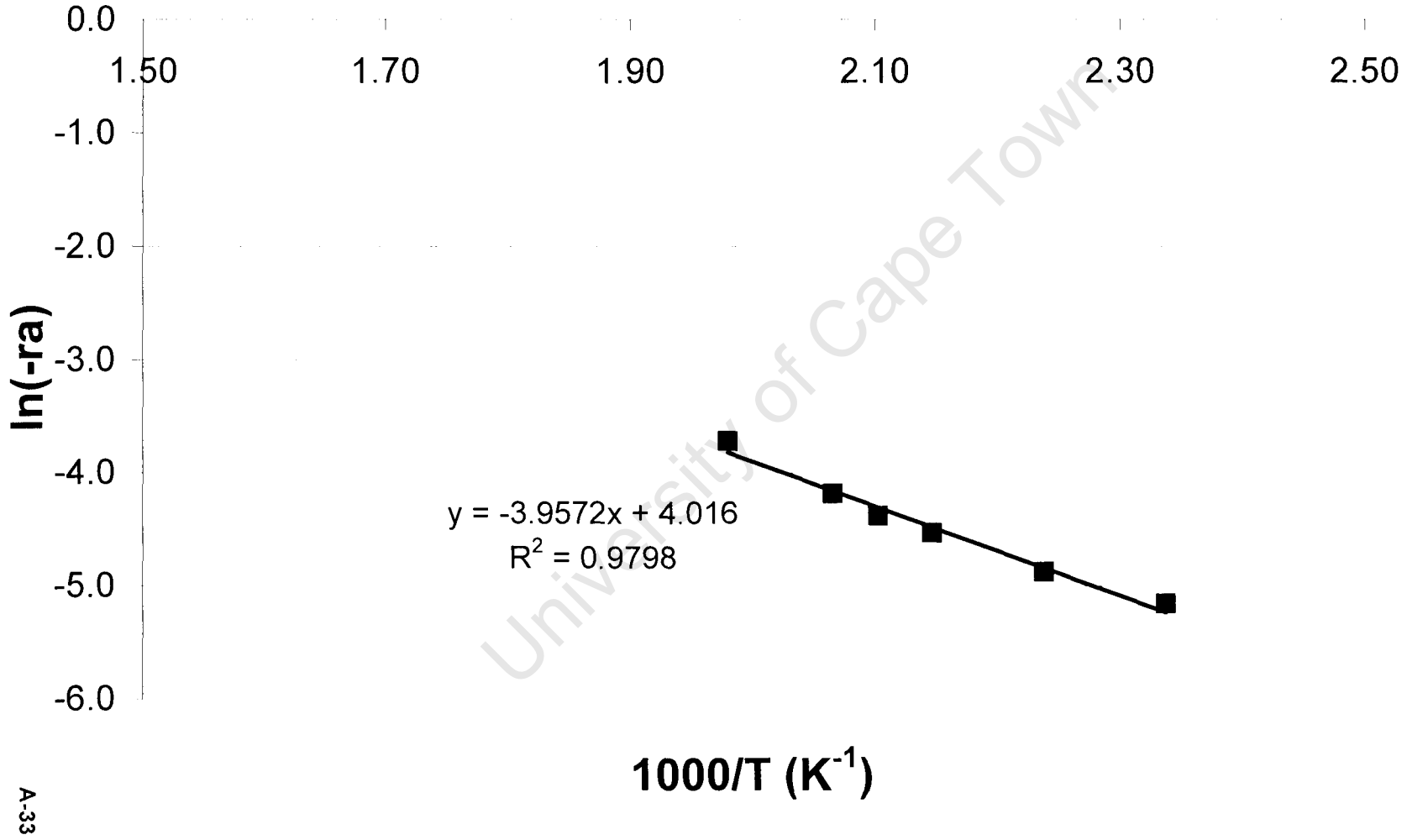

## Determination of Activation Energy for WGC-B

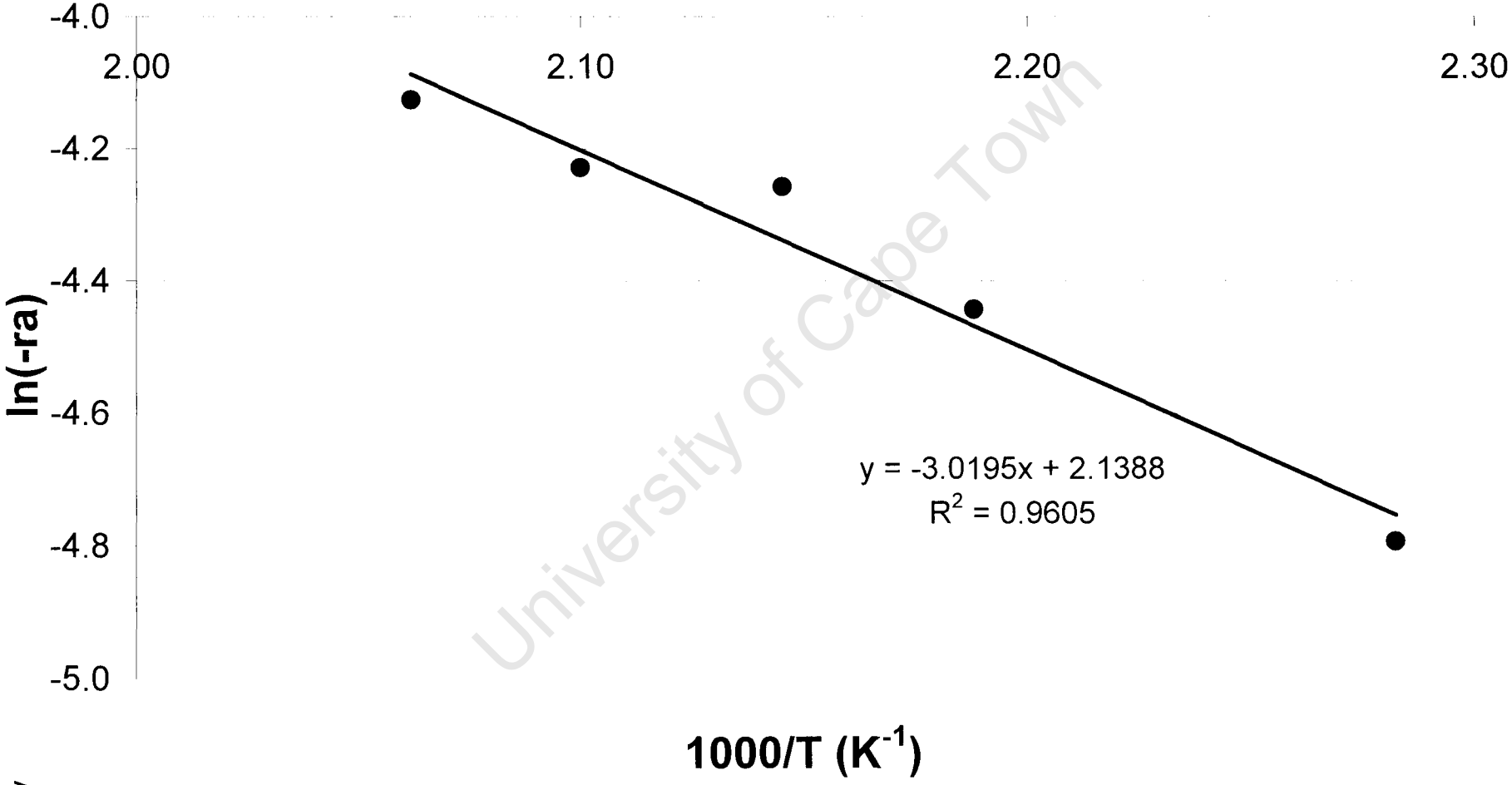

## Determination of Activation Energy for WGC-C